UNCLASSIFIED

AD NUMBER
AD361257
CLASSIFICATION CHANGES
TO: unclassified
FROM: confidential
LIMITATION CHANGES
TO: Approved for public release, distribution unlimited
FROM: Distribution authorized to U.S. Gov't. agencies and their contractors; Administrative/Operational Use; MAY 1965. Other requests shall be referred to Research and Technology Div., Det. 4, Eglin AFB, FL.
AUTHORITY
AFATL ltr, 28 Oct 1975; AFATL ltr, 28 Oct 1975

THIS PAGE IS UNCLASSIFIED

CONFIDENTIAL

ATL-TR-65-35

(UNCLASSIFIED TITLE)

RADIALLY EXPANDING FRAGMENTATION WARHEAD STUDY

Second Summary Report (March 1965)

By

W. R. Porter, Martin Company

May 1965

This material contains information affecting the national defense of the United States within the meaning of the Espionage Laws (Title 18, U.S.C., sections 793 and 794), the transmission or revelation of which in any manner to an unauthorized person is prohibited by law.

Directorate of Armament Development
Det 4, Research and Technology Division
Air Force Systems Command
Eglin Air Force Base, Florida

GROUP-4
Downgraded at 3 year intervals;
Declassified after 12 years.

CONFIDENTIAL

Best
Available
Copy

(Unclassified Title)
RADIALLY EXPANDING FRAGMENTATION WARHEAD STUDY

Second Summary Report (March 1965)

By

W. R. Porter, Martin Company

(This page is Unclassified)

FOREWORD

This report is a summary of investigations completed during the period of April 1964 through January 1965 under contract AF08(635)-4263. In addition, it contains information resulting from a terminal series of experiments completed after the publication of summary report ATL-TDR-64-9 under contract No. AF08(635)-3269. These contracts were administered by Detachment-4, Weapons Division (ATWR), RTD, Eglin Air Force Base, Florida. Detachment-4 project engineer for these contracts was Mr. Edward C. Poston, Jr.

These research programs have been accomplished by the Martin Company, Orlando Division, Orlando, Florida. Martin Company task leader for the overall effort was Mr. W. R. Porter. Other contributing Martin personnel included Messrs S. J. Nicolosi, E. R. Caponi, B. van Zyl, W. H. Burch, D. R. Bragg, J. M. Allred, and T. D. Kitchin. This document was prepared by Mr. W. R. Porter under the direction of Mr. C. A. Borcher, Manager, Engineering Mechanics Research Laboratory.

Acknowledgement is made to Detachment-4 personnel Messrs D. M. Davis, E. C. Poston, Jr., and W. Dittrich for valuable technical consultation and guidance, as well as Captain W. C. Sodoma, A.P.G.C., for successful coordination of rocket sled feasibility demonstrations.

This technical report has been marked in accordance with the DoD Industrial Security Manual by the contractor.

This technical report has been reviewed and is approved.

David K. Dean

DAVID K. DEAN
Colonel, USAF
Chief, Weapons Division

(This abstract is classified confidential.)

ABSTRACT

This document reports on the experimental evolution and analytical confirmation of an explosive layered warhead design capable of projecting 14 layers of fragments into a slowly expanding radial pattern. Major accomplishments leading to the evolved design were:

1 The feasibility of projecting 14 fragment layers was demonstrated in three design variations - spiral cylinders, concentric ring hyperboloids, and spiral hyperboloids.

2 The feasibility of controlling fragment beam spray angles was demonstrated with massive end confinement, hyperboloid shaping, explosive end plates, and combinations of these.

3 The capability of a 14 fragment layer warhead model to meet performance goals under dynamic rocket sled test conditions was demonstrated.

The warhead design that progressed to rocket sled tests at Eglin Air Force Base is a hyperbolic configuration (for beam spray control), 10.75 inches in length and 9.75 inches in diameter, weighing 110 pounds. 30,000 one-quarter inch spherical fragments are projected radially by 3 pounds of sheet explosive. The charge to mass ratio is only 0.036, excluding two 1/2 inch thick steel end plates and a center steel mounting fixture. Single point initiation is effected by an external line wave generator affixed to the spiral wrapping of sheet explosive.

Fragment velocity distributions from static firing test were determined to range from less than 100 feet per second to 1000 feet per second with 90 percent of the velocities below 750 feet per second. 90 percent of the fragment impacts were within a 30 degree beam spray angle. Dynamic rocket sled test results showed uniform radial distributions with an average of 15 to 20 fragment hits per square foot over a radial distance of 20 feet. Warheads were detonated at rocket sled velocities of approximately 1300 feet per second.

In general, work accomplished during this program is discussed in this report in the sequence in which it was performed. The experimental program included study of various techniques of beam spray control, initia-

tion, and scaling effects as derived from static arena testing. The culminating point of the experimental program was the dynamic functional feasibility test. Concurrent with the experimental program, an analytical program, oriented toward predicting velocity performance of multilayered warheads, was conducted; the analytical program confirmed experimental results. The analytical effort employed a modified "Quasi-Wundy" computer code. This modification retained all the advantages of the NOL/White Oak computer program but permitted consideration of the effects of pressure losses resulting from gas venting at the ends of the warhead. Experience with this modification indicates that it can be extended to the consideration of added fragment layers, different fragment materials, differing explosive characteristics and differing design geometries.

Other sections of this report include detailed discussions of test arrangements and instrumentation techniques; data recording and reduction procedures, and methods employed in the fabrication of test models. (The appendix gives detailed design characteristics and test data for the 42 warhead models examined during this program.)

Finally, the conclusion is reported that as many as 14 fragment layers can be explosively projected, at controlled velocities, into uniformly distributed, radial expanding patterns. Recommendations are made for continued research that will result in a feasible hardware configuration ready for end item development.

TABLE OF CONTENTS

Section	Title	Page
Section 1. -	Introduction	1
Section 2. -	Experimental Investigations	3
	A. Approach	3
	B. Significant Results	5
	C. Test Arrangement and Instrumentation	27
	D. Data Reduction	33
	E. Model Fabrication Techniques	38
Section 3. -	Analysis	47
	A. Basic "Quasi Wundy"	47
	B. Limitations of "Quasi Wundy" and Venting Modifications	49
	C. Correlation with Experimental Data	53
Section 4. -	Conclusions	55
Section 5. -	Recommendations	57
References		59
Appendix 1. -	Detailed Data	61

LIST OF ILLUSTRATIONS

Figure	Title	Page
1.	Artist Concept of Hypothetical Space Intercept	2
2.	Experimental Program Flow Chart	4
3.	Cross Sections of Explosive Layered Concepts	5
4.	Inert Model Explosive Layered Warhead Design	6
5.	Full Scale Warhead Test Models	7
6.	Typical Recovery Target Impact Pattern for 14 Fragment Layered Test Model	8
7.	Radiographic Data of Fragment Velocity/Space Distribution for 14 Fragment Layered Test Model	10
8.	Recovery Target Velocity/Space Distribution for 14 Fragment Layered Test Model	12
9.	Warhead Test Model on Rocket Sled	13
10.	CZR Camera Record of Functional Feasibility Demonstration	14
11.	Witness Target Results After Detonation of 14 Fragment Layered Warhead, RE-19	15
12.	Witness Target Results After Detonation of 14 Fragment Layered Warhead, RE-20	16
13.	Design Configuration Beam Spray Achievements	18
14.	Test Model, L/D = 2, Hyperboloid Configuration	20
15.	Estimated Design Parameters for Multi-Layered Hyperboloid Designs	22
16.	Inert Test Model and Sled Mounting Fixture	24
17.	Inert Test Model on Centrifuge Arm	24
18.	CZR Camera Record of Inert Model Sled Test	26
19.	Typical Test Arrangement	27
20.	Penetration vs. Velocity Calibration Curve	28

LIST OF ILLUSTRATIONS (CONTINUED)

Figure	Title	Page
21.	Flash Radiographic Test Arrangement	29
22.	Flash Radiographic Record of RE-23 (14 Layers of Nickel Fragments)	31
23.	Opaque Light Box	32
24.	Typical Eglin Sled Test Arrangement	34
25.	Sled Test Witness Target	35
26.	Typical Polar Plot of Six Layered Test Model	37
27.	Fragment Packaging Techniques	39
28.	Partial Fabrication Test Model RE-14	40
29.	Partial Fabrication Test Model RE-12 (Fragments Encapsulated in Silicon Rubber)	41
30.	Time-Temperature History of Inert Filler Curing Process	42
31.	Test Model Tooling Fixture with Model RE-15 Partially Fabricated	44
32.	Mounting Fixture Assembly	44
33.	Radial Expansion of Fragments	50
34.	Linear Expansion of Detonation Products	51
35.	Pressure-Time History of Detonation	51
36.	Experimental vs. Predicted Fragment Velocities	52

LIST OF ILLUSTRATIONS, APPENDIX 1

Figure	Title	Page
37.	Test Model Design, Round 90	63
38.	Test Model Design, Round 91	64
39.	Test Model Design, Round 93	65
40.	Test Model Design, Rounds 94 and 95	67
41.	Impact Pattern, Round 95	68
42.	Velocity vs. Radial Distribution, Round 95	69

LIST OF ILLUSTRATIONS, APPENDIX 1 (CONTINUED)

Figure	Title	Page
43.	Test Model Design, Round 96	70
44.	Test Model Design, Rounds 98 and 99	72
45.	Impact Pattern, Round 99	73
46.	Test Model Design, Rounds 100 and 101	74
47.	Impact Pattern, Round 101	75
48.	Test Model Design, Rounds 102 and 103	77
49.	Flash Radiography of Test, Round 102	78
50.	Impact Pattern, Round 103	79
51.	Velocity vs. Radial Distribution, Round 103	80
52.	Test Model Design, Round 104	81
53.	Test Model Design, Rounds 105 and 106	82
54.	Impact Pattern, Round 105	83
55.	Velocity vs. Radial Distribution, Round 106	85
56.	Test Model Design, Round 107	86
57.	Test Model Design, Round 108	87
58.	Impact Pattern, Round 108	88
59.	Test Model Design, Round 109	89
60.	Velocity vs. Radial Distribution, Round 109	90
61.	Impact Pattern, Round 109	91
62.	Test Model Design, Round RE-1	93
63.	Impact Pattern, Round RE-1	94
64.	Test Model Design, Round RE-2	95
65.	Impact Pattern, Round RE-2	96
66.	Test Model Design, Round RE-3	97
67.	Impact Pattern, Round RE-3	98
68.	Test Model Design, Round RE-4	100

LIST OF ILLUSTRATIONS, APPENDIX 1 (CONTINUED)

Figure	Title	Page
69.	Impact Pattern, Round RE-4	101
70.	Test Model Design, Round RE-5	102
71.	Impact Pattern, Round RE-5	103
72.	Velocity vs. Radial Distribution, Round RE-5	104
73.	Test Model Design, Round RE-6	105
74.	Test Model Design, Round RE-7	106
75.	Impact Pattern, Round RE-7	107
76.	Test Model Design, Round RE-8	109
77.	Test Model Design, Rounds RE-9 and RE-10	110
78.	Test Model Design, Round RE-11	111
79.	Test Model Design, Round RE-12	113
80.	Test Model Design, Round RE-13	114
81.	Test Model Design, Round RE-14	115
82.	Impact Pattern, Round RE-14	116
83.	Test Model Design, Round RE-15	118
84.	Velocity vs. Radial Distribution, Round RE-15	119
85.	Test Model Design, Round RE-16	120
86.	Test Model Design, Round RE-17	121
87.	Test Model Design, Round RE-17	122
88.	Warhead Test Model RE-17	123
89.	Impact Pattern, Round RE-17	124
90.	Velocity vs. Radial Distribution, Round RE-18	125
91.	Test Model Design, Round RE-21	127
92.	Test Model Design, Round RE-22	129

LIST OF TABLES

Table No.	Title	Page
1.	Beam Spray Control Technique Comparison	17
2.	Rocket Sled Time-Velocity History	25
3.	Explosive Characteristics DuPont DetaSheet C	39

SECTION 1 - INTRODUCTION

Experimental and analytical research on the Radially Expanding Fragmentation Warhead was initiated for the Air Force in November 1962 under contract no. AF08(635)3269. Prime objective of this contract, as illustrated conceptually by Figure 1, was to examine various means of explosively projecting multi-layers of fragments into a slowly expanding, uniform radial pattern. The most significant results of this initial effort included:

1 Establishing the feasibility of explosively projecting multiple layers of fragments (four, six, and eight) into radially expanding patterns by a warhead design concept utilizing alternate layers of fragments and sheet PETN explosive;

2 Establishing the feasibility of controlling fragment radial velocities to obtain uniform growth patterns by varying the gage thickness of explosive between fragment layers.

3 Achieving desired pattern and velocity distributions for charge to metal ratios of 0.080 and less.

4 Devising a semi-empirical analytical technique to assist in the selection of warhead design parameters and prediction of velocity performance.

5 Defining specific areas for further performance improvement.

Other details pertinent to the research accomplishments under contract AF 08(635)3269 are set forth in Air Force Technical Documentary Report No. ATL-TDR-64-9, Reference 1.

Prime objective of the program to be accomplished under contract AF 08(635)4263, and as defined by Reference 2, was early exploitation of the explosive layered warhead design concept to:

1 Project added fragment layers (14 or more) into uniform radial distribution patterns with diametric growth rates of between 500 and 1000 feet/second;

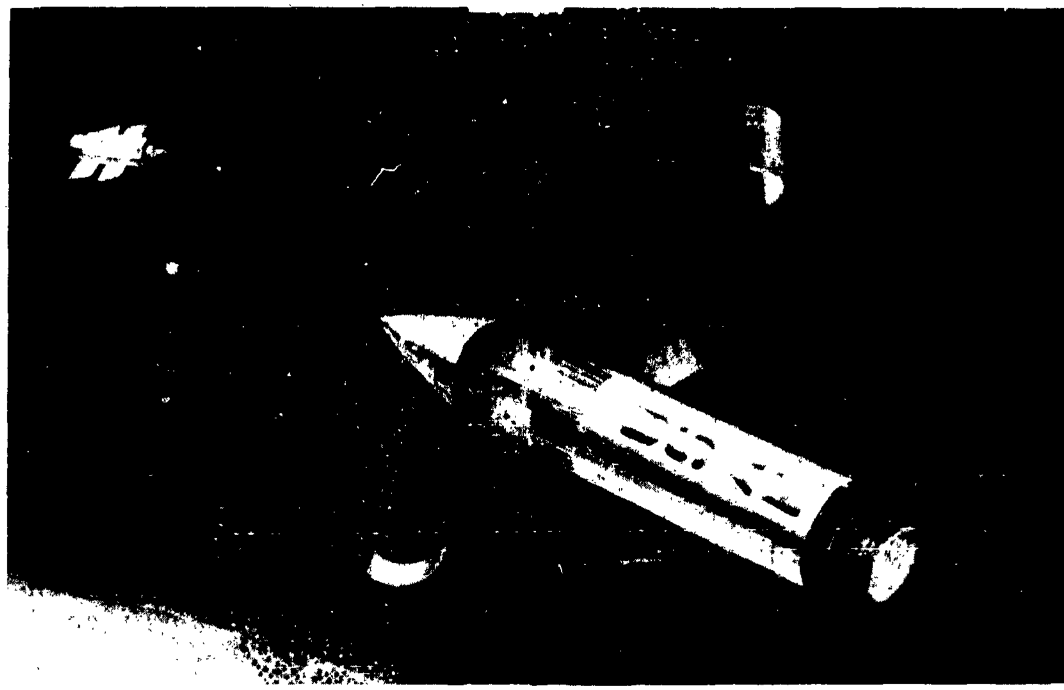

Figure 1. Artist Concept of Hypothetical Space Intercept

2 Investigate alternate means of controlling fragment beam spray angles without adding excessive warhead parasitic weight;

3 Determine practical means of initiating thin explosive layers;

4 Determine the scaling effects of different fragment materials, shapes, and sizes, as well as the effects of length to diameter and charge to mass ratios.

5 Establish more practical means of fabricating test models;

6 Demonstrate dynamically on Eglin rocket sled facilities the functional feasibility of the Explosive Layered Warhead Concept to project 14 or more layers of fragments into slowly expanding, uniform radial distribution patterns.

This report summarizes achievements in each of the above major areas of investigation and discusses in detail items such as significant results, test arrangements and instrumentation, rocket sled feasibility demonstrations, test model fabrication techniques, analytical procedures, and gives complete data on the various model designs tested toward exploiting the Explosive Layered Warhead design concept.

SECTION 2 - EXPERIMENTAL PROGRAM

This section summarizes the experimental portion of the Radially Expanding Fragmentation Warhead Study. It discusses the approach followed, sets forth significant accomplishments, describes techniques employed in the collection and reduction of data, and discloses fabrication procedures. Detailed data pertinent to each test are included in Appendix 1 of this report.

A. APPROACH

The general approach followed throughout the experimental program is outlined in flow chart form in Figure 2. Experimentation progressed on the basis of first sampling in each major investigatory area and then proceeded down the most appropriate series networks. As preliminary results showed promise, effort was diverted from the more complex work areas and oriented toward the ultimate objective of successfully projecting 14 layers of fragments into controlled radial distribution patterns.

Experimentation was initiated with two major variations of the Explosive Layered Concept - that of a concentric ring design and that of a spiral wrap configuration (Figure 3). Following the planned program and evolving from experimental results, the most promising of these variations (spiral wrapping) was continued into the demonstration model development phase and the culminating dynamic functional feasibility demonstrations.

All warhead models were tested in an arena using a Celotex recovery target to collect fragments from a sampling sector of the warhead. For most models tested, fragments in this sector were marked in order that their velocity and trajectory could be correlated with their location in the warhead. However, as the number of fragment layers was increased and angular beam spray reduced, the multiplicity of fragment impacts in a small target area destroyed the first layers of Celotex and negated any reasonable correlation of fragment recovery with their location in the original test model. Hence, flash x-ray radiographic techniques were employed to provide more precise measurements of fragment velocities and to confirm uniformity of the radial distribution patterns.

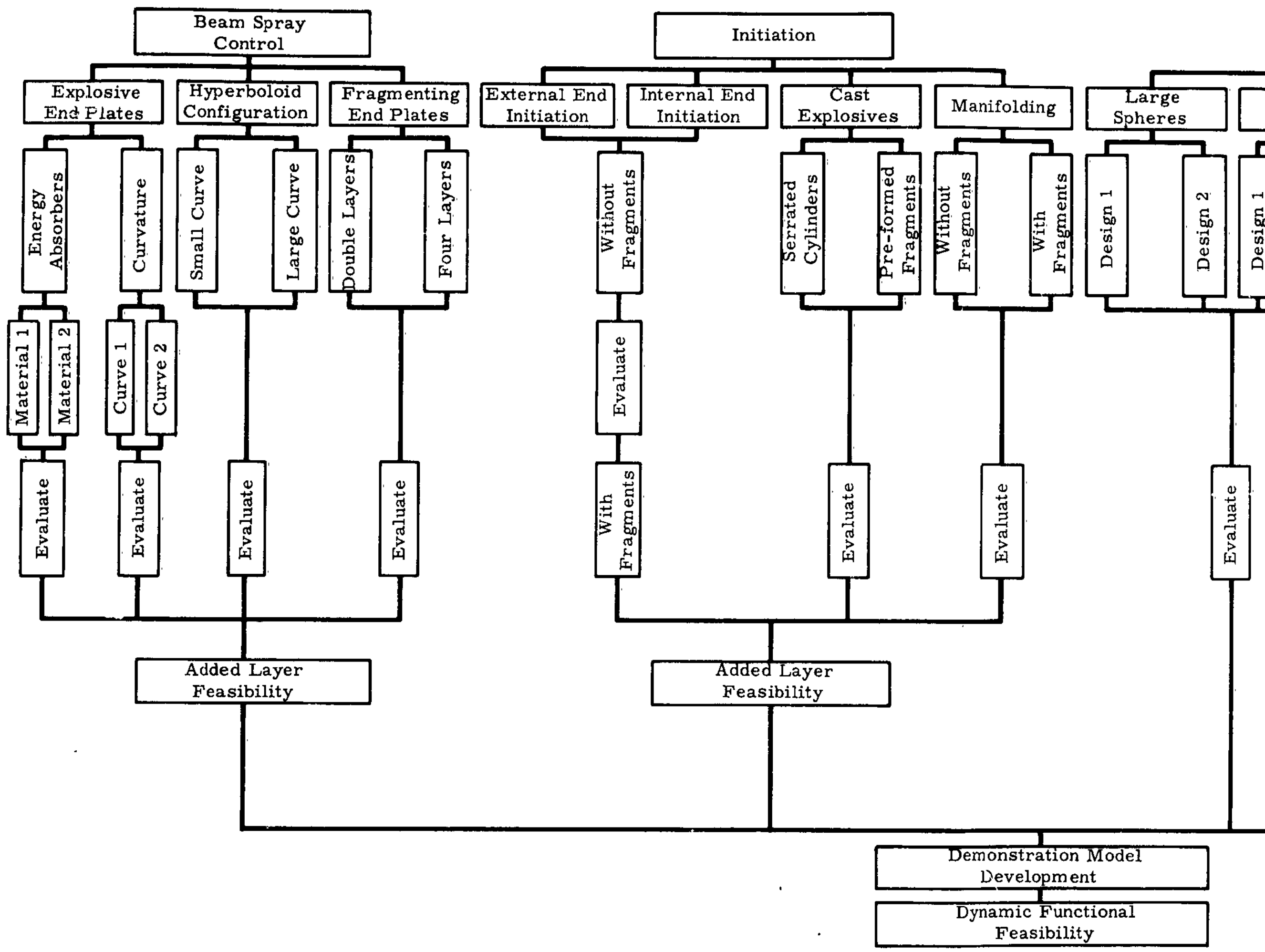

Figure 2. Experimental Program Flo

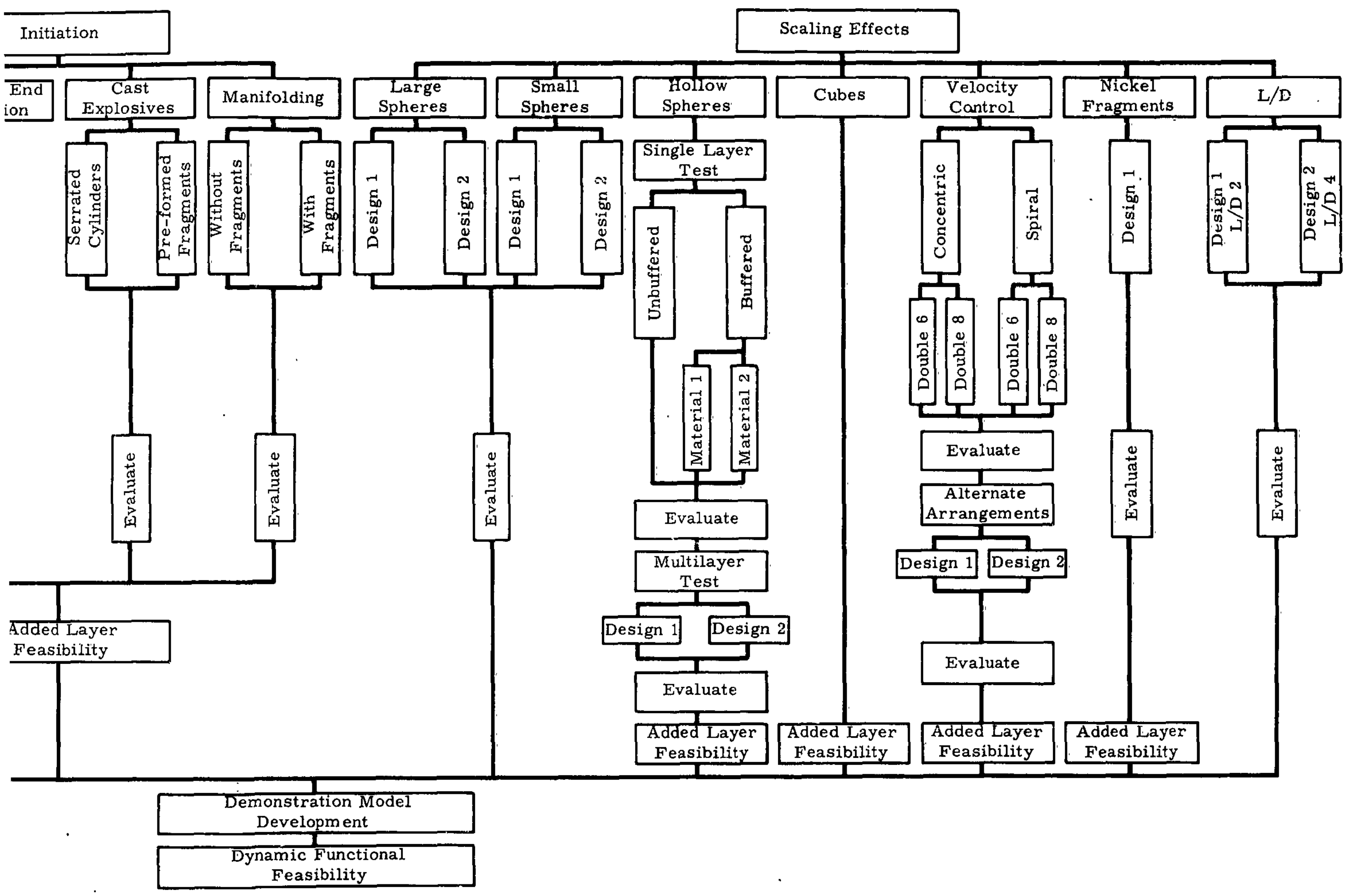

Figure 2. Experimental Program Flow Chart

2

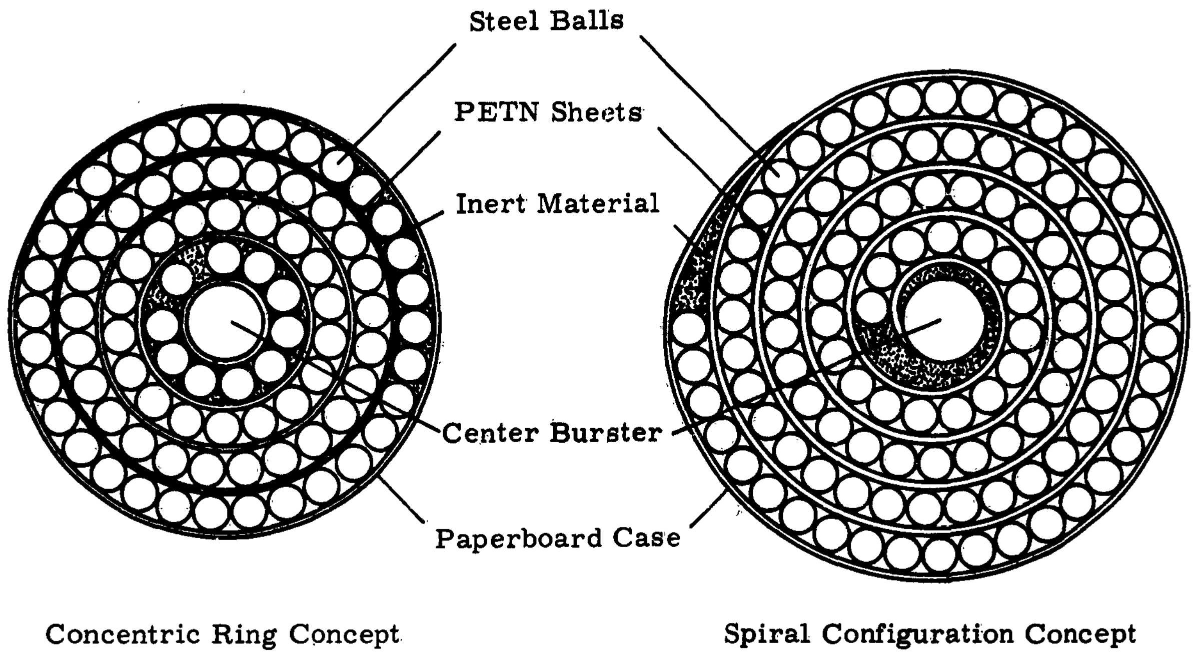

Figure 3. Cross Sections of Explosive Layered Concepts

B. SIGNIFICANT RESULTS

This research program has resulted in the evolution of an Explosive Layered Warhead design capable of projecting 14 layers of fragments into a slowly expanding, uniform, radial pattern. Figure 4, a 1/2 scale sectionalized inert model, illustrates the warhead's general design characteristics, which include:

1 A hyperbolic shape for beam spray control,

2 A 10.75 inch length by 9.75 inch diameter,

3 A total weight of 110 pounds,

4 30,000 one-quarter inch steel fragments,

5 3 pounds of sheet PETN explosive,

6 An external line wave generator to permit single point initiation,

7 A charge to mass ratio of only 0.036, exclusive of two 1/2 inch thick steel end plates and a center steel mounting fixture.

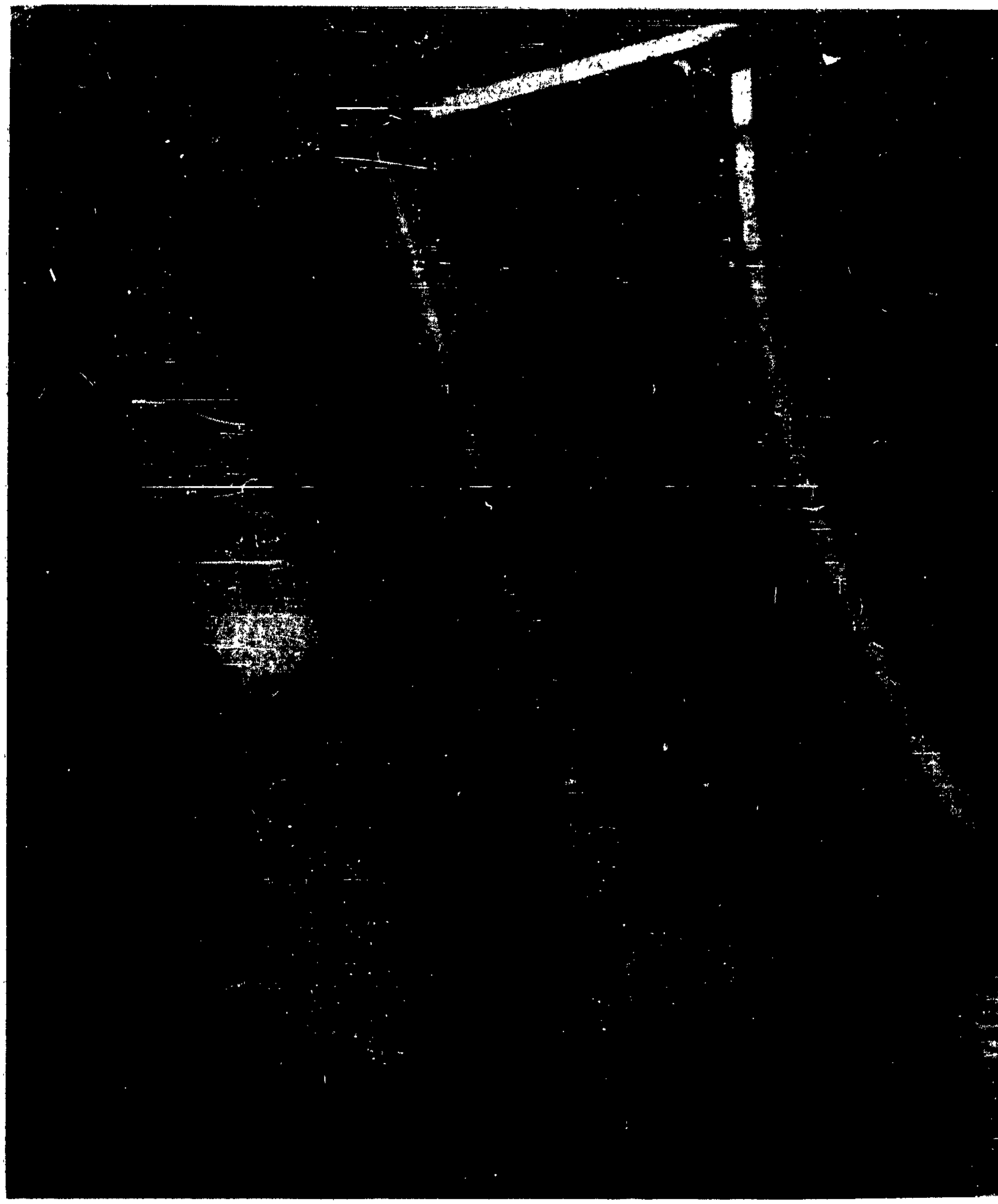

Figure 4. Inert Model Explosive Layered Warhead Design

Two full scale test models incorporating these design characteristics are shown in Figure 5.

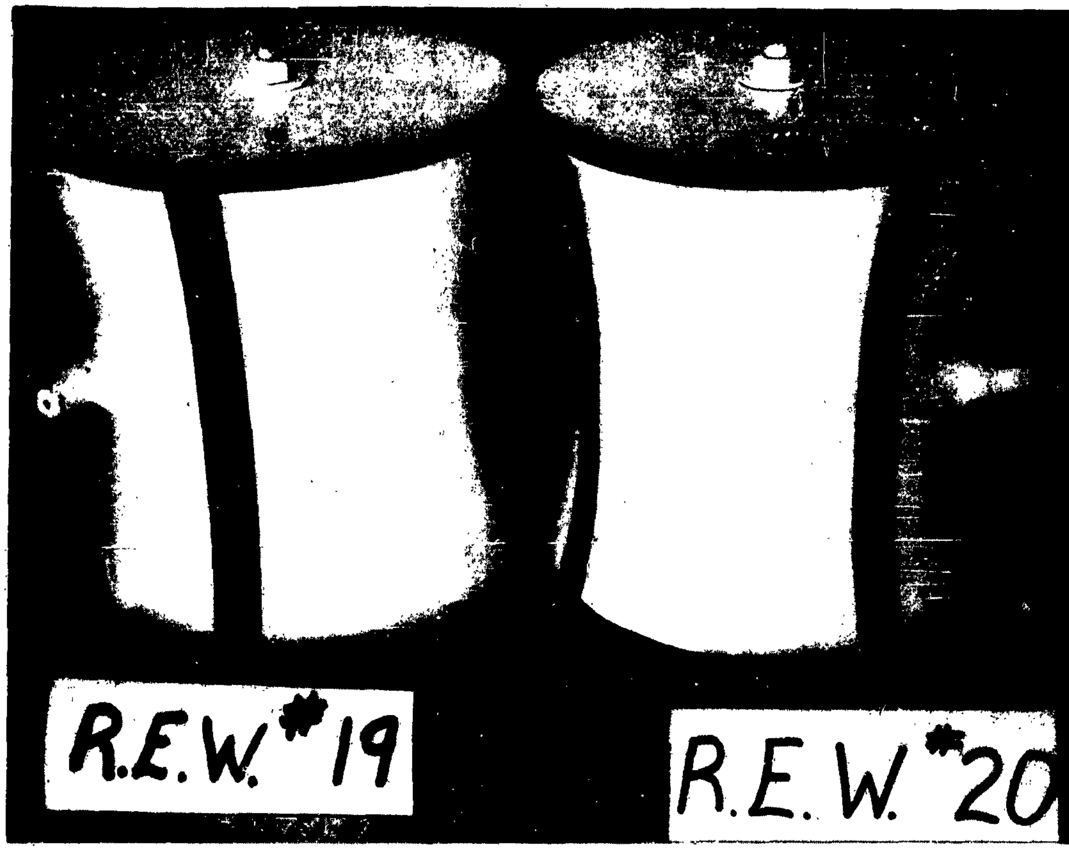

Figure 5. Full Scale Warhead Test Models

Performance capabilities of this design as determined from static arena test are:

1 Fragment velocity distributions from less than 100 to 1000 feet per second, with 90 percent of the fragments at velocities below 750 feet per second;

2 90 percent of fragment impacts within a 30 degree beam spray angle (Figure 6).

Figures 7 and 8 provide experimental evidence as to the design's ability to achieve the reported velocity/space distributions. Figure 7 is a flash radiographic mosaic of the fragment pattern formation from a sample section of one such warhead test, and Figure 8 is a similar presentation

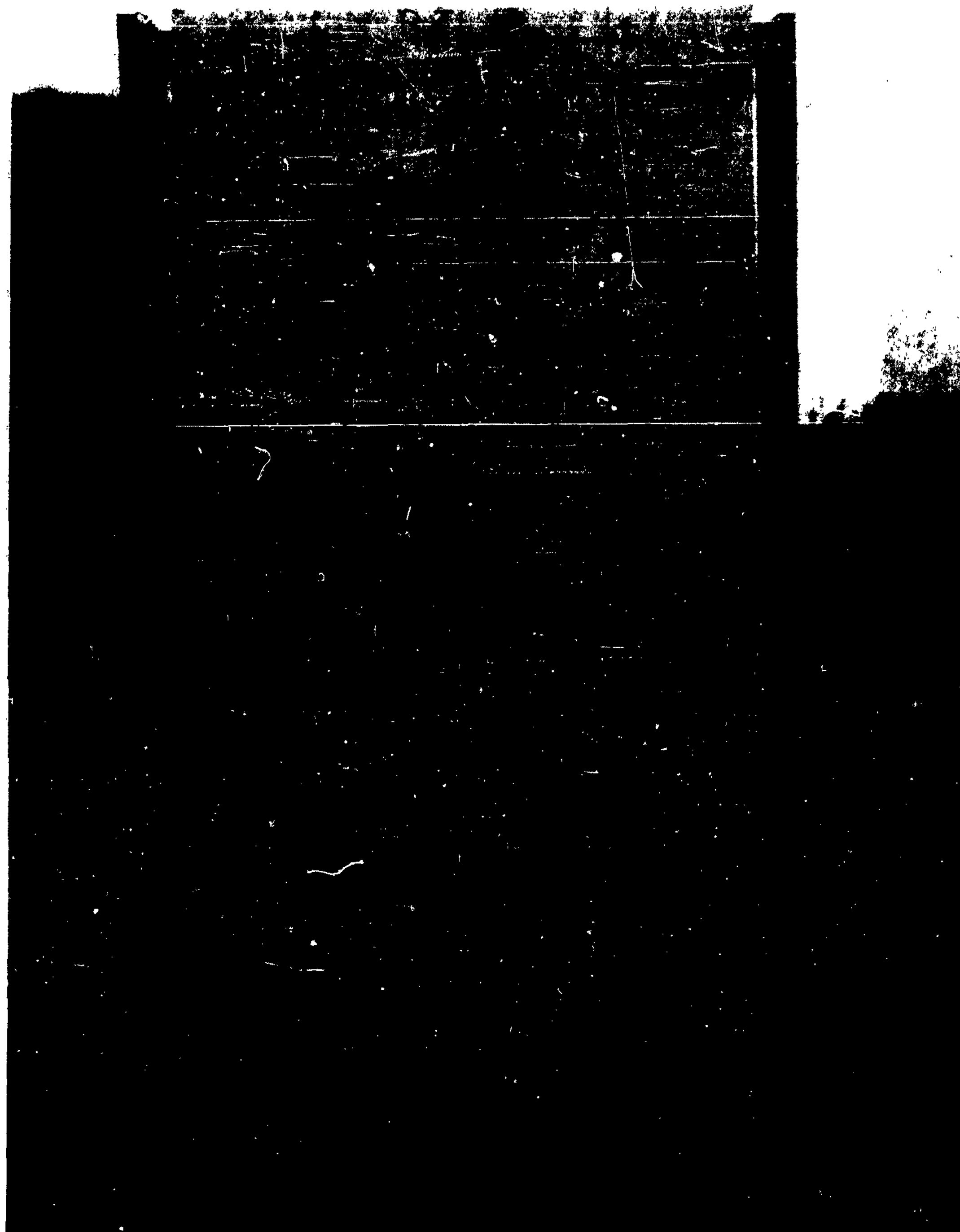

Figure 6. Typical Recovery Target Impact Pattern for 14 Fragment Layered Test Model

derived from fragment recovery data.* Both of these presentations show how the fragments' distributions would appear to an observer viewing the pattern formation, at a given instant in time, down the warhead's longitudinal axis.

In addition, the warhead's ability to function under dynamic conditions has been demonstrated through rocket sled testing (Figures 9 and 10). On two successive trials the warhead successfully detonated at sled velocities of approximately 1300 feet per second and created uniform radial distribution patterns with an average of 15 to 20 fragment hits per square foot on a witness target located forward of the warhead's point of detonation. Figure 11 shows the results of the first firing trial and Figure 12 shows the fragment distributions achieved on a strengthened target.

Further detailed discussion of results recorded during the experimental portion of this program as applicable to each major work area - beam spray control, initiation, scaling, projection of added fragment layers, and dynamic feasibility demonstrations - is given in subsequent paragraphs.

* Although this figure shows fragments grouped in distinct bands, it is emphasized that this effect is exaggerated because of the multiplicity of fragment hits within the same area and the accuracy with which fragment penetration can be related to impact velocity. The radiograph of Figure 7 confirms this observation.

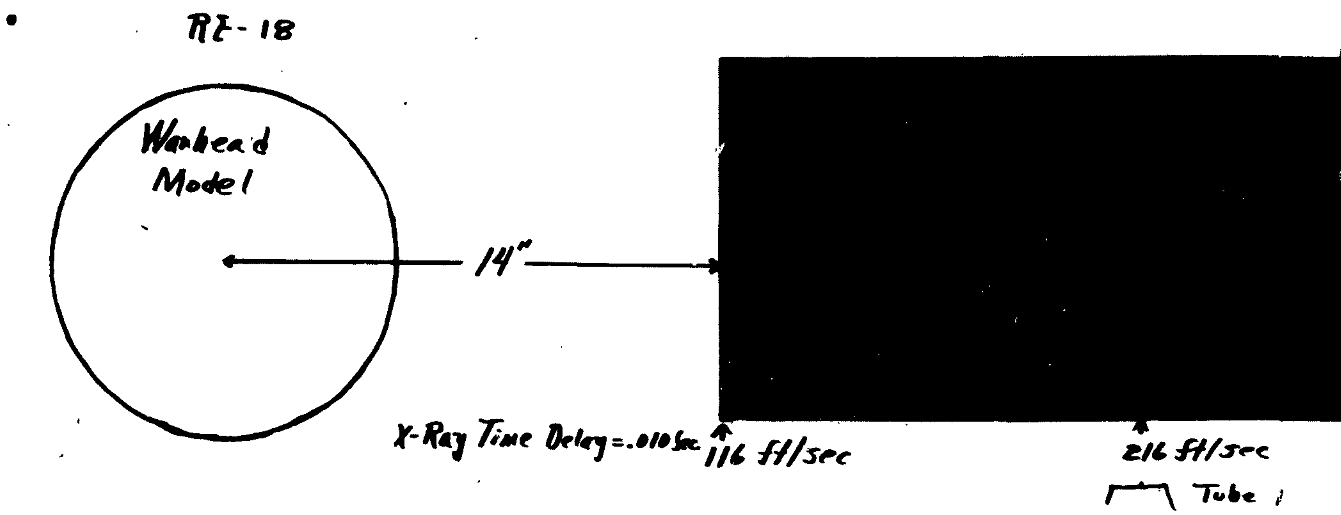

Figure 7. Radiographic Data of Fragment Veloc
14 Fragment Layered Test M

diographic Data of Fragment Velocity/Space Distribution for
14 Fragment Layered Test Model

616 ft/sec
Tube

81(

Figure 7 (Con

816 ft/sec 866 ft/sec 933 ft/sec

Tube 4 Tube 5

Figure 7 (Cont)

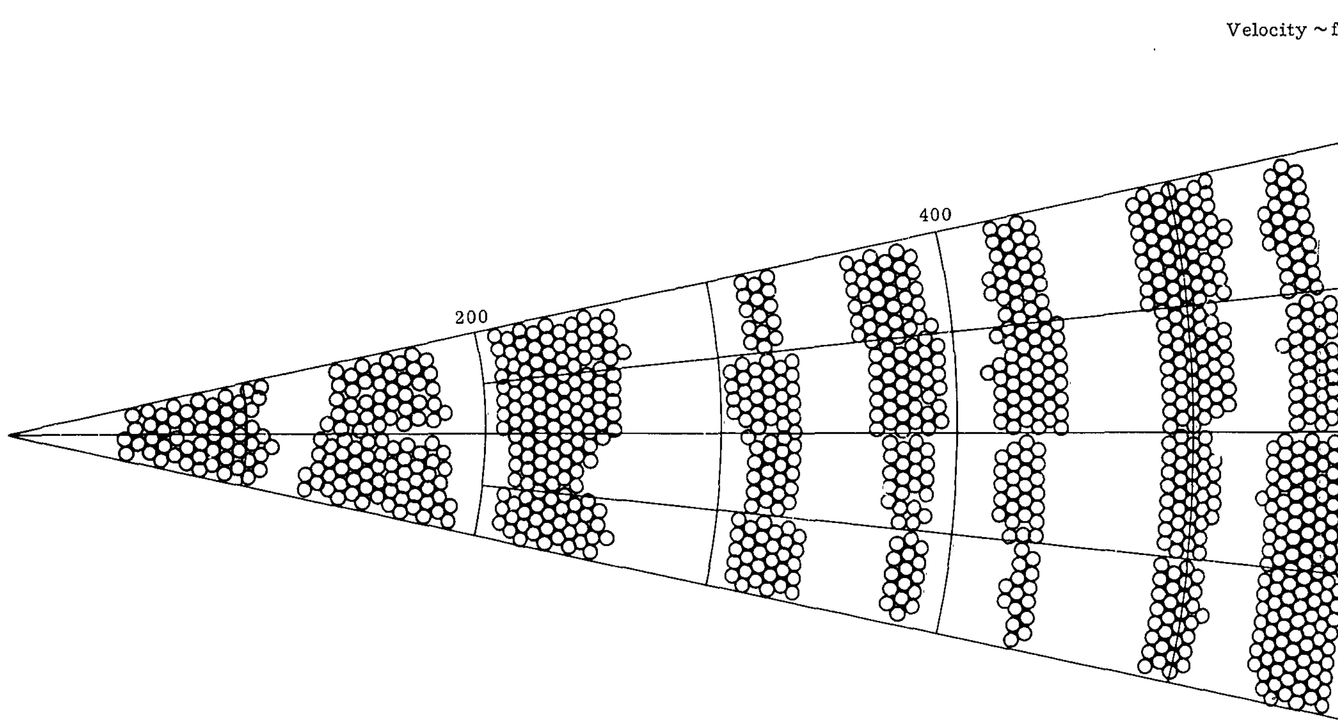

Note: Apparent banding of fragments results from multiplicity of hits within same area and accuracy with which recovery can be related to impact velocity.

Figure 8. Recovery Target Velocity/Space
Layered Test Mo

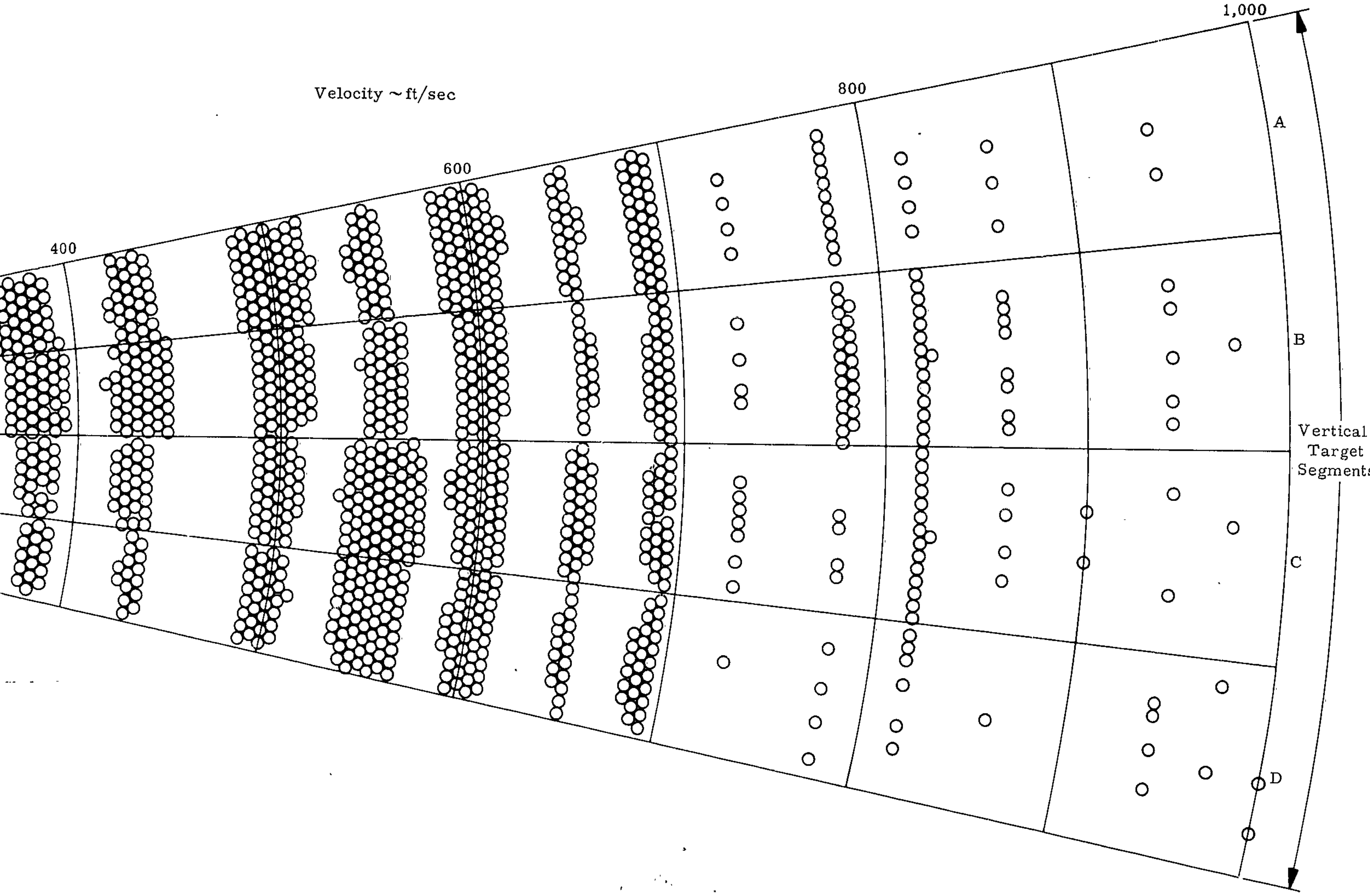

Recovery Target Velocity/Space Distribution for 14 Fragment Layered Test Model

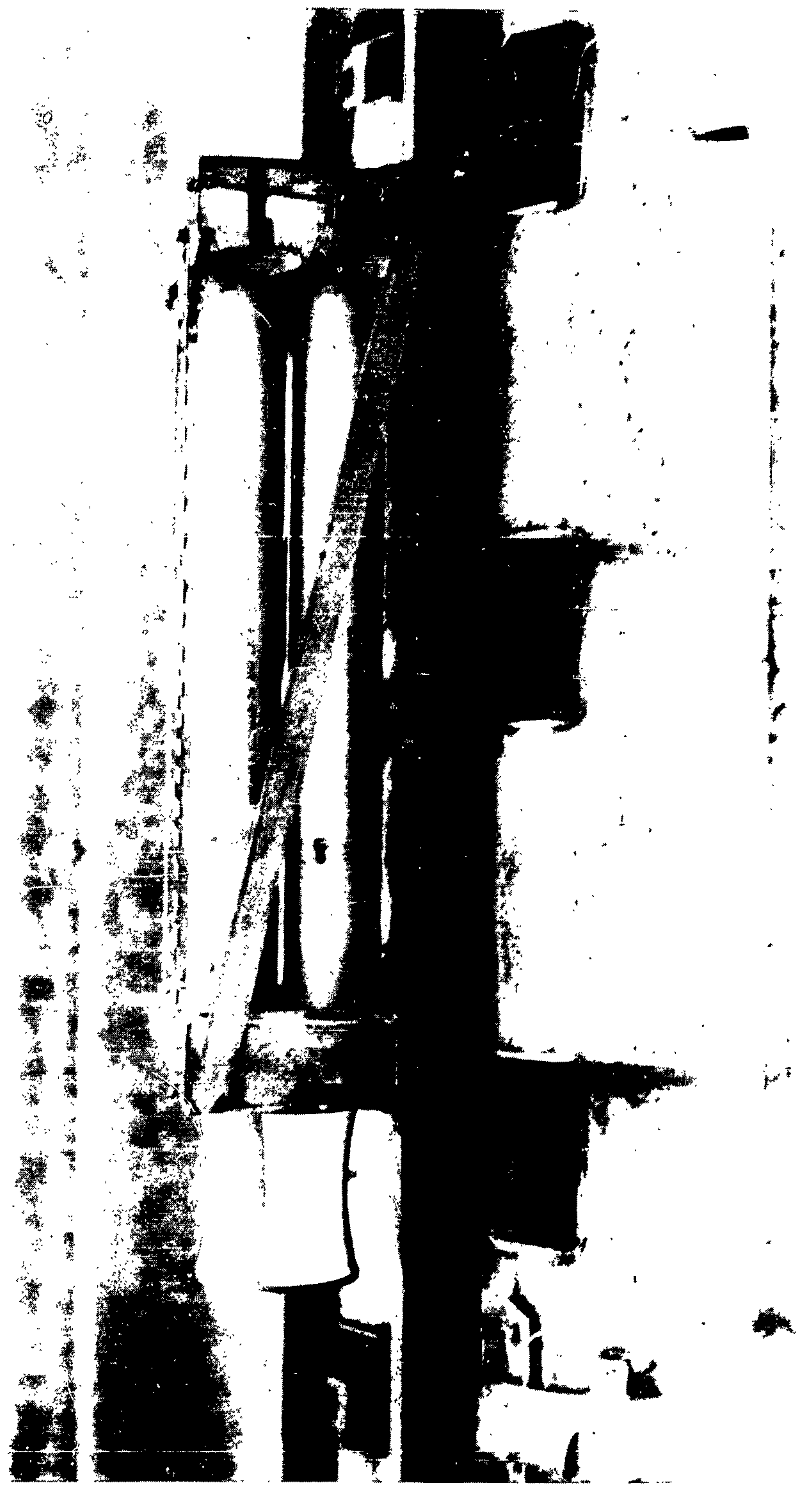

Figure 9. Warhead Test Model on Rocket Sled

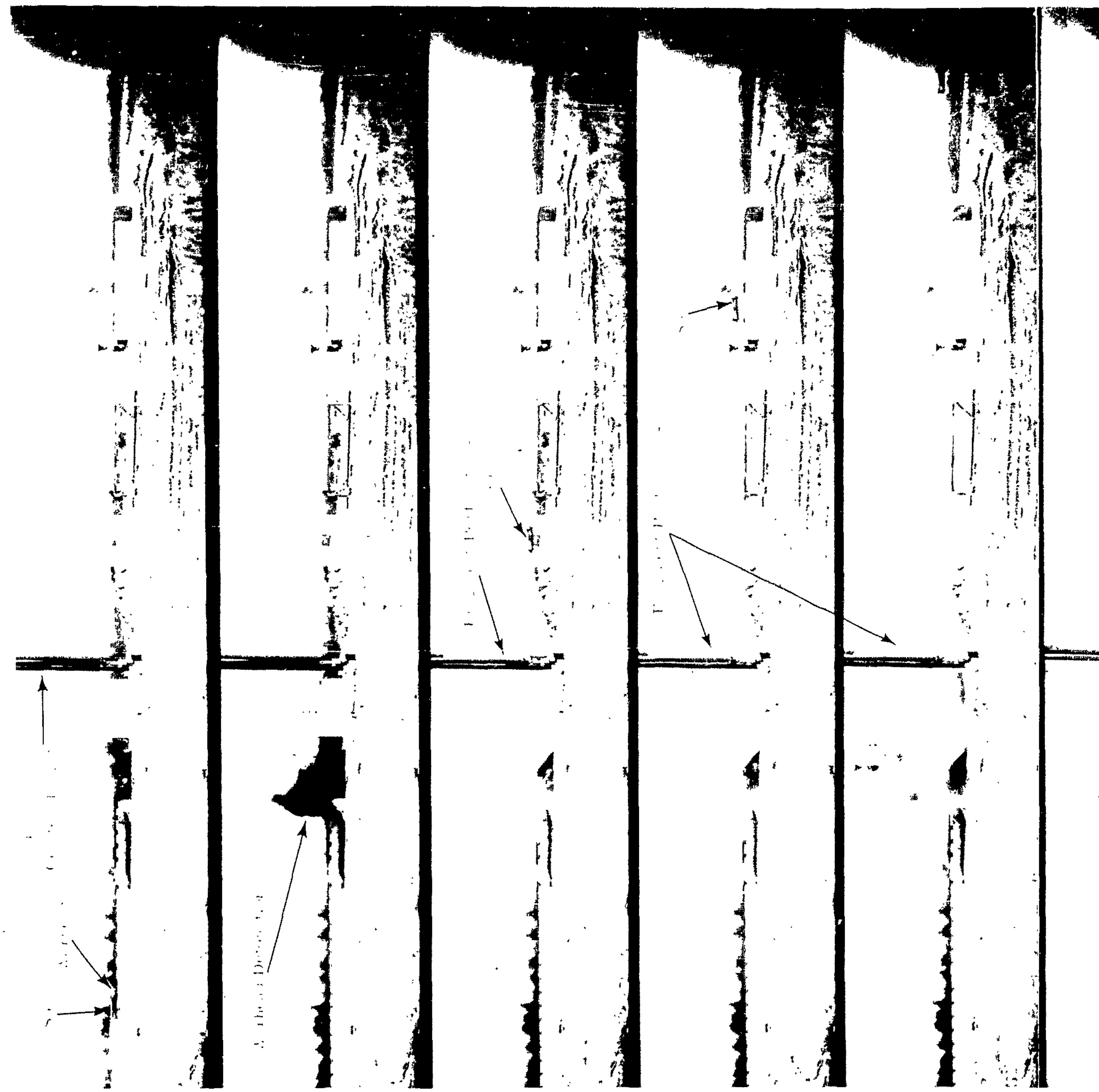

Figure 10. CZR Camera Record of Functional F

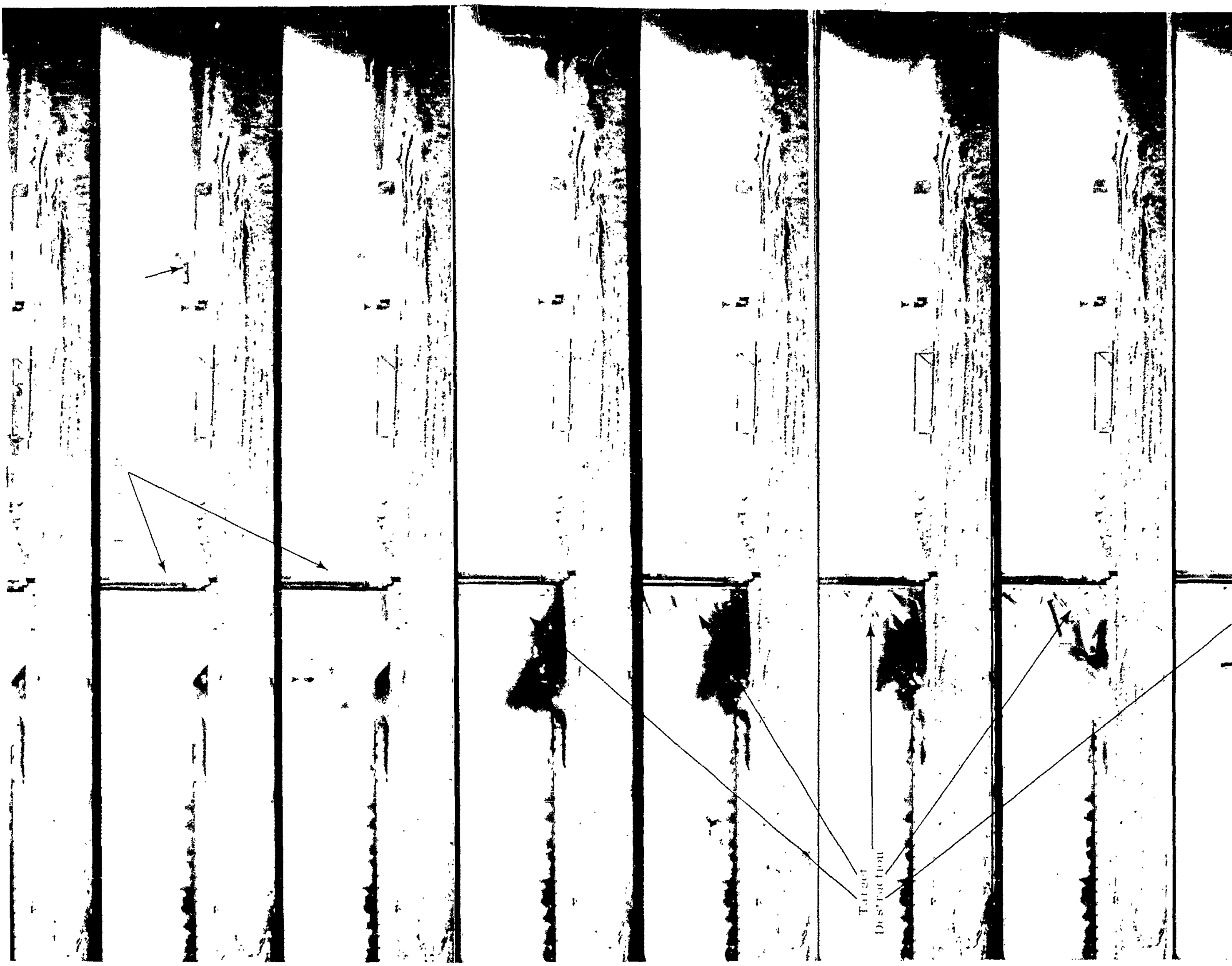

Figure 10. CZR Camera Record of Functional Feasibility Demonstration

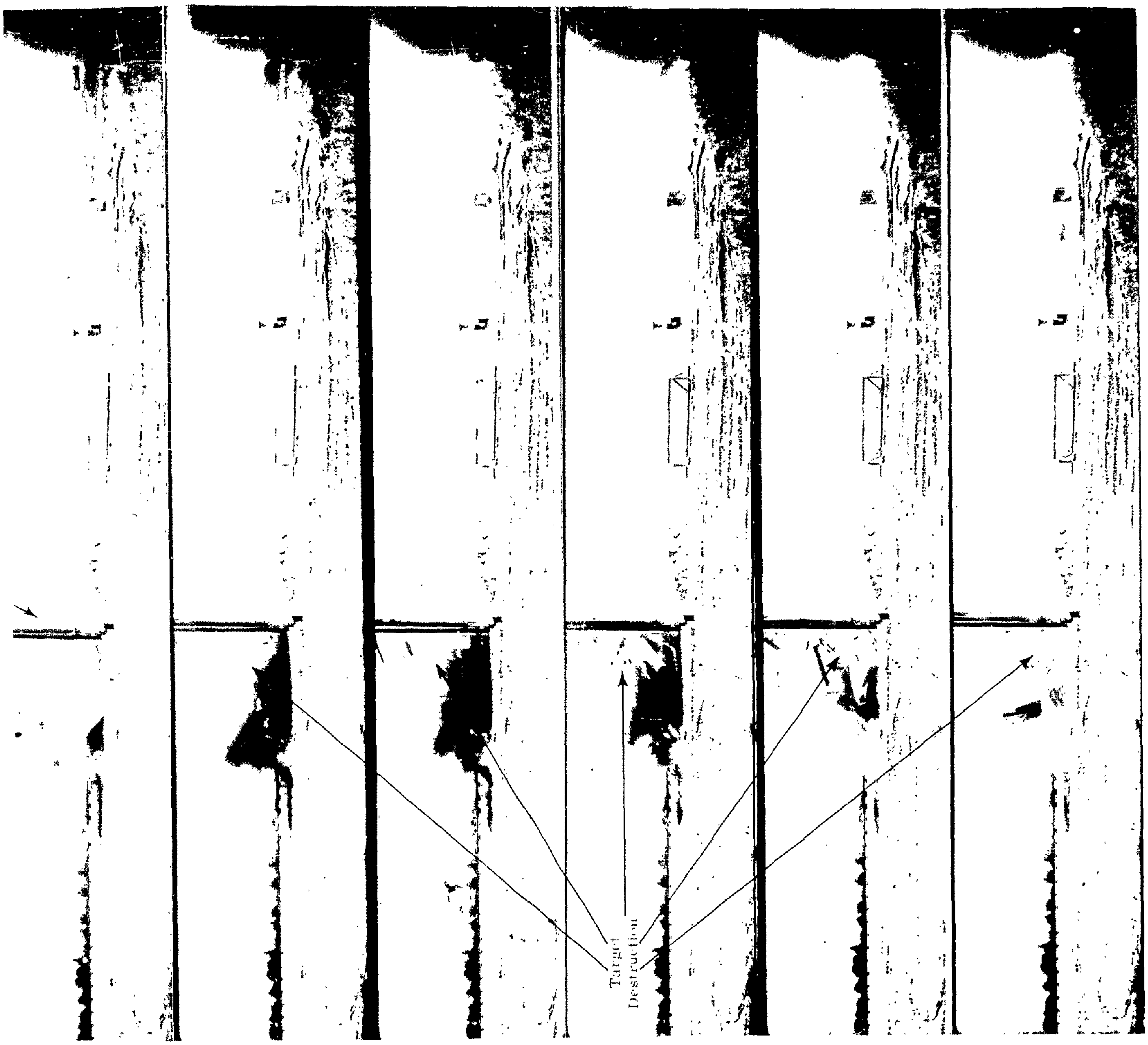

ecord of Functional Feasibility Demonstration

3

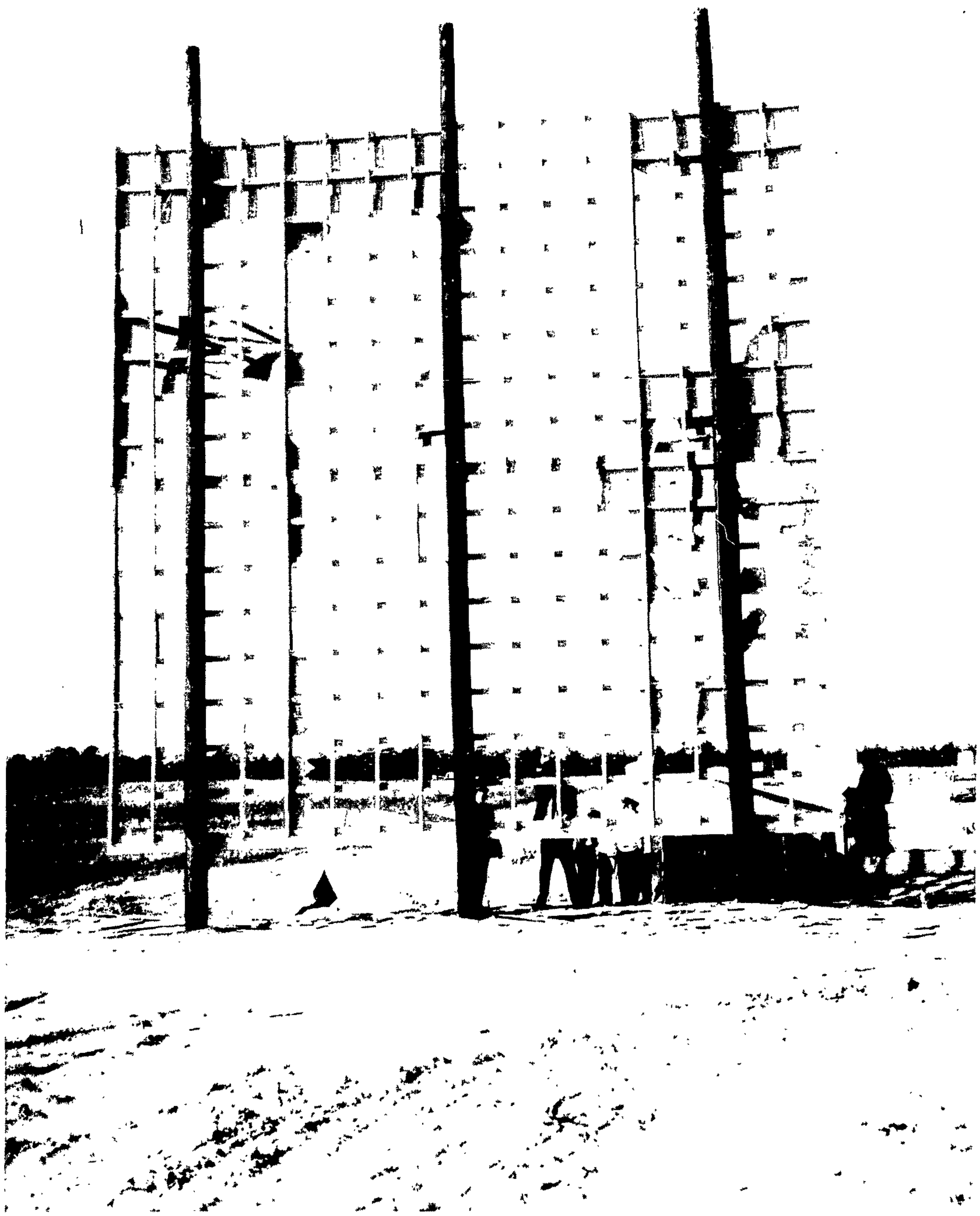

Figure 11. Witness Target Results After Detonation of 14 Fragment Layered Warhead, RE-19

Figure 12. Witness Target Results After Detonation of
14 Fragment Layered Warhead, RE-20

1. BEAM SPRAY CONTROL

Data resulting from this program show that techniques such as massive end plates, fragmenting end plates, explosive end plates, configuration shaping, and combinations of these are all effective in controlling fragment beam spray angles. Table 1 summarizes the control potential as well as advantages and disadvantages of the various techniques considered, and Figure 13 graphically depicts beam spray control achievements of the various designs.

Based on the information presented in the above referenced table, a beam spray control technique incorporating hyperboloid configuration shaping and 1/2 inch thick steel end plates was selected for the development of final feasibility demonstration models. This technique was selected because it provided a narrow beam spray angle (90 percent fragments within 30 degrees),

TABLE 1 - BEAM SPRAY CONTROL TECHNIQUE COMPARISON

TECHNIQUE	CONTROL POTENTIAL	ADVANTAGES	DISADVANTAGES
Massive end plates (1" thick) and cylindrical design configurations	35° maximum spray angle for 6, 8 and 10 fragment layers (Ref. 1 and Test Model 106, Appendix 1.) 75% fragment hits within 25° for 14 fragment layers. (Test Model RE-1, Appendix 1)	Simplified fabrication; structural capability to withstand dynamic loadings; structural compatibility with cantilever mounting or orientation systems. Compatible with single and dual initiation techniques.	Excessive parasitic weight.
Fragmenting end plates (1" thick) and cylindrical design configurations	Same order of beam spray control as with solid steel end plates. (Test Model RE-7, Appendix 1)	Reduced parasitic weight; efficient utilization of allowable metal weight; increased fragment density in center of expanding disc; structural compatibility with cantilever mounting techniques. Compatible with single and dual initiation techniques.	Slight fabrication complexity.
Hyperboloid shaping and 1/2" thick steel end plates	12 to 20 degrees for fragment layers depending upon design curvature (Test Models 94, 95, 102, 103 and RE-2; Appendix 1).	More effective control than achievable with cylindrical configuration; structural compatibility with dynamic loading and system mounting fixtures; compatible with single or dual initiation techniques.	Parasitic weight.
Hyperboloid shaping and fragmenting end plates	Approximately same degree of control as above hyperboloid designs (Test Models, 108, RE-14, and RE-15; Appendix 1)	All advantages of above hyperboloid design plus more efficient utilization of allowable weight and a means of increasing fragment density in center of expanding disc.	Slight fabrication complexity.
Hyperboloid shaping and explosive end plates	Provides essentially the same degree of control as other techniques: 87% fragments within 12° for 4 layer design; 83% fragments within 20° for 8 layer design; 84% fragments within 30° for 13 layer design (Test Models 107, RE-3 and RE-8; Appendix 1).	Minimum parasitic weight; provides means of initiating all explosive layers in concentric ring designs.	Requires dual initiation points. Appears to be incompatible with spiral design models. May require additional structure for compatibility with dynamic loading and mounting fixtures.

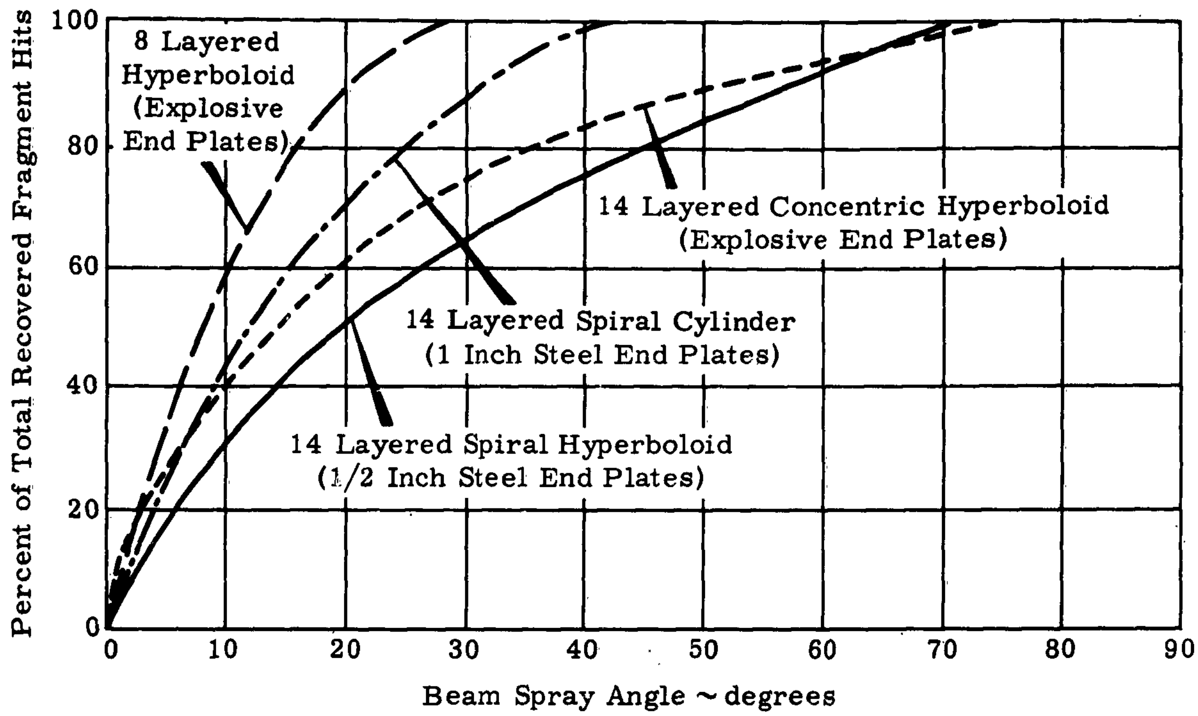

Figure 13. Design Configuration Beam Spray Achievements

and was compatible with other pertinent design consideration such as spiral explosive layering,* single point initiation, and minimization of parasitic weight. The same degree of beam spray control was achieved with both spiral and concentric ring designs. However, the spiral design provided the potential for evolving a warhead model capable of better meeting dynamic structural requirement.

Solid steel end plates were selected for this design simply to expedite model fabrication and to ensure sufficient structural integrity for the dynamic sled test. For future development, replacement of the solid steel end plates with fragmenting end plates will reduce parasitic weight of the overall warhead and provide more effective fragments in the center of the expanding radial fragment pattern.

* Spiral design concept was selected because of its convenient adaptability to the projection of added fragment layers (Paragraph 4).

2. INITIATION

Following completion of the initial summary report (Reference 1) and progressing toward the goal of achieving reduced fragment velocities, difficulties were encountered in obtaining complete detonation of thin gaged sheet explosive (0.042 and 0.025 inch thicknesses) in six and eight layered test model designs (numbers 90, 91, 92, 93, 97; Appendix 1). Initially this difficulty was attributed to unreliable initiation of the thinner gaged sheet explosive since it had never been observed with 0.084 inch thick explosive in either the spiral or concentric ring design configurations.

Subsequent experimentation with sheet explosive in flat continuous strips and spiral wrapped packages, without fragments, revealed that initiation was being accomplished and that incomplete detonation was most likely resulting from other causes, possibly fabrication procedures or the design concept itself.

Precautions such as the use of special explosive adhesives and reinforced taping procedures at each explosive splice were evaluated. Nevertheless, incomplete detonations were still observed.

Simultaneous with the incomplete detonation observations, attempts were initiated to eliminate any tendency for the spiral designs to create voids in the center of the expanding fragment package. Implementation of this objective was simply the removal of center explosive burster charges, the void of which was to be subsequently filled with a center mounting spindle or fragments. Upon filling this center void with fragments, complete detonations of the thin gaged explosive were thereafter achieved (Test Models 104, 105, 106, 109; Appendix 1). Hence, it is reasoned that the absence of structure within the center of externally initiated spiral designs permitted shock and pressure waves to separate explosive splices and prevent complete detonations.

For concentric ring designs, wherein a central explosive burster is always used, no difficulties were encountered in achieving complete detonation with 0.084 inch thick explosive through as many as eight fragment layers. However, when the thinner gaged explosives were employed complete detonation was not achieved beyond six fragment layers. This possibility had been anticipated with the ultimate solution of incorporating a manifolding initiation technique.

Problem resolution was quite simple and resulted as a by-product of the explosive end plate beam spray control experiments. By insuring that the explosive end plate discs were in intimate contact and secure (explosive adhesive) with each concentric ring of explosive, a simple manifolding technique was derived and complete detonation of multiple concentric explosive layers was achieved (Test Models 107, RE-3, RE-8, RE-14, RE-15; Appendix 1).

3. SCALING

Scaling experiments included investigations into overall configuration length to diameter ratio effects, alternate arrangements of fragment and explosive layering, as well as effects of fragment material, size, and shapes. Results of these investigations are summarized accordingly in the following paragraphs.

a. Length to Diameter Ratio - For six fragment layered hyperboloid concentric ring designs, Figure 14, increasing the model's length to diameter ratio from 1 to 2 appears not to decrease the explosive layered design concept's ability to project fragment layers at graduated velocities. To retain small beam spray angles, a hyperboloid curvature greater than that employed herein is recommended.

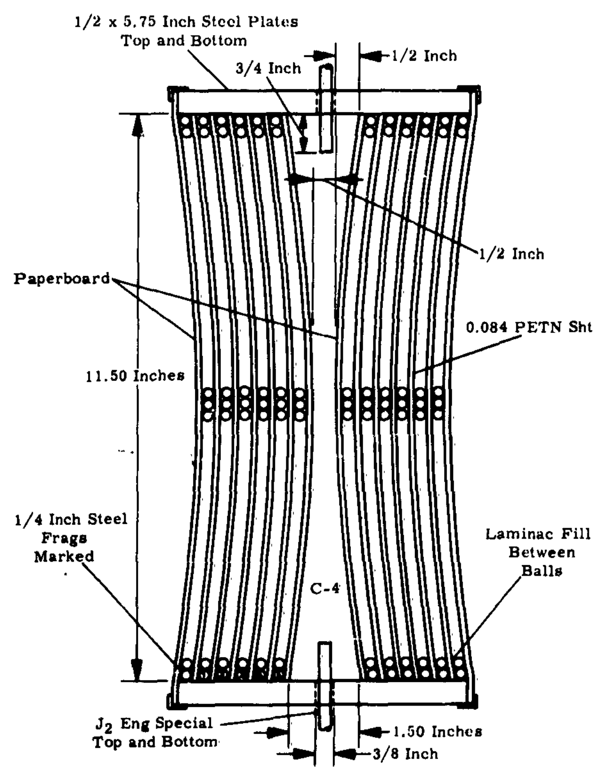

Figure 14. Test Model, L/D = 2, Hyperboloid Configuration

b. Alternate Fragment/Explosive Layering Arrangements - Double fragment layers in concentric ring design results in incomplete detonation when explosive end plate discs are not used (Test Models 98 and 99; Appendix 1). On the other hand, double fragment layers in spiral design configurations reduce overall velocity performance by approximately 20 percent in comparison to single fragment layers (Reference 1), thus more closely achieving required velocity distributions. (Test Models 100, 101, 105, 106; Appendix 1). Hence, this packaging arrangement was selected for subsequent test with added fragment layers.

c. Fragment Materials - The innermost layers of nickel fragments in designs employing center explosive bursters can be expected to be deformed (RE-11, Appendix 1). On the other hand, as many as 14 layers of nickel fragments can be projected from spiral hyperboloid configurations (no center bursters) without any fragment deformation, (RE-23; Appendix 1).

A number of tests utilizing hollow brass spheres affixed to small strips of sheet explosive were conducted to investigate the feasibility of incorporating such fragments in radial explosive projectors. The resulting data indicate that the hollow brass spheres deformed excessively when exposed to explosive forces and do not appear to be a practical fragment for the current radially expanding warhead designs.

d. Fragment Size--Increasing fragment size from 1/4 inch diameter spheres to 1/2 inch diameter spheres in concentric ring designs without explosive end plates results in incomplete detonation of the test model (RE-9 and 10; Appendix 1). This is attributed to the added distance between explosive layers. On the other hand 1/2 inch diameter spheres in designs utilizing explosive end plates (RE-21; Appendix 1) can be successfully projected and provide essentially the same velocity distributions for equivalent charge to mass ratios as utilized in designs employing 1/4 inch diameter spheres. It is believed that the larger size fragments can be successfully projected in either the spiral or concentric ring design configuration utilizing either cylindrical or hyperboloid shaping; however, this must be confirmed experimentally.

e. Fragment Shape--Use of cubical fragments as opposed to spherical fragments, while retaining an equivalent charge to mass ratio, provides a more concentrated impact pattern and approximately a 20 percent increase in fragment velocities (RE-22; Appendix 1).

4. ADDED FRAGMENT LAYERS

As many as fourteen layers of fragments have been projected by both the concentric ring and spiral explosive layering design concepts. The

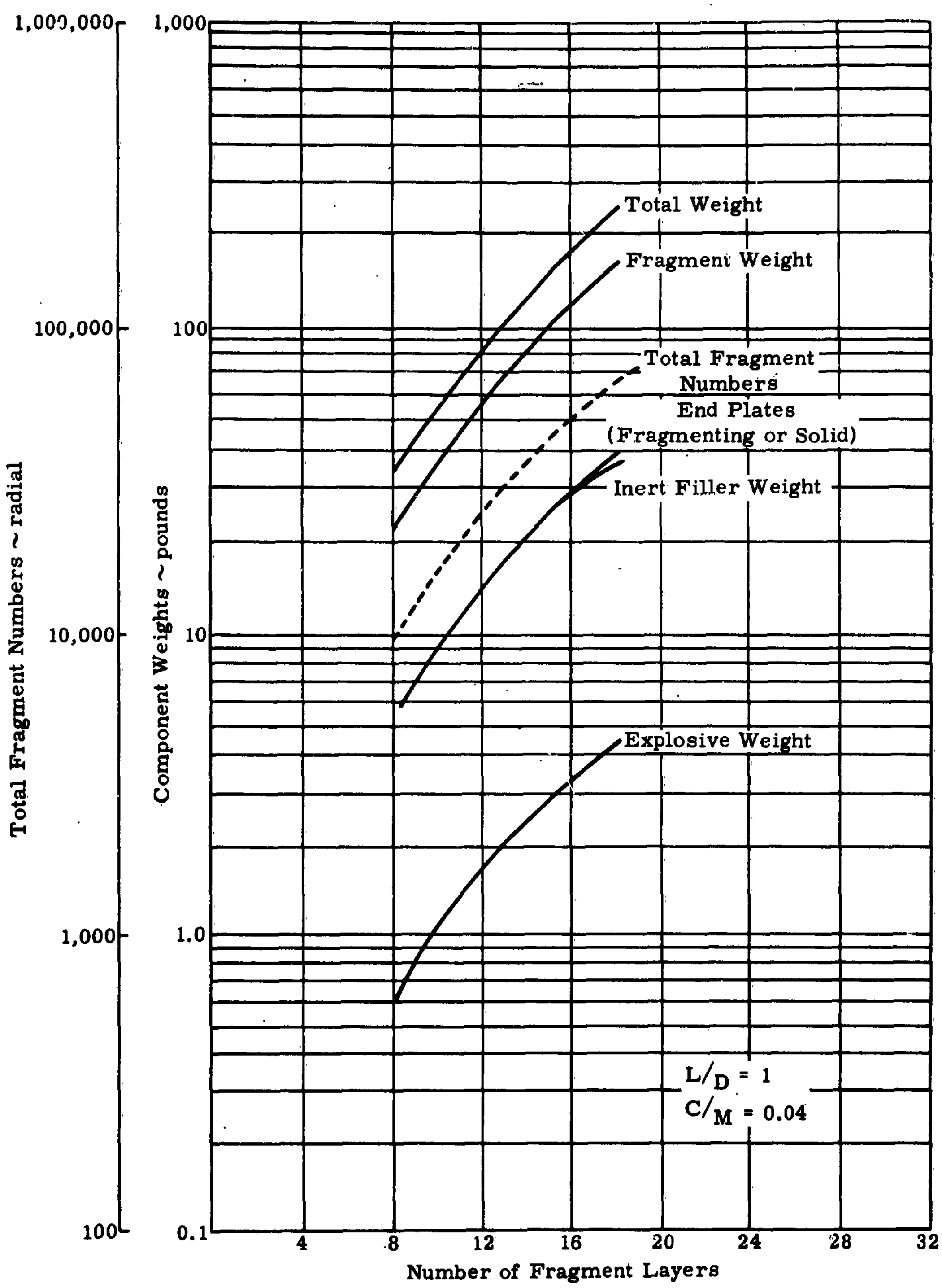

Figure 15. Estimated Design Parameters for Multi-Layered Hyperboloid Designs

maximum number of fragment layers which can be projected by these techniques is believed to be considerably more than fourteen but is yet to be confirmed. Figure 15 illustrates design parameter projections which appear to be easily achievable with hyperboloid design in the immediate future. On the basis of exploratory scaling data generated during this study, extrapolation beyond the points shown on Figure 15, as well as utilization of other fragment sizes, shapes, and materials should present no major unresolvable problems.

5. DYNAMIC FEASIBILITY DEMONSTRATIONS

Design requirements for the rocket sled feasibility demonstrations included:

1 Maximum longitudinal force of 40 to 45 "g".

2 Track roughness factor of 6 "g" and a safety factor of 6.

3 Preferable usage of cantilever mounting fixture for securing warhead to rocket sled.

Towards meeting these requirements an inert test model was first designed, subjected to centrifuge testing, and then dynamically tested on the Eglin rocket sled.

This inert model was of the spiral hyperboloid configuration which weighed 130 pounds, contained approximately 34,500 fragments in fourteen layers, and an explosive simulant of 0.06 inch thick rubber. Figure 16 shows the finished warhead model and rocket sled mounting fixtures prior to final assembly and case finishing.

Centrifuge forces which this model successfully withstood are listed below:

1 Longitudinal Position (Figure 17):

35.6 "g" at inside end plate

47.7 "g" at center of gravity

57.0 "g" at outside end plate

2 Lateral Position:

26.7 "g" on test No. 1

37.7 "g" on test No. 2

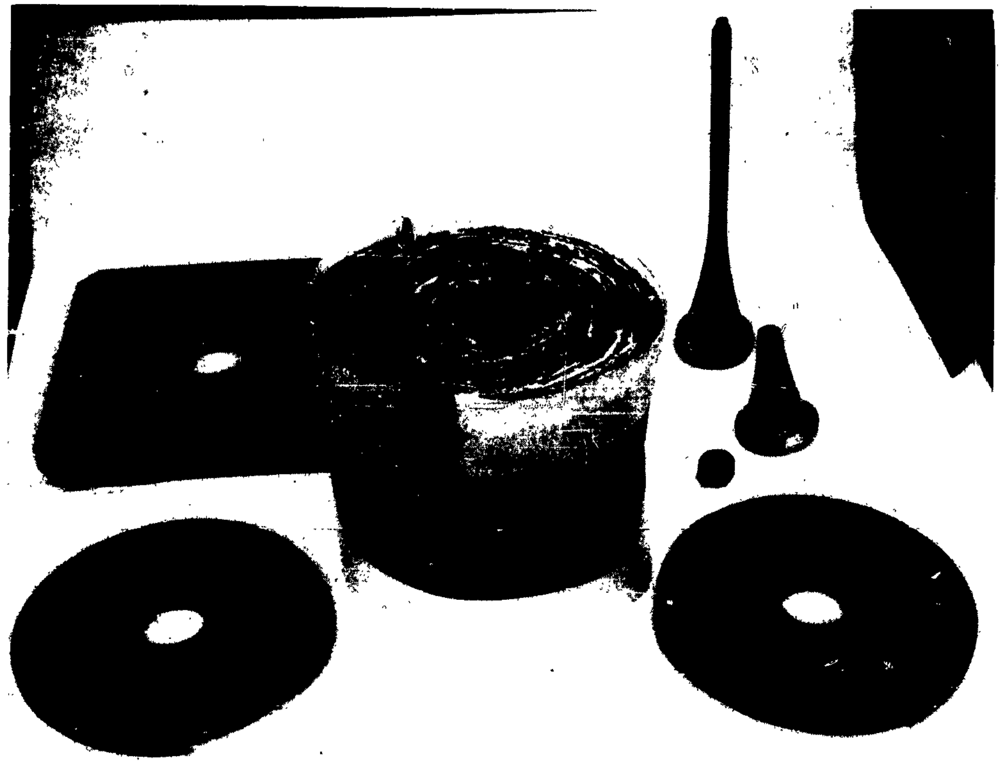

Figure 16. Inert Test Model and Sled Mounting Fixture

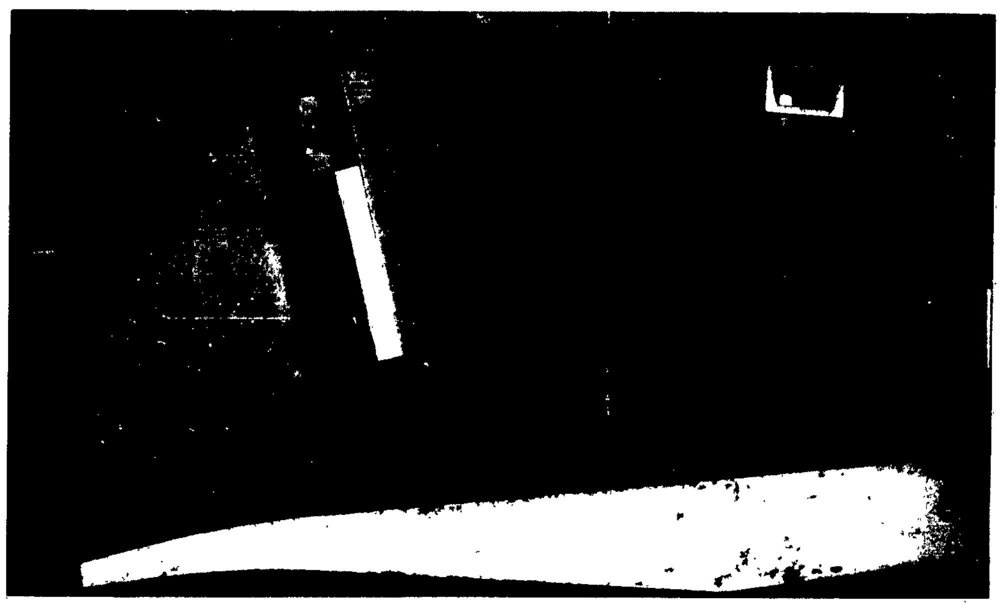

Figure 17. Inert Test Model on Centrifuge Arm

This inert model successfully withstood the rocket sled test in mid-December 1964. Peak sled velocity achieved during this test was approximately 1300 feet per second. Figure 18, a CZR camera photographic record, shows the model completely intact during and at the end of the sled run. (Table 2 shows sled velocities achieved during this test.)

TABLE 2 - ROCKET SLED TIME-VELOCITY HISTORY

PROJ. 2508W4

SLED SHOT 16 DECEMBER 1964

TIME INTERVALS Msec	VELOCITY Ft/Sec	FT. FROM MUZZLE	TIME INTERVALS Msec	VELOCITY Ft/Sec	FT. FROM MUZZLE
0	0	1788	40.8	1225	675
123.3	405	1725	41.3	1210	625
90.	556	1675	41.5	1205	575
74.5	672	1625	42.	1190	525
65.2	767	1575	42.5	1175	475
		(1525)			
114.	878	1500	43	1163	425
		(1475)	43.5	1150	375
51.	982	1425	43.7	1143	325
48	1043	1375	44	1135	275
115.7	1095	1325	44	1135	225
43.5	1150	1275	44.6	1120	175
42.5	1175	1225	44.8	1115	125
41	1220	1175	45	1110	75
40.5	1235	1125	45.5	1100	25
39.4	1270	1075			
39.1	1280	1025			
38.9	1285	975	Total Initial Wt.	1032 Lb.	
39	1282	925	Wt. After Burnout	840 Lb.	
39.2	1276	875			
39.8	1255	825			
40.2	1245	775			
40.3	1240	725			

NOTE: These data provided by Detachment - 4.

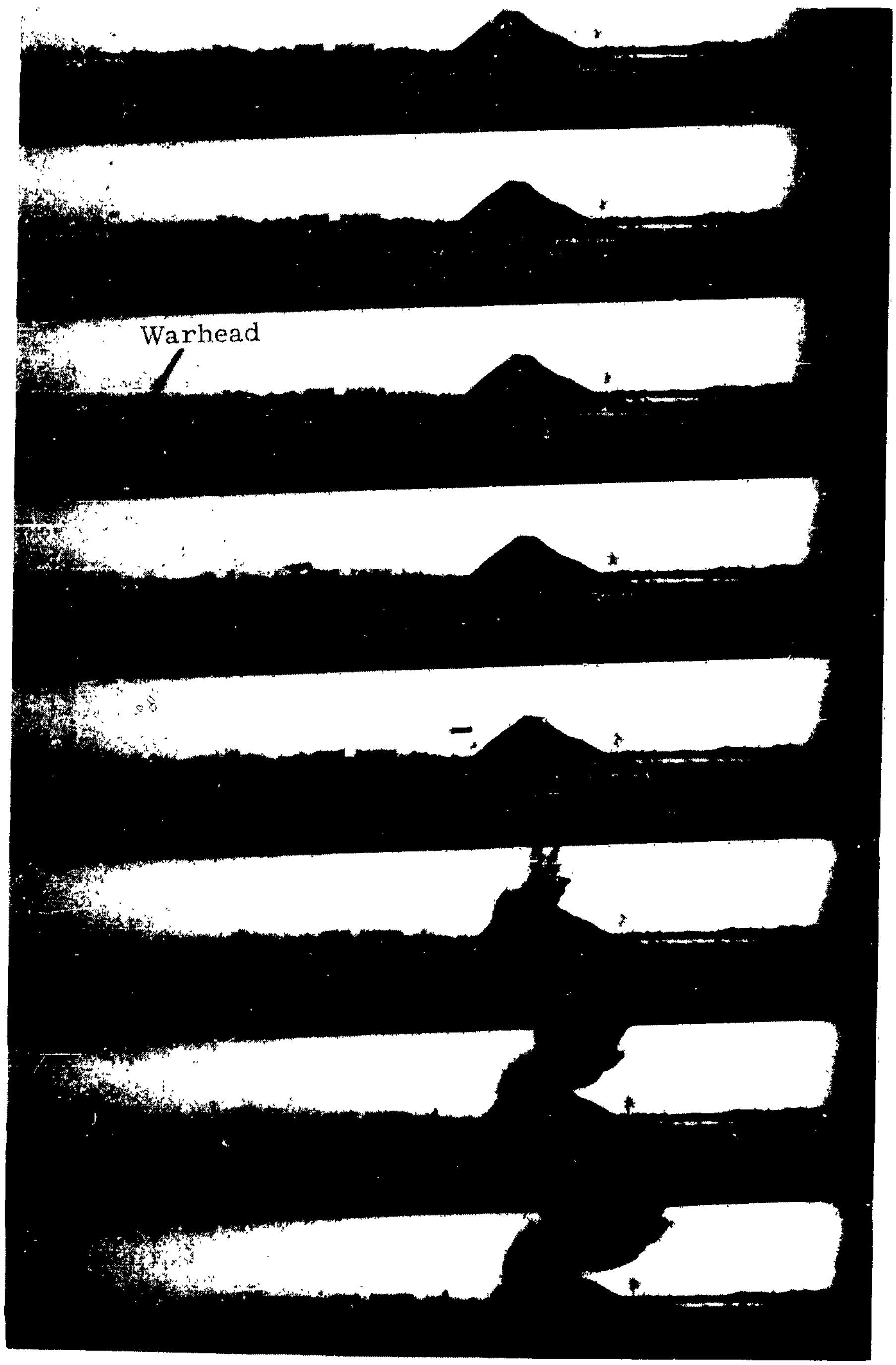

Figure 18. CZR Camera Record of Inert Model Sled Test

In mid-January 1965 two similar explosive loaded test models (RE-19 and RE-20; Appendix 1) successfully demonstrated their performance capability under the same dynamic sled test conditions. RE-19 was fired approximately 28 feet in front of a Celotex witness target at a sled velocity of 1300 feet per second. Although the witness target was completely destroyed by the fragmentation and blast effects, examination of target debris indicated a uniform fragment distribution pattern with 15 to 20 fragment hits per square feet over a radius of approximately 20 feet. RE-20 was fired four feet closer to the target and again created a distribution pattern of 15 to 20 fragment hits per square foot over a radius of 15 feet.

C. TEST ARRANGEMENT AND INSTRUMENTATION

A typical test arena employed during this program (Figure 19) consists of:

1 A gridded Celotex recovery target to determine fragment beam spray angle and to estimate fragment velocity/space distribution patterns;

2 A 180 degree Celotex witness panel arena to confirm radial continuity of the beam spray angle;

3 Five flash radiographic channels to determine maximum fragment expansion rate and to confirm uniformity of the distribution pattern;

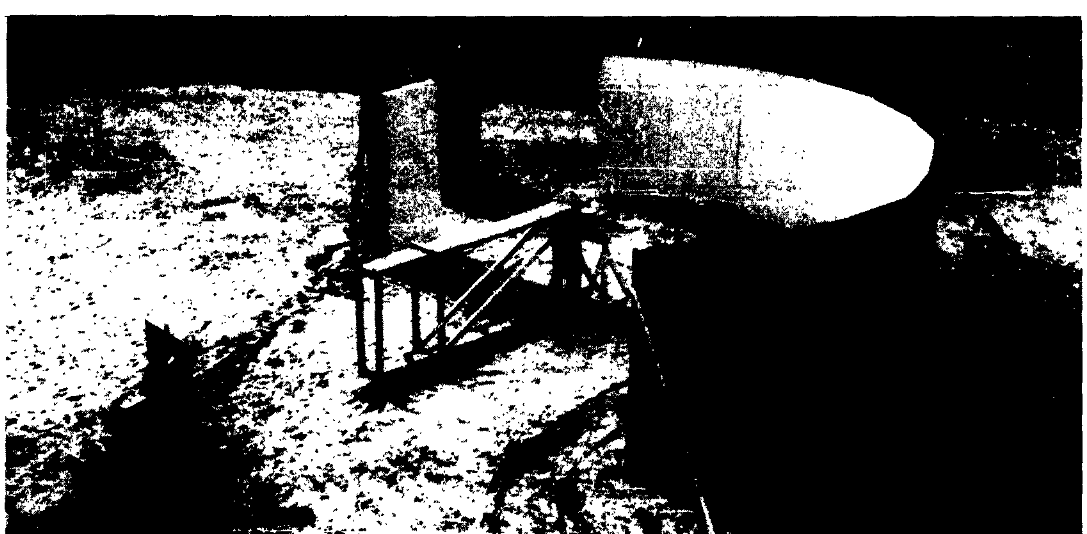

Figure 19. Typical Test Arrangement

4 Fastax camera and opaque flash box to provide independent fragment velocity measurements.

Further discussion of the individual elements within this arrangement follows.

1. CELOTEX RECOVERY TARGETS

All recovery targets are constructed of the same type Celotex (Building Board, Finish 20, Federal Specification LLL-1-535 1/2 inch thick sheets) and packed as nearly alike as possible, the number of layers varying in accordance with expected impact velocities. The face of each recovery target is marked with a grid of one-foot squares. Through careful correlation of fragment impact location with depth of penetration, and the previously described calibration curve (Figure 20 and Reference 1), estimates of both fragment velocities and space distribution are determined.

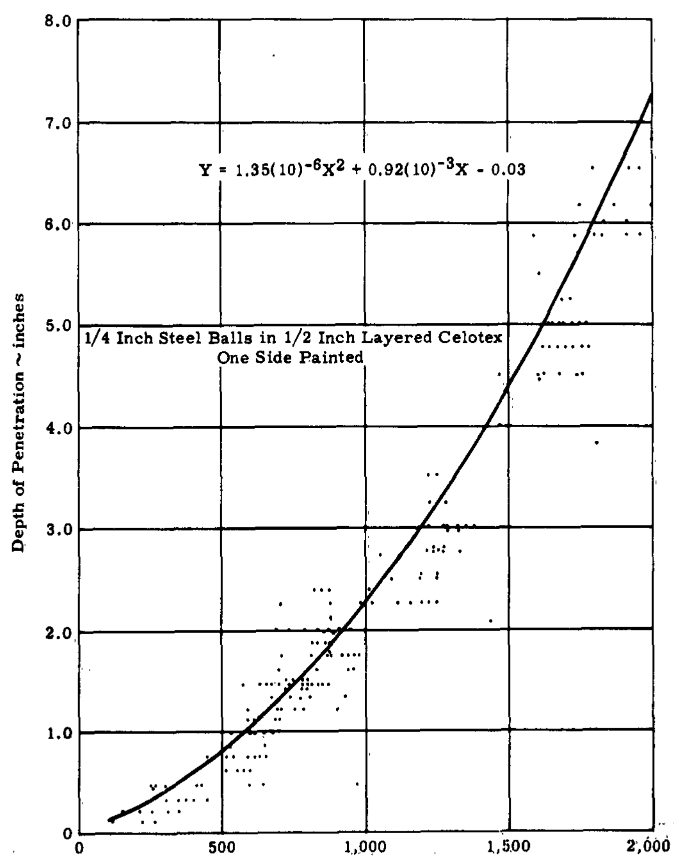

Figure 20. Penetration versus Velocity Calibration Curve

2. FLASH RADIOGRAPHIC TECHNIQUE

The flash radiographic technique employed is illustrated in Figure 21. Five 150KV X-ray tubes of the Field Emission type (Model 730) are located at 2-foot intervals in the ground plane. Four feet above these tubes and within protective barriers is a 10-foot-long mosaic of X-ray film. At a pre-determined time after warhead detonation all X-ray tubes are flashed simultaneously, providing a direct view of these fragments between the film and X-ray sources (Figure 22). From this presentation, fragment velocities can be reasonably well calculated since all distances are measured by surveying techniques and since the time between warhead detonation and X-ray flash is precisely recorded on a Tektronix Model 555 oscilloscope. (Double exposures of fragment patterns were prevented by the use of lead apertures over each tube, thereby eliminating cross-radiation.)

3. FASTAX CAMERA AND OPAQUE LIGHT BOX

To obtain an independent measure of low velocity fragments a technique utilizing a Fastax camera focused on an opaque light box is employed. In concept, photoflash bulbs within the light box (Figure 23) are flashed at sequential time intervals after warhead detonation and, as individual fragments perforate the thin opaque covering, light flashes are recorded on the camera record. Other details pertinent to this technique include:

Figure 21. Flash Radiographic Test Arrangement

(The reverse side of this page is blank.)

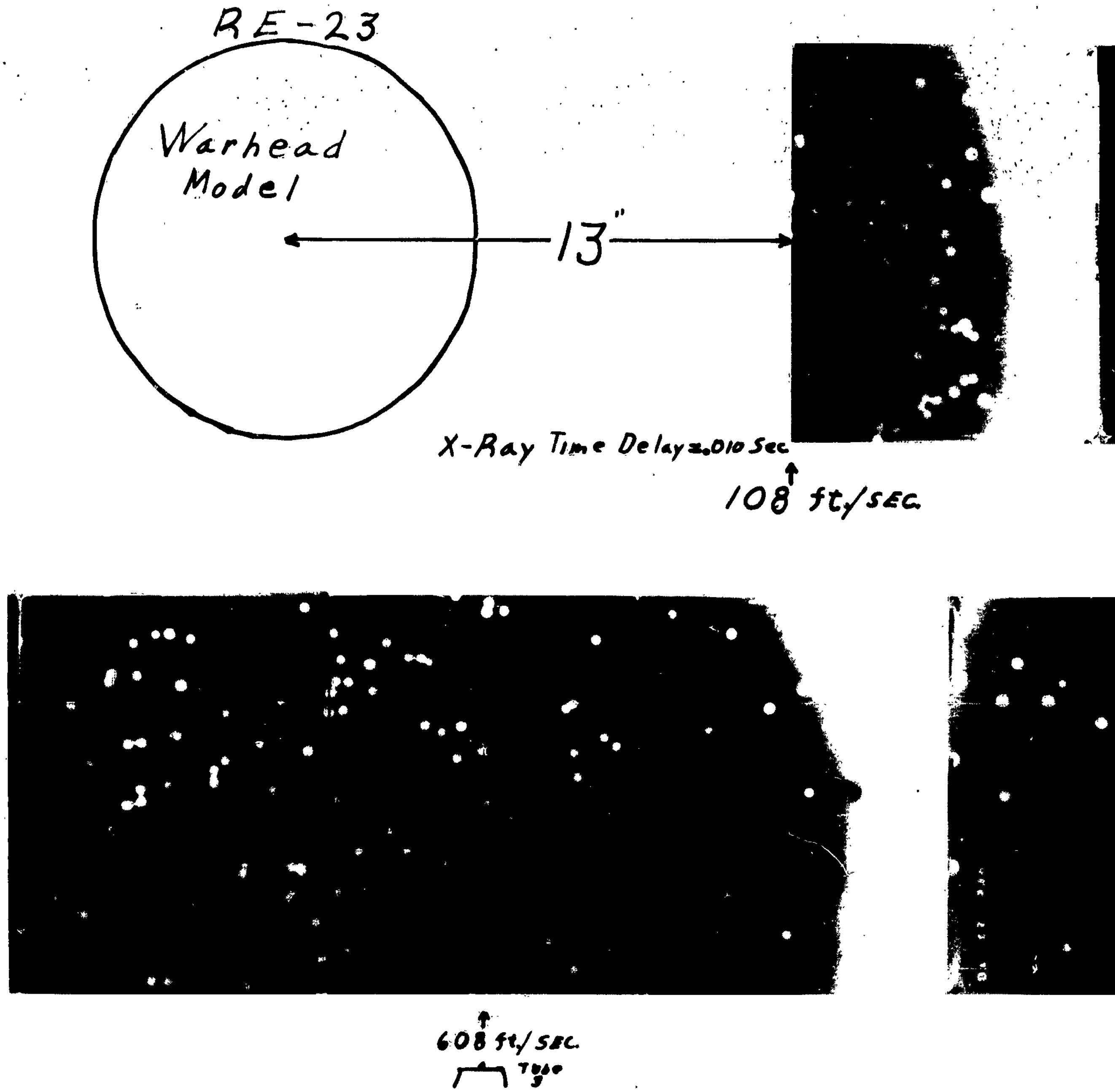
RE-23
Warhead Model
13"
X-Ray Time Delay=.010 Sec
108 ft/SEC.
608 ft/SEC.

1

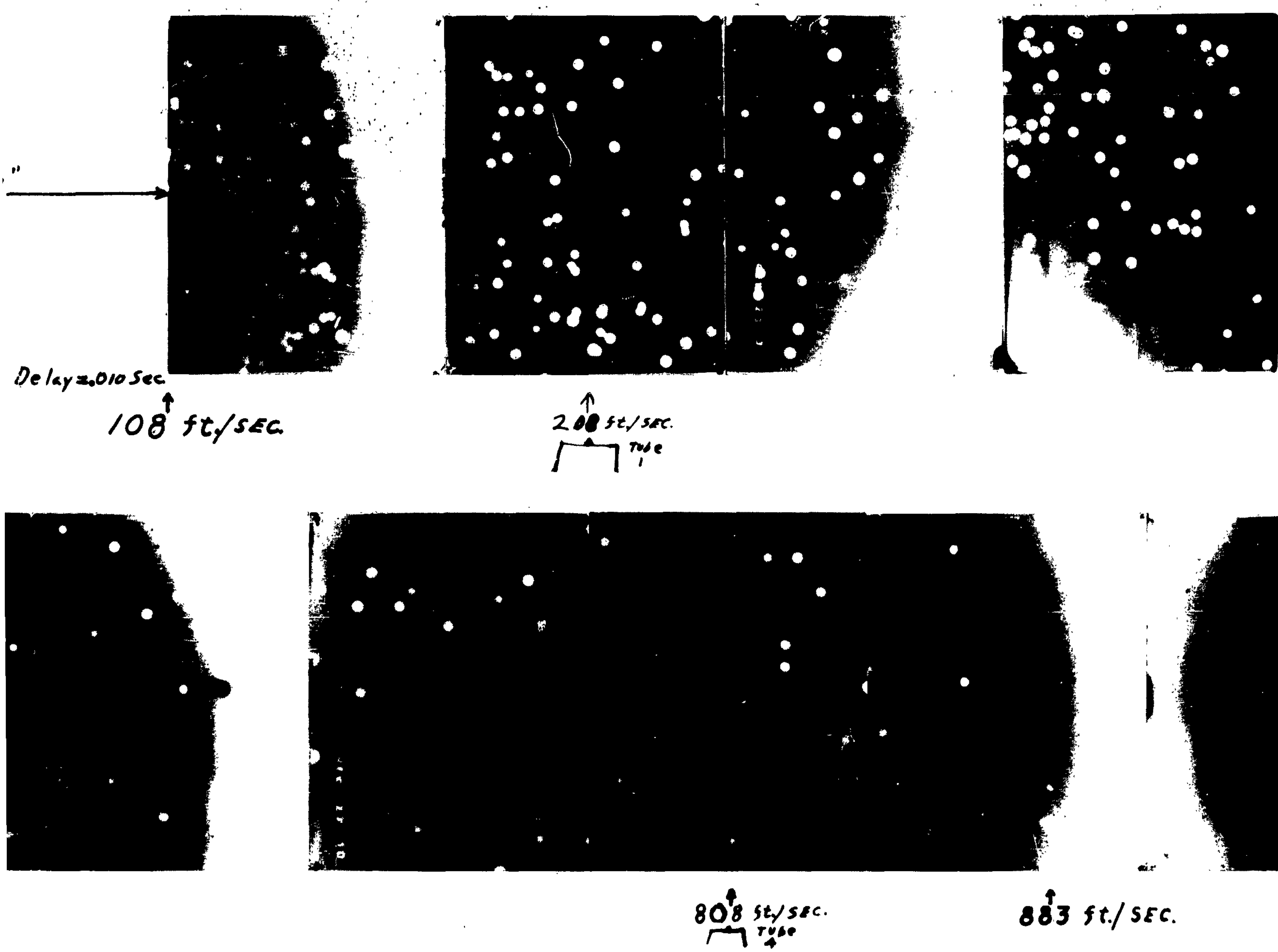

Figure 22. Flash Radiographic Record of RE-23
(14 Layers of Nickel Fragments)

2

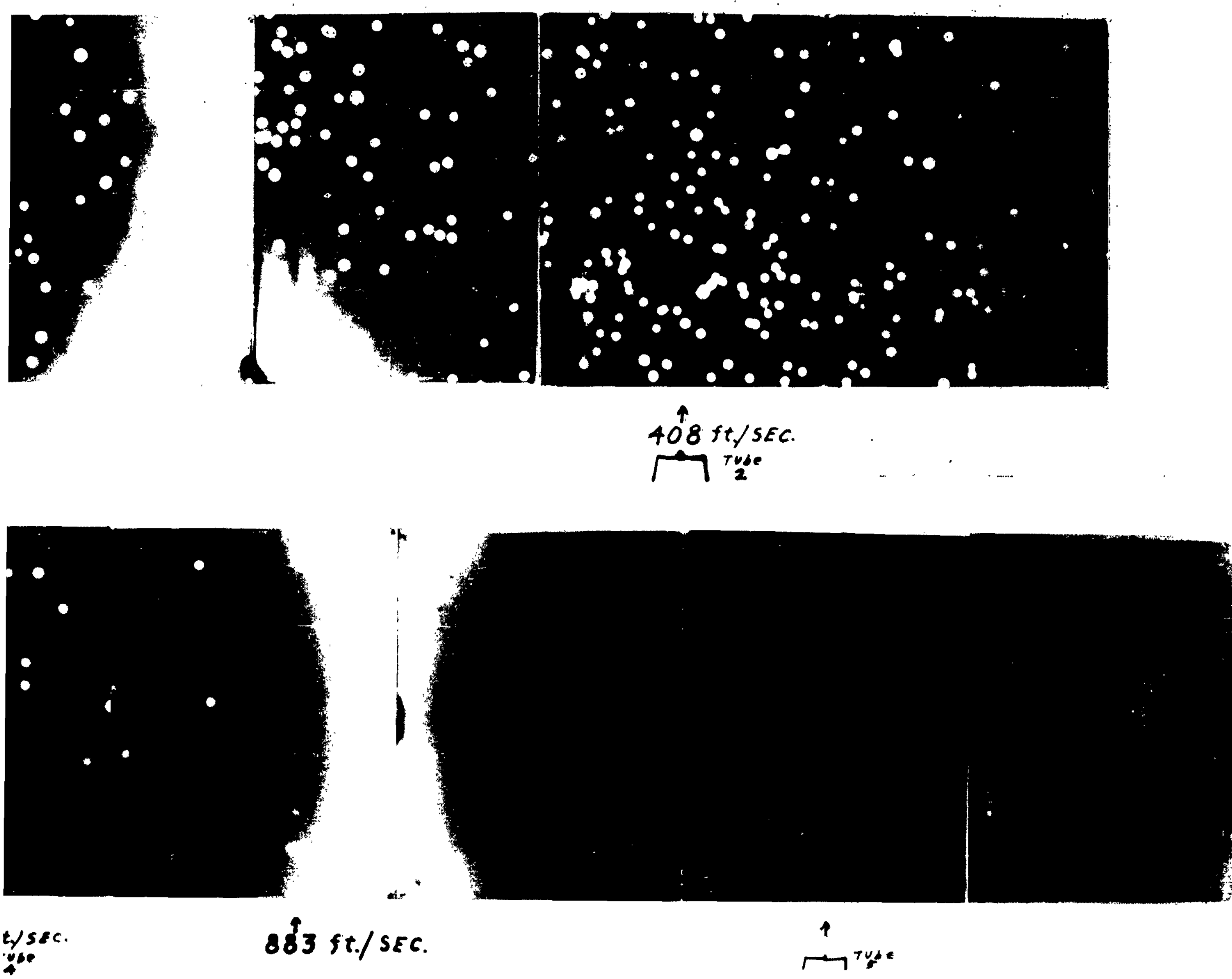

ographic Record of RE-23
Nickel Fragments)

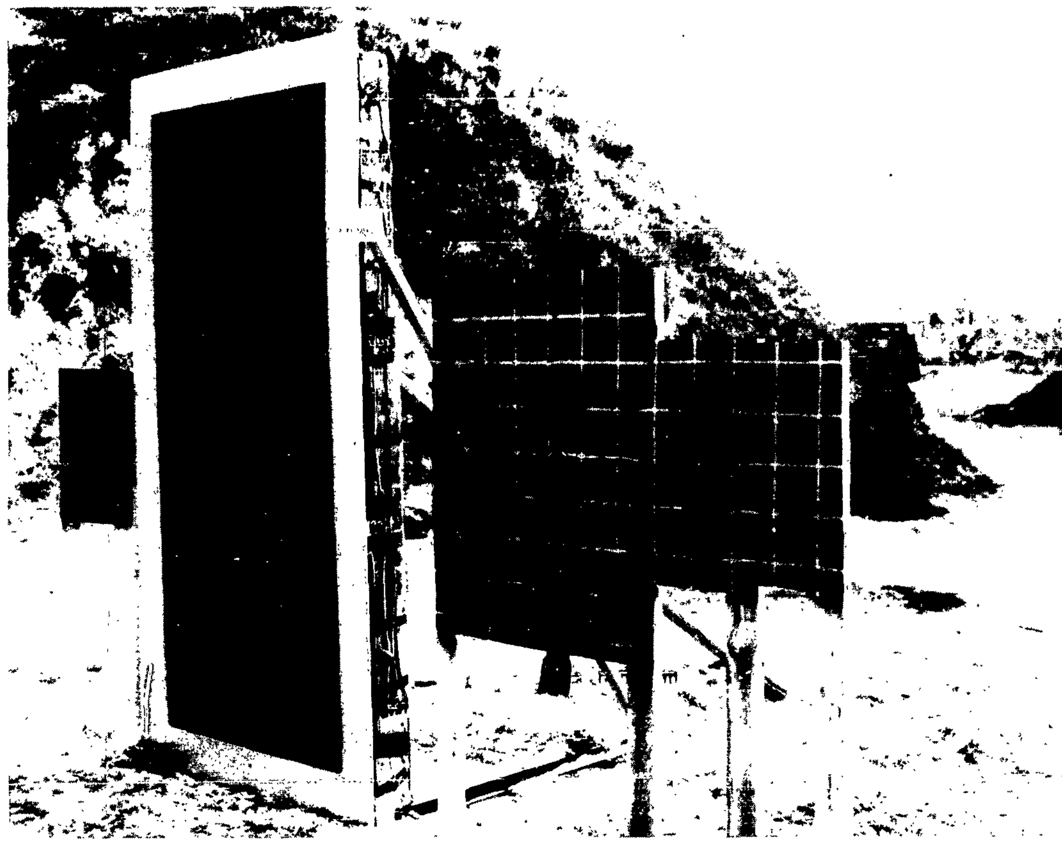

Figure 23. Opaque Light Box

1 Light Box size - 4 by 8 feet by 6 inches,

2 Opaque covering - 0.004 inch thick polyvinyl,

3 Flash bulbs - Twenty-four (Press 25) bulbs in three individual circuits sequenced at 6 millisecond time intervals,

4 Fastax camera - Wollensak Model WF-4 with one-millisecond timing light; pulse generator; industrial timer "Goose" Model J-515; 5000 to 8000 frames per second.

4. FIRING CIRCUIT

The electrical pulse for initiating warhead test models is of the capacitor discharge type utilizing a 4 microfarad capacitor charged to 10,000 volts. The basic design for the unit was obtained from the Ballistic Research Laboratories, Aberdeen Proving Grounds, Maryland (Reference 3).

5. SLED TEST ARRANGEMENT

Dynamic functional feasibility demonstrations were accomplished at the Eglin Air Force Base rocket sled test facilities. Figure 24 schematically illustrates the general test arrangement and includes:

1 A 2000 foot monorail track, 900 feet of which was used for testing Radially Expanding Fragmentation Warhead Models;

2 A sled propelled by eight 5 inch HVAR rocket units;

3 Screen box triggering and capacitor discharge circuitry for warhead initiation at the end of the sled run;

4 A 32 foot by 32 foot Celotex witness target placed 25 feet from the end of the sled track and located so as to sample the warhead's fragment distribution pattern in the upper right hand quadrant, Figure 25;

5 Two CZR cameras (30 to 70 frames per second) for determining terminal sled velocity and point of warhead detonation, as well as providing photographic evidence of fragment target interactions;

6 Three 16 mm Fairchild Model 100 high speed cameras (1000 frames per second) for viewing fragment impacts on the target's face;

7 Four 35 mm 1/2 frame Fastax cameras (4000 frames per second) to obtain a side view of the fragment pattern formation;

8 One 35 mm Mitchell documentary camera (48 frames per second).

D. DATA REDUCTION

Data resulting from the previously described test arrangement include:

1 Fastax film records for fragment velocity measurements,

2 Still photographic records of the impact patterns,

3 Fragment recovery records giving fragment location, depth of penetration, and where possible the fragment layer identification,

4 Flash X-ray radiographic records.

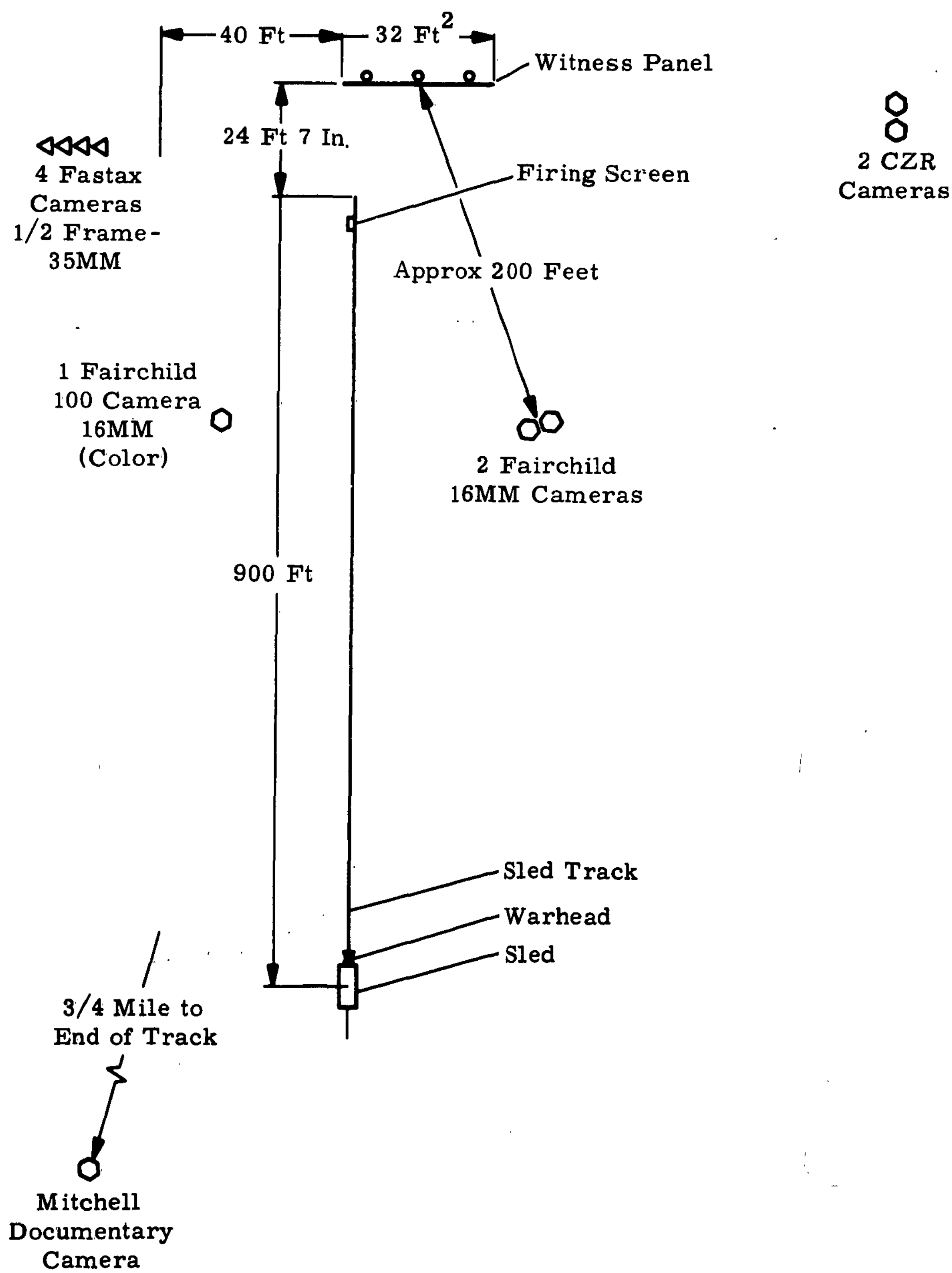

Figure 24. Typical Eglin Sled Test Arrangement

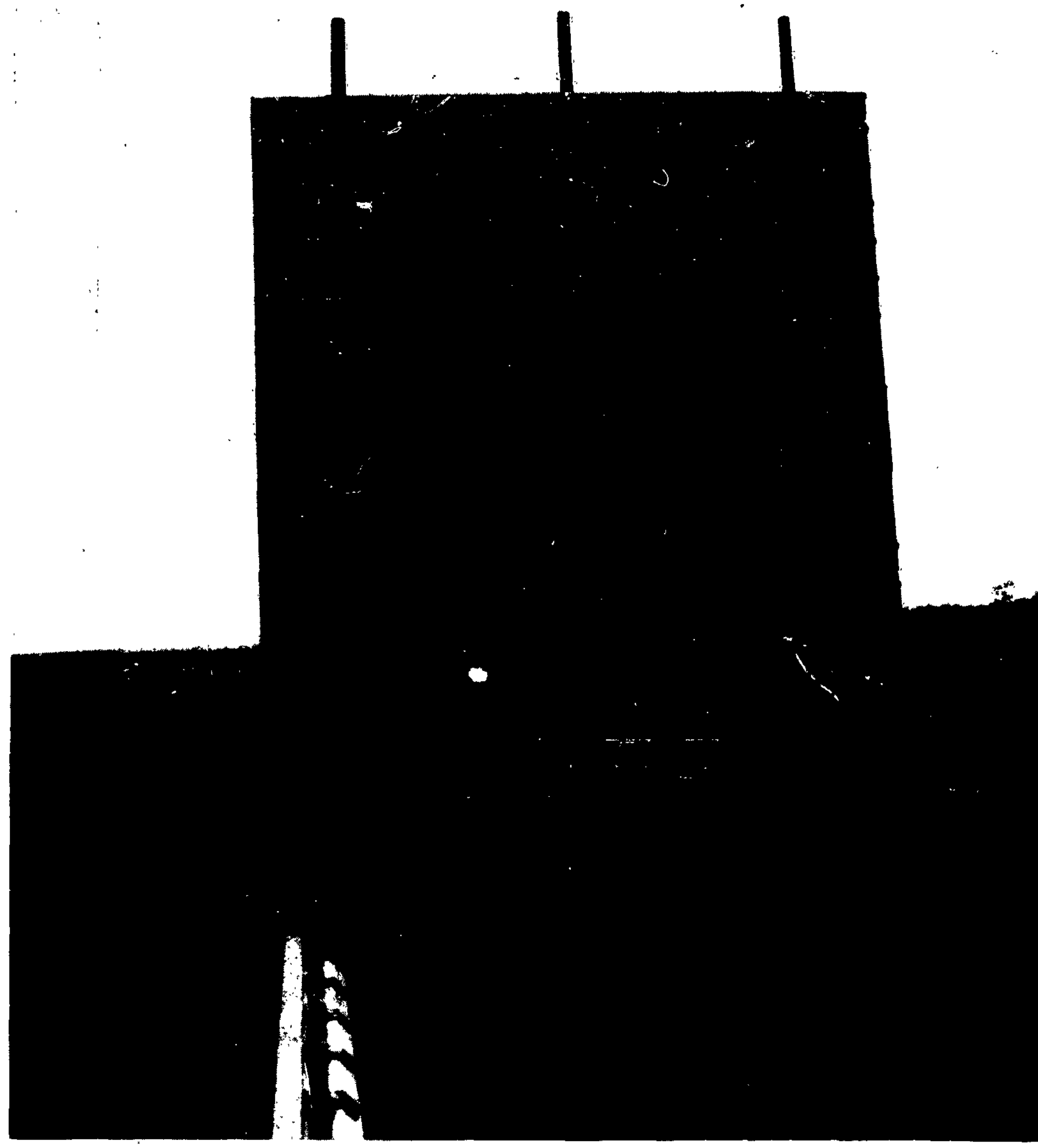

Figure 25. Sled Test Witness Target

i. FASTAX VELOCITIES

Fastax camera records are reviewed through the use of a photographic film analyzer (L-W Photo Optical Data Analyzer Model 225). By projecting this film and recording framing rates, elapsed time from warhead detonation to fragment impact is determined. As the number of fragment layers is increased and the beam spray angle reduced, the multiplicity of fragment impacts within a small area presents a nearly impossible task of determining velocity for individual fragments. However, for the larger test models (10 to 14 layers) this technique is very useful in establishing maximum fragment velocities and confirming the continuation of fragment impacts well into the very low velocity region of 100 feet per second or less.

2. IMPACT PATTERNS

Following each test firing the individual fragment impact points are numbered and permanent photographic records made (Appendix 1). By counting the number of impacts within various horizontal bandwidths on the gridded recovery target and relating these to arena geometry and distance measurements, the percentages of fragments within given beam spray angles are determined.

3. POLAR DISTRIBUTION PLOTS

Figure 26 is a typical polar plot of a 6-layered test model illustrating the model's velocity/space performance. It shows how the fragment pattern would appear to an observer viewing its formation, at a given instant in time, along the warhead's longitudinal axis. Average fragment velocities are plotted radially along with angular position and fragment row location as shown by the coded data points. These velocities have not been corrected for air retardation. However, considering the short distances involved, the error introduced is approximately 1 percent or less of the initial velocities within the velocity interval of interest. Again, with the large multilayered test models and reduced beam spray angles, the multiplicity of fragment impacts negated accurate recovery of fragments. Hence, the costly procedure of marking fragments was discontinued in the 14-layered test models and recovery progressed on the basis of obtaining a gross indicator of the test model's velocity/space performance.

4. FLASH X-RAY RADIOGRAPHY

Flash X-ray radiographs (Paragraphs B and C) provided the primary means of instrumentation for large multiple layered test models. It is emphasized that this technique samples only those fragments within the radiation cone and passing between the radiation source and X-ray film plates. These data must still be correlated with those resulting from impact patterns and witness panels to obtain an overall insight as to the test model's performance.

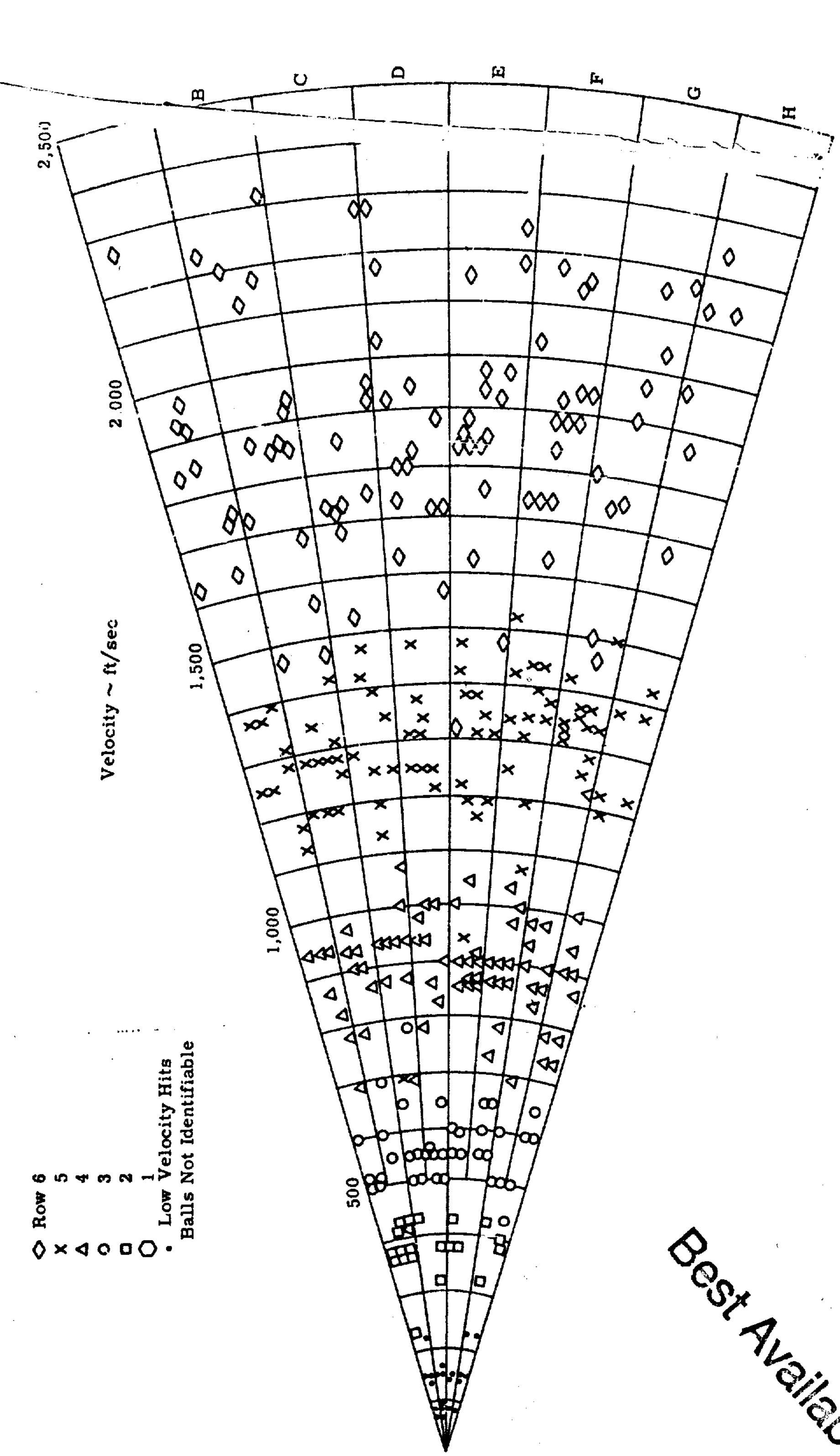

Figure 26. Typical Polar Plot of Six Layered Test Model

E. FABRICATION PROCEDURES

Design drawings and descriptions of the various types of warhead models fabricated for this program are given in Appendix 1. Because of the wide number of variables investigated, each test model was hand made. Discussion of the more salient features pertinent to the fabrication of these devices follows.

1. FRAGMENTS

The type of fragments employed in this program includes 1/4 and 1/2-inch diameter steel spheres (SKF 36-300, Grade 200, Polished); 1/4 inch steel (SAE-1019) cubes; and 1/4 inch hollow brass spheres. Spheres were used in the majority of tests because of economics and ready availability.

Identification marking of fragments was accomplished with simple steel stamps after heat treating the fragments to a hardness of Rockwell B-85. Marked fragments were used only in the test model's sector where recovery was to be accomplished.

2. EXPLOSIVE

Explosives used during this program include Composition C-4, Cyclonite (RDX) and rubberized sheet explosive (DuPont Detasheet "C" - MIL-E-46676 (MU) Flexible Explosive). Sheet explosive was used in all explosive layered designs and for explosive end-plate experiments. Major characteristics of the DuPont Detasheet are summarized in Table No. 3 and Reference 4.

Fabrication procedures employed with the sheet explosive involved simply cutting the explosive to the required size and covering it completely with cloth gun tape. It was found that this tape prevented deterioration of the rubberizing material in the sheet explosive during a subsequent inert filler curing process. When necessary to increase the length of the explosive sheet, edges of separate sheets were feathered and spliced with DuPont explosive adhesive 4684.

3. FRAGMENT PACKAGING

Investigations into possible means of improving the technique of packaging fragments were conducted. Improvement goals are superior quality test models and reduced fabrication time. Techniques considered as illustrated by Figure 27 include:

1 Encapsulating fragments in a pliable sheet, such as Sylgard 182 and Silastic RTV-501 Silicone Rubber,

TABLE 3 - EXPLOSIVE CHARACTERISTICS DuPONT DETASHEET C

PROPERTIES	QUANTITIES
Explosive Content & Material	63% PETN - 8% NC
Detonation Velocity	7000 meters/sec
Density	1.48 grams/cc
Flexibility Range	-65 to 160°F
Storage Life	Over 4 years at ambient temperatures
Thermal Stability	24 hrs at 250°F 1 hr at 275°F
Hot Bar Ignition Temperature	Instantaneous at 565°F 5 seconds at 456°F 15 seconds at 380°F 30 seconds at 353°F
Impact Sensitivity	56 inches (5 KG Drop Test)
Static Sensitivity	0.9 joule (30 KV discharged through a capacitance of 2000 mf)
Minimum Tensile Strength	30 psi (20 in./min. crosshead travel)
Range of Percent Elongation	15 to 150
Minimum Propagation Thickness	0.025 inch (unconfined)

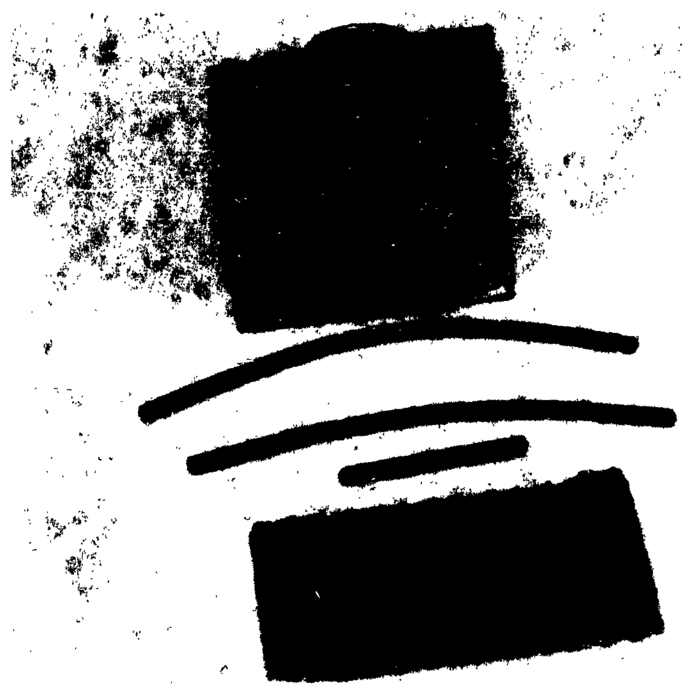

Figure 27. Fragment Packaging Techniques

2 Pre-casting fragments in a frangible material such as Laminac,

3 Securing fragments to a double coated pressure sensitive tape, (Minnesota Mining No. 400).

Of these approaches, the pressure sensitive tape proved to be most useful, economical, and time saving. Figure 28 shows a preliminary fabrication stage of one test model wherein this tape was employed. Previous fragment packaging techniques for a model such as this required as much as eight hours to "lay-up" a single external fragment layer. With the pressure tape, time required to "lay-up" the same external fragment layer is reduced to one hour.

Figure 28. Partial Fabrication Test Model RE-14

The technique of encapsulating fragments in Silastic Rubber (Figure 29) also showed promise. However, since test model designs were evolving toward a hyperbolic concept further investigation was suspended because of the problem of fitting a flat surface to a complex curvature. On the one model tested, RE-12, data show the fragments to move as a solid group rather than in the desired graduated manner. Whether this is a result to be expected from the encapsulating technique cannot be determined on the basis of only one test.

4. INERT FILLER

Upon completion of fragment packaging by the various techniques previously described, the resulting package was filled with an inert bonding material. Aside from securing fragments firmly in place, it is believed that this filler improves energy coupling to the fragments to prevent fragment fracture at the time of detonation.

Figure 29. Partial Fabrication Test Model RE-12
(Fragments Encapsulated in Silicon Rubber)

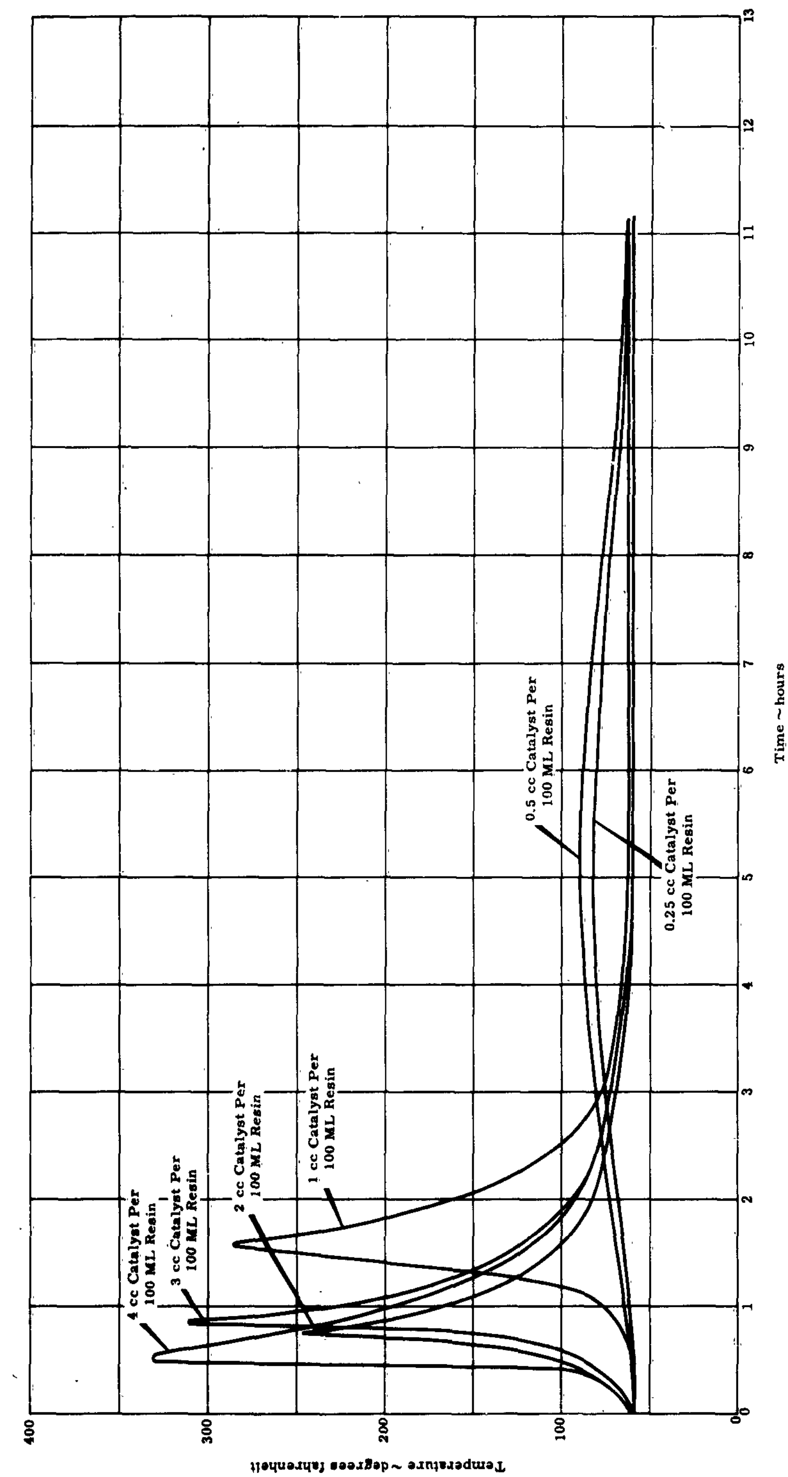

Figure 30. Time-Temperature History of Inert Filler Curing Process

Two types of inert fillers were used:

1 Epon 820 with Versamid 140 catalyst,

2 Laminac No. 4116 with Lubersol DDM catalyst.

Since these materials generate heat during their curing process, time temperature histograms of various sample mixtures (Figure 30) were made to ensure safety of the overall fabrication process. In all combinations of the Epon type filler, no significant temperature rises were recorded, and samples of bare sheet explosive potted in these mixtures detonated completely. On the other hand, test samples of bare sheet explosive potted in the Laminac mixtures resulted in incomplete detonations. However, when similar explosive samples were protected by gun tape and potted in the Laminac mixtures, complete detonation was obtained.

To further exploit the use of an Epon type filler, one large 14 fragment layered test model was fabricated with this material and test fired in the arena. Examination of recovered fragments and flash radiographic records showed that the inert filler did not shatter completely, thereby preventing a uniform distribution of fragments. Hence, use of Laminac filler and taped explosive was continued with no more than 2 cc of catalyst per 100 ml of resin. Further investigations toward the use of an Epon type filler is strongly recommended to eliminate any potential fabrication hazard. In addition, it is believed that the long term hydrocarbon out-gasing of Epon materials is more compatible with sheet explosive than those emitted by Laminac compounds. Hence, they offer the advantage of a long shelf life for an ultimate production weapon.

5. FOURTEEN FRAGMENT LAYERED TEST MODELS

To fabricate large multiple fragment layered test models, a simple tooling fixture as depicted by Figure 31 was employed for either concentric ring or spiral design configurations.

Fabrication of spiral designs starts with the placement of a steel mounting cone (Figure 32) and steel end plates in this fixture. The spindle was wrapped with pressure sensitive tape and the buildup of alternate layers of sheet explosive (*) and discrete fragments initiated. By simply revolving the tooling fixture and adding appropriate longitudinal strips of pressure sensitive tape, this buildup was continued until the required

(*) Sheet explosive was cut in longitudinal strips to permit fabrication of spiral hyperboloid test models.

Figure 31. Test Model Tooling Fixture with Model RE-15 Partially Fabricated

Figure 32. Mounting Fixture Assembly

numbers of fragment layers were in place. The resulting fragment/explosive package was removed from the fixture, placed in a wood mold,(**) one end plate was removed, and the inert filler added. After a two hour curing period, the warhead was removed from the mold, reassembled in the tooling fixture, and an external line wave generator secured to the sheet explosive. Case finishing included an external wrapping of fiberglass (Type EC11A-0.75 x 0.007 inch), epoxy filling, sanding, and painting.

(**) Internal surfaces of the mold were coated with a Teflon spray release agent.

(The reverse side of this page is blank.)

SECTION 3 - ANALYSIS

A unique computer code has been developed to assist in deriving an alternate analytical technique for predicting velocity performance of multiple fragment layered radial projectors. The basic code, "Quasi-Wundy," was prepared by the Naval Ordnance Laboratory/White Oak and incorporates the main features of the Dynamic Pressure Differential approach, as defined in Reference 5. This program is unique in that it provides:

1 A pressure-time history of the gas released by the explosive;

2 A time history of compression and tension waves in the fragments due to shock propagation;

3 A history of energy transfer from the explosive to the fragments;

4 A velocity-time history for each layer of fragments.

For direct application to warhead models evolved during this program, the basic Quasi-Wundy code, because of its one dimensional nature, did not consider the effect of pressure losses resulting from venting of explosive gases at each end of the warhead. Hence, a modification to account for these losses was derived and successfully incorporated into the overall program.

Further discussions of the basic computer program, end venting modifications, and extent of correlation with experimental data are given in the following paragraphs.

A. BASIC "QUASI-WUNDY"

The original computer code is a device for the numerical solution of the standard hydrodynamic equations commonly used in problems involving fluid flow. The four basic equations comprising this set are:

$$\frac{\partial u}{\partial t} = - \frac{1}{\rho(j)} \frac{\partial P}{\partial j} \qquad \text{(equation of motion)} \qquad (1)$$

$$\frac{\partial E}{\partial t} = - P \frac{\partial V}{\partial t} \qquad \text{(conservation of energy)} \qquad (2)$$

$$\frac{\partial u}{\partial j} = \rho(j)\, \frac{\partial V}{\partial t} \qquad \text{(conservation of mass)} \qquad (3)$$

$$P = P(E,\, V) \qquad \text{(material equation of state)} \qquad (4)$$

where: j = Lagrangian coordinate

x = spatial (Eulerian) coordinate

ρ = mass density

P = pressure

u = particle velocity

V = specific volume, $\left(\frac{1}{\rho}\right)$

E = specific internal energy

t = time

The Lagrangian coordinate, j, is used here because it simplifies the equations for computer calculations using finite difference methods. Each "j" is a label attached to a particle of fluid; the label travels with the particle through all computations. It is converted to the more significant spatial coordinate, x, by integrating the velocity over time:

$$x\,(j,\, t) = \int_{t\,=\,0}^{t} u\,(j,\, t)\;dt \qquad (5)$$

The computer code, as its name implies, is a quasi-one-dimensional solution to these equations; this means that only one spatial coordinate is used, but by choice of appropriate geometrical factors, spherical and cylindrical symmetries can be taken into account as well as slab symmetry. The geometrical modifications are shown more clearly by considering the equation for the mass between the centers of two particles j and (j + 1):

$$M = \int_{x\,(j,\, t)}^{x\,(j\,+\,1,\, t)} \rho\,(x)\; A\,(x)\; dx \qquad (6)$$

where A is the cross-sectional area of the flow at x. For true one-dimensional flow, A = 1; for cylindrical symmetry, A = $2\pi x$; for spherical symmetry, A = $4\pi x^2$.

To take into account the presence of shocks in the detonation process, the Von Neumann-Richtmeyer "q" method is used. This method adds an artificial viscosity term, q, to the pressure in equations (1) and (2). This term is:

$$q = \begin{cases} \left(\frac{C_o^2}{V}\right)\left(\frac{\partial u}{\partial j}\right)^2 , & \frac{\partial u}{\partial j} < 0 \\ 0 , & \frac{\partial u}{\partial j} \geq 0 \end{cases} \tag{7}$$

The effect of the artificial viscosity term is to spread a shock front over more than one computational zone; this makes the slope of the pressure across the zone low enough to be manageable for finite difference computations performed by the program, thus avoiding an oscillatory solution. C_o is a constant which adjusts the width of the shock front.

An equation of state, usually experimentally determined, expresses the behavior of a given material under varying values of the flow parameters; from it, compressions, tensions, magnitude of shock, etc., within the materials are determined at each computational step. The equation of state used for gases, including detonation products, is the "gamma gas law"

$$E = \frac{PV}{(\gamma - 1)} \tag{8}$$

γ is a constant characteristic of the material; for explosive gases, it is determined by

$$\gamma = \left(\frac{D^2}{2E_o} + 1\right)^{\frac{1}{2}} \tag{9}$$

where D = detonation velocity of the explosive

E_o = chemical energy of detonation per unit mass of explosive

The equations of state used for solid materials are usually more complex, having different forms in different pressure ranges. They normally come from curve-fitting to purely experimental data.

B. LIMITATIONS OF "QUASI-WUNDY" AND VENTING MODIFICATIONS

Quasi-one-dimensional solutions to explosion hydrodynamics problems are clearly subject to inaccuracies in predicting the performance of actual rounds, due mainly to the escape of detonation products in directions other than along the single coordinate considered. In the case of cylindrical radial fragment projectors, energy can escape axially through the ends of the round, depending upon the amount of end confinement present. This escape of gases causes a drop in gas pressure within the round below that computed by "Quasi-Wundy," and thus results in lower fragment velocities than those predicted.

To allow for venting of energy in the computations without resorting to prohibitively expensive two-dimensional computations, Martin Orlando has modified the basic Wundy program to artificially incorporate the resulting pressure drops. An outline of the method follows:

Consider a cylindrical charge propelling a layer of fragments radially, as shown in Figure 33. Wundy in its unmodified form gives a good approximation of the pressure-time history of gaseous detonation products acting on the fragments only near the round's center. Near the ends of the round, the pressure drops rapidly due to loss of gases from the ends. Thus, the fragments near the ends reach lower velocities than those near the center. To predict their velocities, an accurate pressure-time history is needed.

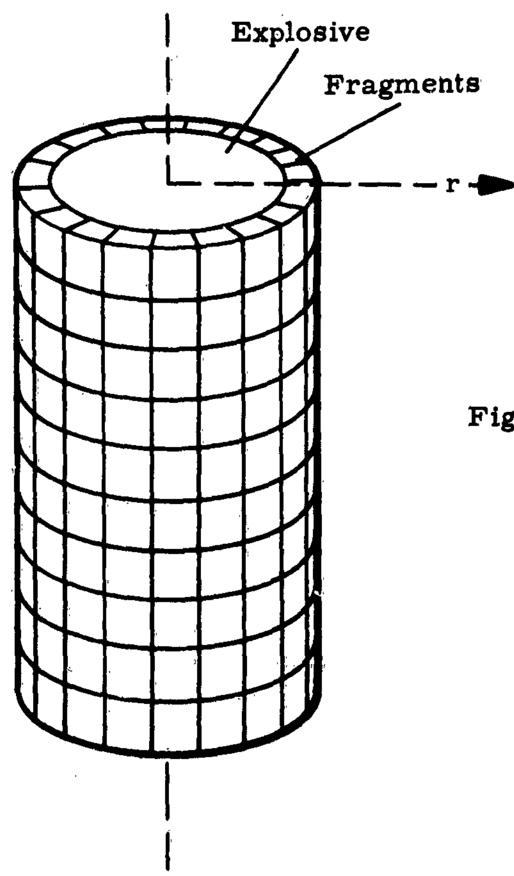

Figure 33. Radial Expansion of Fragments

To obtain this p-t curve, Wundy is used in the slab-symmetry mode to predict the rate of expansion of detonation products from each end of the cylinder of explosive, as shown in Figure 34. Figure 35 shows the type of curves obtained. Notice the much more rapid pressure drop at the ends than at the center. This data is fed into a "vent" subroutine in the modified program. When the modified program is then used to calculate the round's radial expansion, the pressure calculated at each computational cycle is reduced by a factor from the vent subroutine appropriate to the time and the distance from round center. Thus a pressure-time history closely approximating the actual one acting on the fragment is used to predict the fragment's velocity.

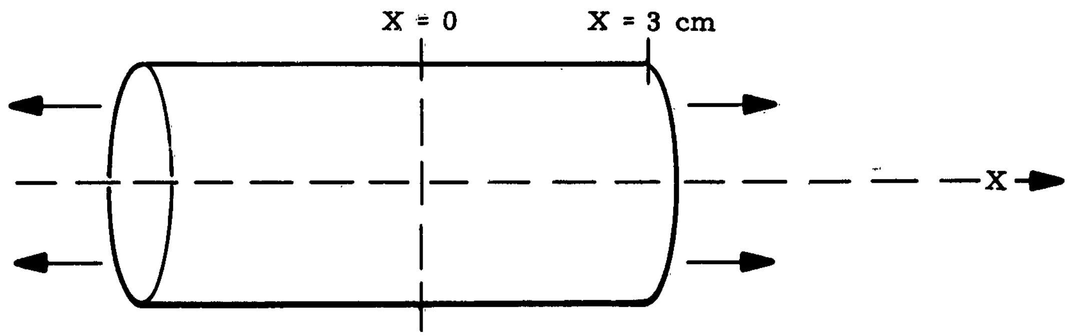

Figure 34. Linear Expansion of Detonation Products

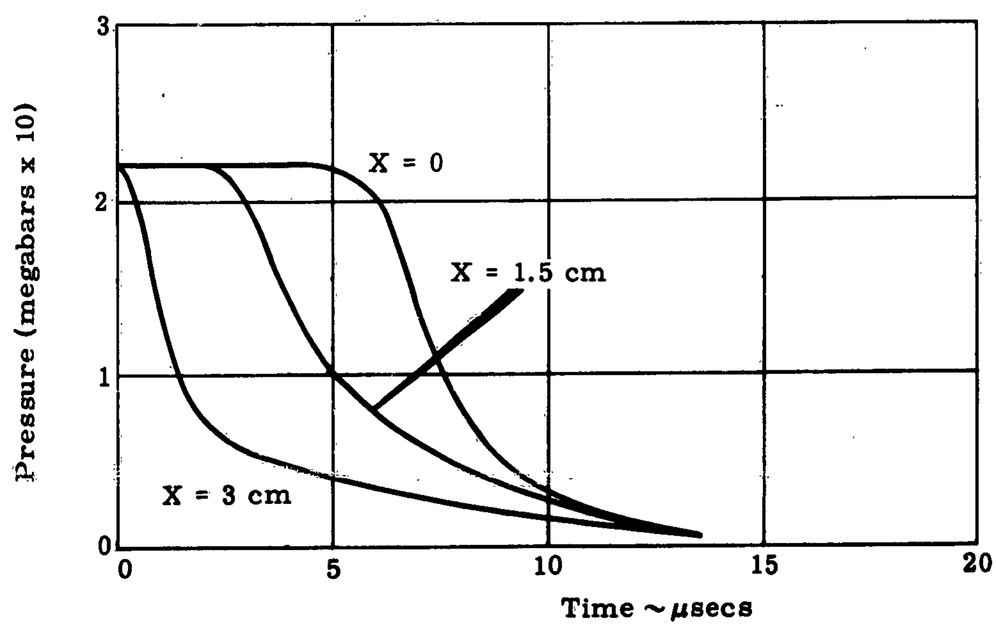

Figure 35. Pressure-Time History of Detonation

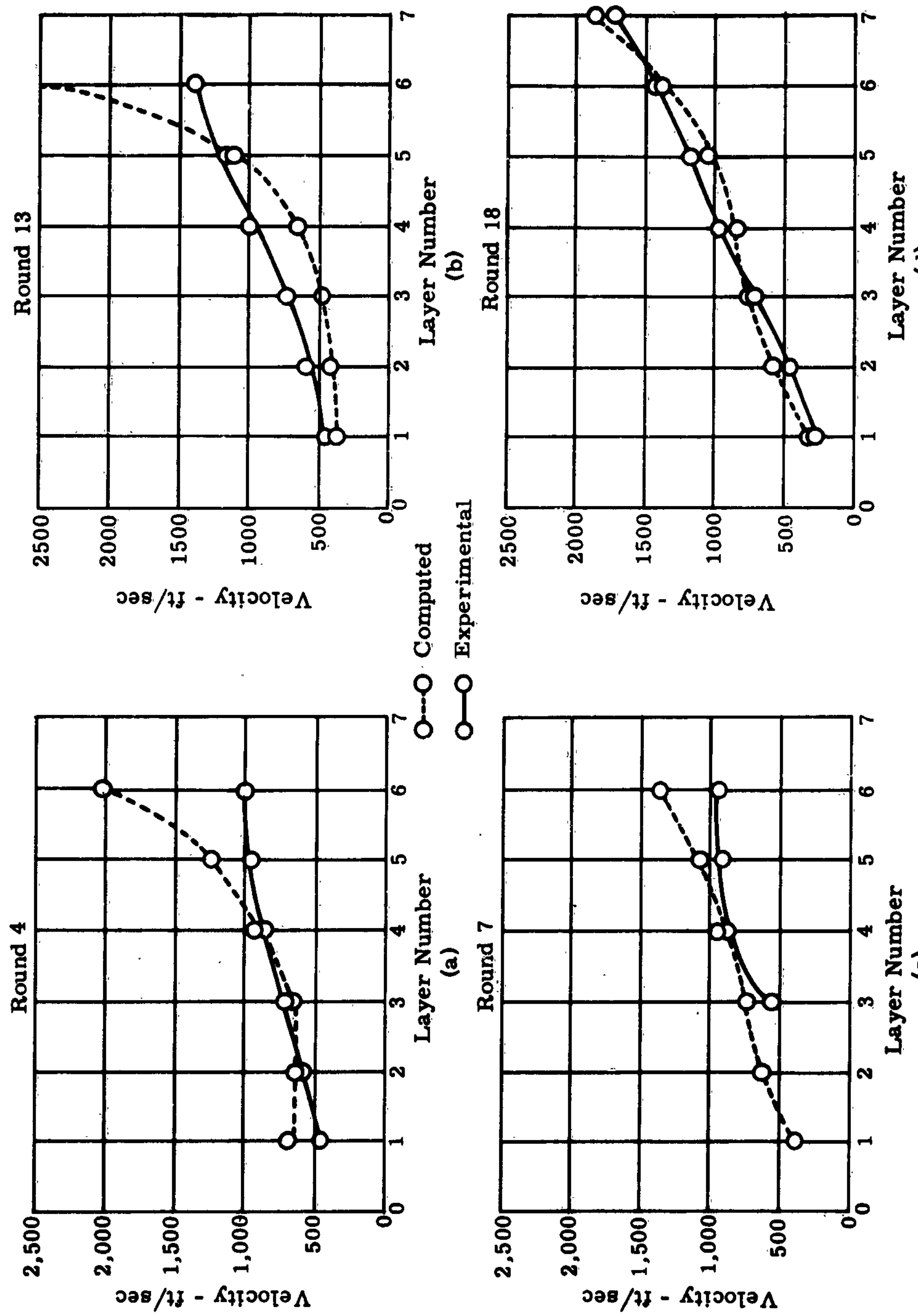

Figure 36. Experimental versus Predicted Fragment Velocities

C. CORRELATION WITH EXPERIMENTAL DATA

Agreement of computer calculated velocities with those observed experimentally was encouraging, although limited. Closest correlations, on the whole, were observed in the "middle" fragment layers, e.g., the second through fifth layers of a six-layer test model. The curves of Figure 36 illustrate this tendency. Notice that in Figure 36 (a) predicted velocities of the inner layer and the outer two layers are considerably higher than those observed. This computer run was made using the unmodified program; therefore, gases in the center burster and inner explosive layers, instead of escaping, continue to accelerate the inner fragment layer to unrealistically high velocity. This tendency can be seen to be corrected in 36 (b), (c) and (d), where the "vent" subroutine was incorporated.

The high velocities predicted for the outer one or two layers, seen in all plots of Figure 36 is believed to be due to the one-dimensional character of "Wundy" which renders it unable to take the discrete nature of fragments into account. It treats each fragment layer as an expanding cylindrical shell with an integral surface. In an actual test model, considerable gas escapes through the interstices between fragments, reducing the energy transfer. This effect is believed to be of considerable importance only for the outer one or two layers, where the large pressure drop to the atmosphere leads to rapid gas loss between the fragments. This hypothesis is supported by the experimental data obtained from test model RE-18, as shown in Figure 36 (d). This round consisted of alternating explosive layers and double fragment layers, with a final exterior explosive sheet. One would expect considerably less pressure exchange between layers due to the increased impedance to gas flow of two intersticed fragment layers, as well as the increased external pressure due to detonation of the outer explosive sheet. Figure 36 (d) immediately confirms this expectation; velocity correlation is better than on any previous round considered.

The program, as now operating, is unable to differentiate between two adjacent fragment layers within a round; for this reason each double fragment layer is represented in the computer input data as a single steel layer of thickness equal to that of two intersticed layers of balls. Thus the computer predicted velocity of each group in Figure 36 (d) represents the average velocity of fragments from a double fragment layer.

A modification to the program which will incorporate the effects of interlayer pressure exchange has been conceived and can be incorporated into the program for future use.

(The reverse side of this page is blank.)

SECTION 4 - CONCLUSIONS

The following major conclusions are based on the data resulting from this study:

1 Fourteen layers of fragments can be explosively projected into uniform radial distribution patterns by three variations of the explosive layered design technique - spiral cylinders, concentric ring hyperboloids, and spiral hyperboloids.

2 Fragment beam spray angles for large multi-layered warhead models can be controlled to the order of 30 degrees or less by massive end confinement, fragmenting end plates, hyperboloid shaping, explosive end plates, and combinations of these.

3 Fragment radial velocities can be controlled to achieve distributions ranging from less than 100 to 1000 feet per second with 90 percent of the fragments at velocities below 750 feet per second.

4 A fourteen layered spiral hyperboloid warhead weighing 110 pounds and containing 30,000 fragments and 3 pounds of explosive for a charge to mass ratio of only 0.036 can provide the required performance under dynamic rocket sled test conditions.

5 Long sheets of thin gaged sheet explosive in spiral configurations can be readily initiated by the use of a line wave generator. However, care must be exercised during the warhead fabrication process to insure integrity of explosive splices.

6 Nickel fragments can be projected equally as well as steel fragments by the Spiral Hyperboloid warhead design.

7 It appears impractical to use hollow brass spheres in explosive layered warhead designs.

8 Cubical fragments instead of spherical fragments tend to provide an improved distribution pattern and higher velocities for equivalent charge to mass ratios.

9 Increasing length to diameter ratio from one to two does not degrade performance capability of the Explosive Layered Warhead design technique.

SECTION 5 - RECOMMENDATIONS

It is recommended that research be continued toward evolving a feasible hardware model of a multilayered fragmentation warhead representative of end item configuration. Specific areas in which further research is recommended are:

1 Design study and analysis to establish specific warhead design(s) compatible with anticipated system usage including considerations of size and weight, beam spray angle, expansion rate, distribution density, total weight and space allocations, dynamic loadings, and environmental conditions;

2 Fabrication and static arena testing of selected warhead design(s) to confirm capability to meet performance requirements including effects of structural elements and potential mounting fixtures;

3 Structural testing to evolve configuration(s) capable of withstanding anticipated dynamic and environmental conditions including static bending test, as well as centrifuge and vibration test under ambient and low temperatures.

4 Fabrication and arena testing of end-item warhead configurations after subjecting them to vibration, centrifuge, and low temperature environments.

5 Demonstrate functional feasibility under dynamic rocket sled test conditions.

6 The performance capability of the spiral hyperboloid can be further improved and more efficient utilization of weight achieved by incorporating fragmenting end plates and optimizing the design of structural members.

7 Modification of the "Quasi-Wundy" computer code to consider gas pressure venting can accurately predict the velocity performance of large multi-layered warhead designs. In the future, this modified program can be used to reduce the number of experimental test firings.

(The reverse side of this page is blank.)

REFERENCES

1 ATL Technical Documentary Report, No. 64-9, Project No. 2835, "Radially Expanding Fragmentation Warhead Study," Summary Report, W. R. Porter - Martin Company, Orlando, Florida, March 1964, Confidential.

2 "R&D Exhibit No. ASQW62-48A," Detachment-4, Weapons Division, R.T.D., Air Force Systems Command, Eglin Air Force Base, Florida, January 1964, Confidential.

3 Technical Note No. 1470, Ballistic Research Laboratories, Aberdeen, Maryland, "Simultaneity of Explosion Times of Engineers Special Detonators," E. Bonner, L. Bryant, J. Trimble, August 1962, Unclassified.

4 DuPont Explosive Specialties, Section 2, "Detasheet," Flexible Explosive, A-33087.

5 OR 3807P, The Martin Company, "Radially Expanding Fragmentation Warhead Study," January 1964, Confidential.

(The reverse side of this page is blank.)

APPENDIX 1

This appendix presents detailed data on all warhead models that have been test fired. It presents data pertinent to specific design concepts, delineates test objectives, and where possible shows the results of particular design variable changes. Round numbers 90 through 109 were accomplished as a terminal series of firings following the publication of summary report ATL-64-9 under contract AF 08(635)3269. Rounds RE-1 through RE-23 include the large 14 fragment layered test models and were accomplished under contract AF 08(635)4263.

Rnd. No.	Round Description	Parameters Varied	Test Objective	Results and Comments
90	Type - Spiral Cylinder Fragment Nos., 3772 Fragment Wt. (Grams), 3961 Explosive Wt. (Grams), 244 End Plate Wt. (Grams), 2055 Inert Filler Wt. (Grams), 549 Total Wt. (Pounds), 15.2 C/M, 0.054 Figure No. 37	0.042" Explosive sheet out-outside tab line initiated.	Test end line initiation of thin gage PETN	Inner four layer velocities not recorded - probable initiation problem.
91	Type - Spiral Cylinder Fragment Nos., 1694 Fragment Wt. (Grams), 1799 Explosive Wt. (Grams), 66 End Plate Wt. (Grams), 1189 Inert Filler Wt. (Grams), 368 Total Wt. (Pounds), 7.5 C/M, 0.030 Figure No. 38	0.025" Explosive sheet. 1/2" RDX center burster explosive brought into center and into contact with blasting cap.	Initiation potential and feasibility of reducing overall average velocity.	Little gradient 600-800 FPS - same results as RDS 70 and 71; probable initiation problem.
92	Type - Spiral Cylinder Fragment Nos., 1624 Fragment Wt. (Grams), 1705 Explosive Wt. (Grams), 104 End Plate Wt. (Grams), 1053 Inert Filler Wt. (Grams), 200 Total Wt. (Pounds), 6.7 C/M, 0.055	Same as 91 except using 0.042 explosive sheet.	Same as Round 91	Confirmed results of Round 91.
93	Type - Spiral Cylinder Fragment Nos., 1550 Fragment Wt. (Grams), 1628 Explosive Wt. (Grams), 53 End Plate Wt. (Grams), 1066 Inert Filler Wt. (Grams), 201 Total Wt. (Pounds), 6.5 C/M, 0.029 Figure No. 39	0.025" Explosive sheet.	Investigate end line initiation of 0.025 PETN and reduction of overall initial velocities.	Little gradient avg. 400-600 FPS - probable incomplete initiation.

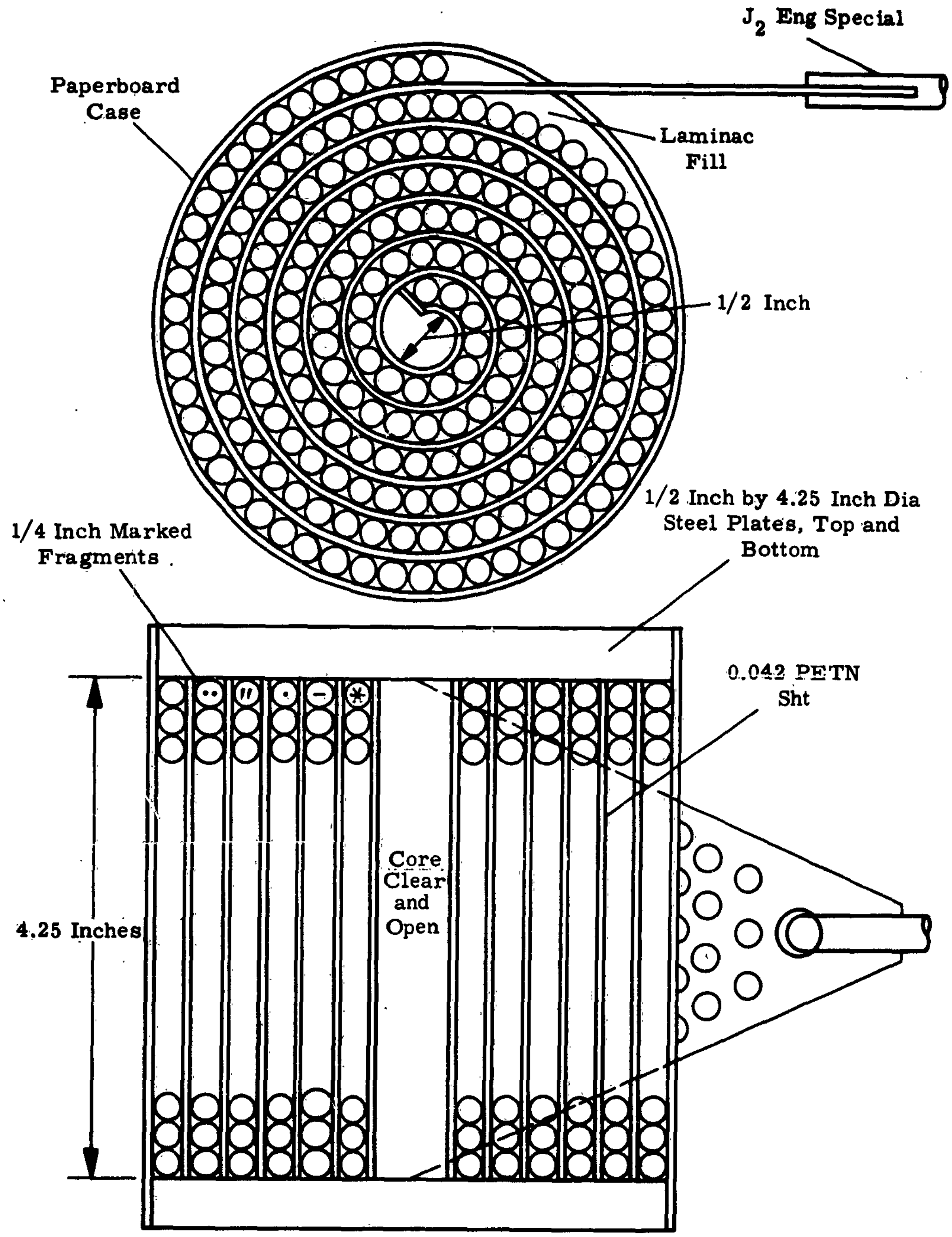

Figure 37. Test Model Design, Round 90

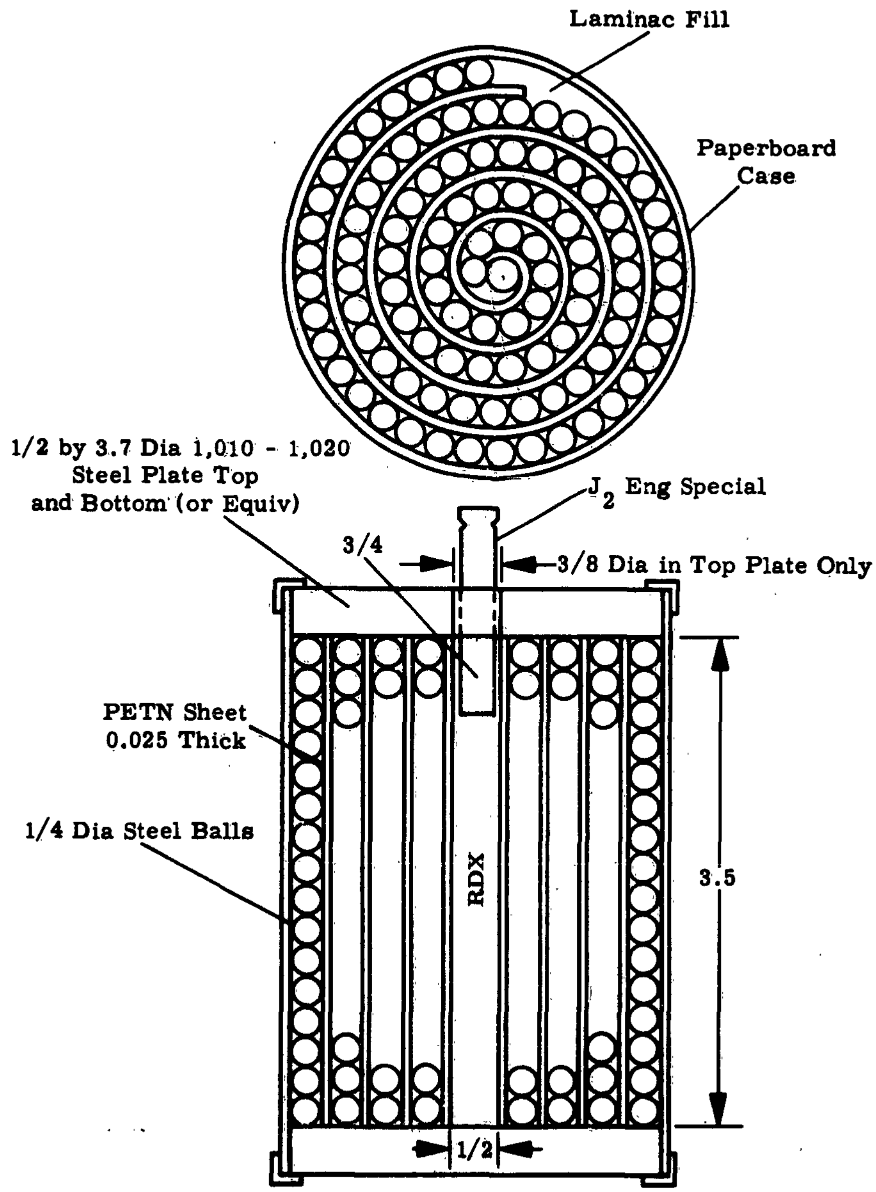

Figure 38. Test Model Design, Round 91

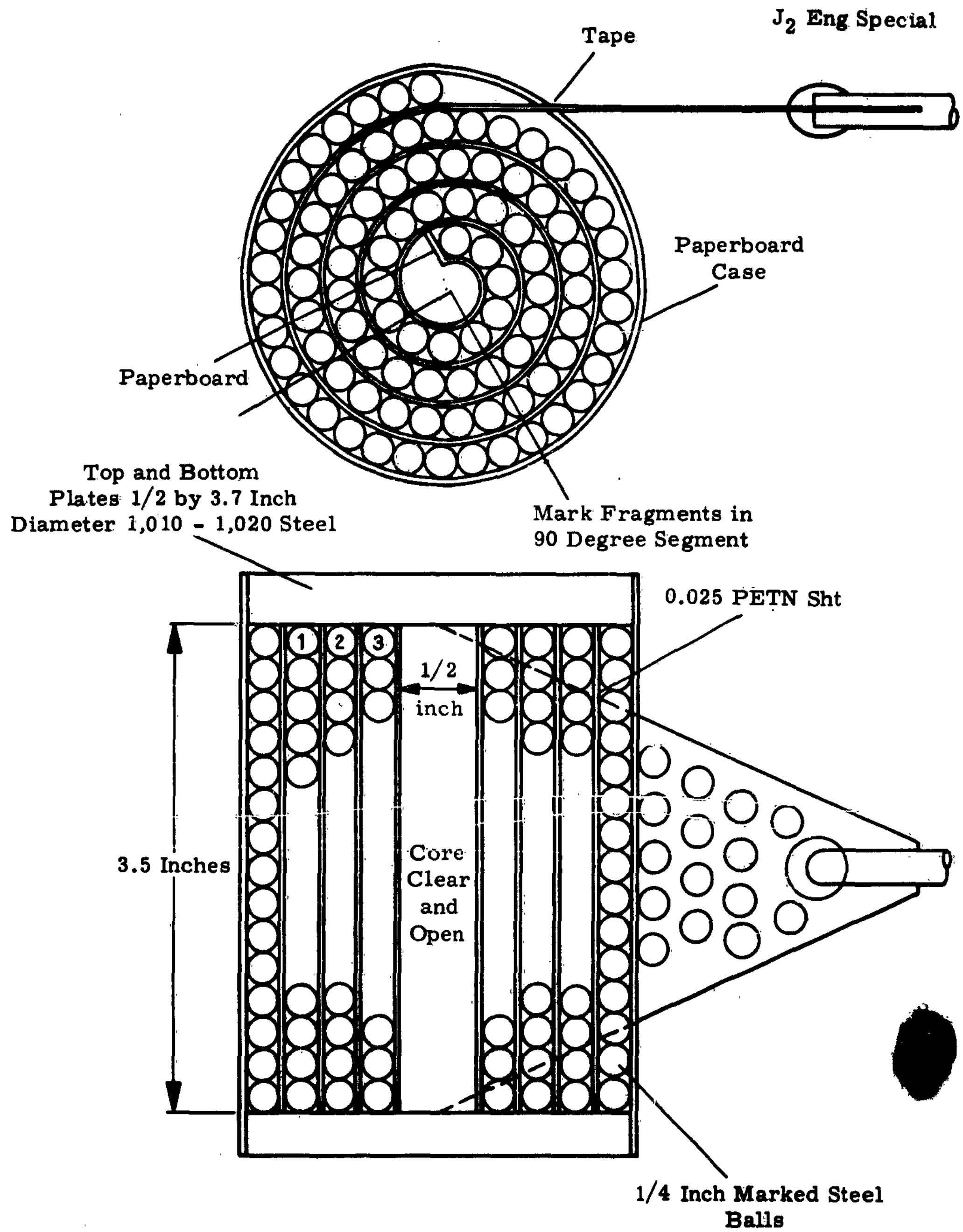

Figure 39. Test Model Design, Round 93

Rnd. No.	Round [redacted]tion	Parameters Varied	Test Objective	Results and Comments
94	Type - Concentric Hyperboloid Fragment Nos., 4510 Fragment Wt. (Grams), 4736 Explosive Wt. (Grams), 505 End Plate Wt. (Grams), 2913 Inert Filler Wt. (Grams), 548 Total Wt. (Pounds), 19.2 C/M, 0.096 Figure No. 40	Reshaping of model geometry. 0.084 sheet explosive.	Investigate feasibility of hyperboloid configuration for beam spray control.	Gradient 300-1900 FPS; Beam spray - approx. 20° - good control potential.
95	Type, Same as Round 94 Fragment Nos., 4383 Fragment Wt. (Grams), 4600 Explosive Wt. (Grams), 514 End Plate Wt. (Grams), 2907 Inert Filler Wt. (Grams), 427 Total Wt. (Pounds), 18.6 C/M, 0.102 Figure No. 40	Same as Round 94	Same as Round 94	Impact Pattern Figure 41. Confirmed results of round No. 94. Beam spray 21°. Polar Plot Figure 42
96	Type, Concentric Ring Fragment Nos., 1130 Fragment Wt. (Grams), 1187 Explosive Wt. (Grams) 75 End Plate Wt. (Grams), 1104 Inert Filler Wt. (Grams), 183 Total Wt. (Pounds), 5.6 C/M, 0.033 Figure No. 43	0.042" Explosive sheet	Initiation potential and feasibility of reducing overall avg. velocity.	Gradient 400-1100 FPS, Apparent complete initiation, good velocity reduction potential.
97	Type, Spiral Fragment Nos., 3281 Fragment Wt. (Grams), 3937 Explosive Wt. (Grams), 243 End Plate Wt. (Grams), 1930 Inert Filler Wt. (Grams), 524 Total Wt. (Pounds), 14.6 C/M, 0.054	Repeat of Round 90	Investigate detonation propagation over splices in explosive.	Layers to inside of splice not recovered confirming interruption at splice.

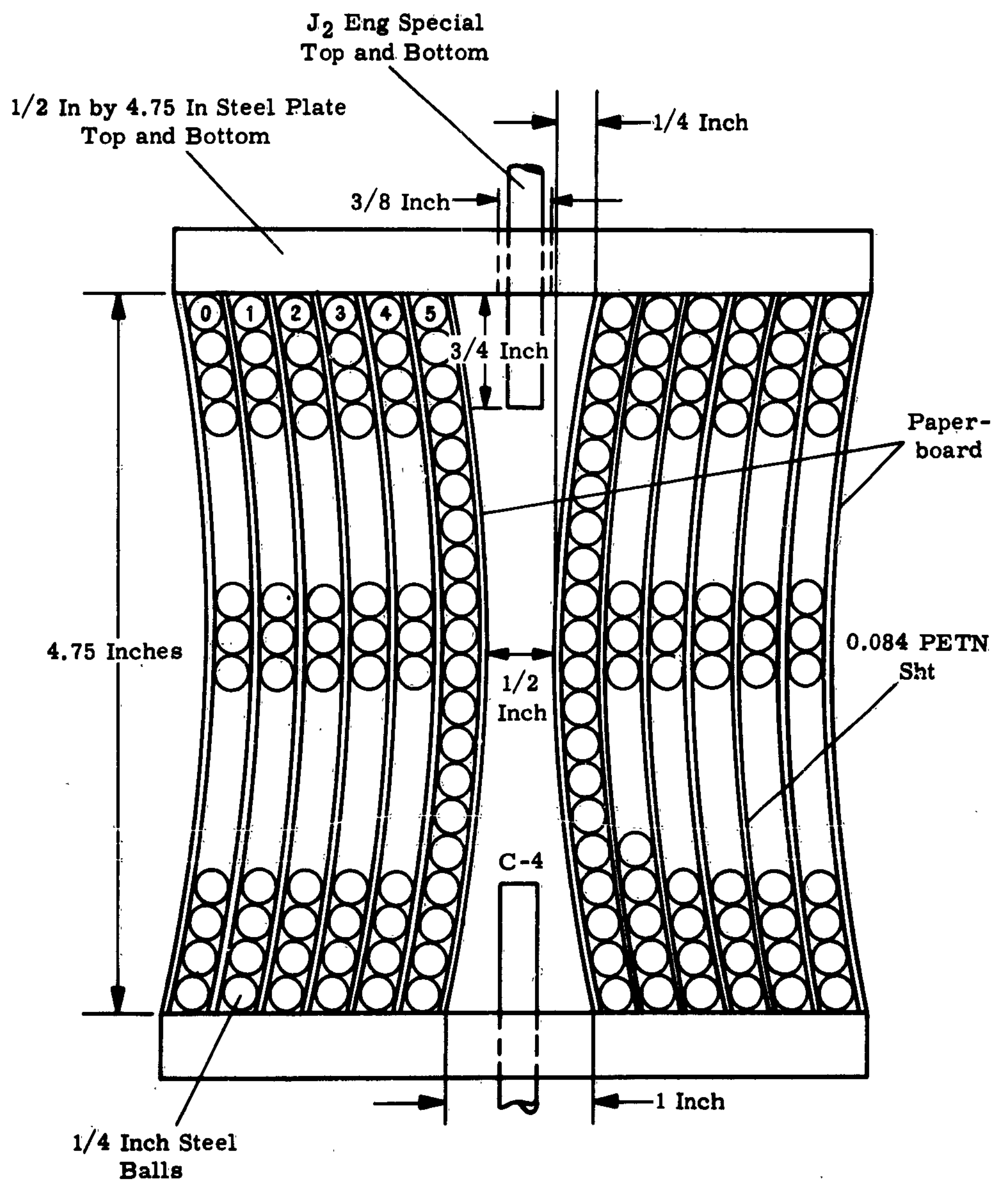

Figure 40. Test Model Design, Rounds 94 and 95

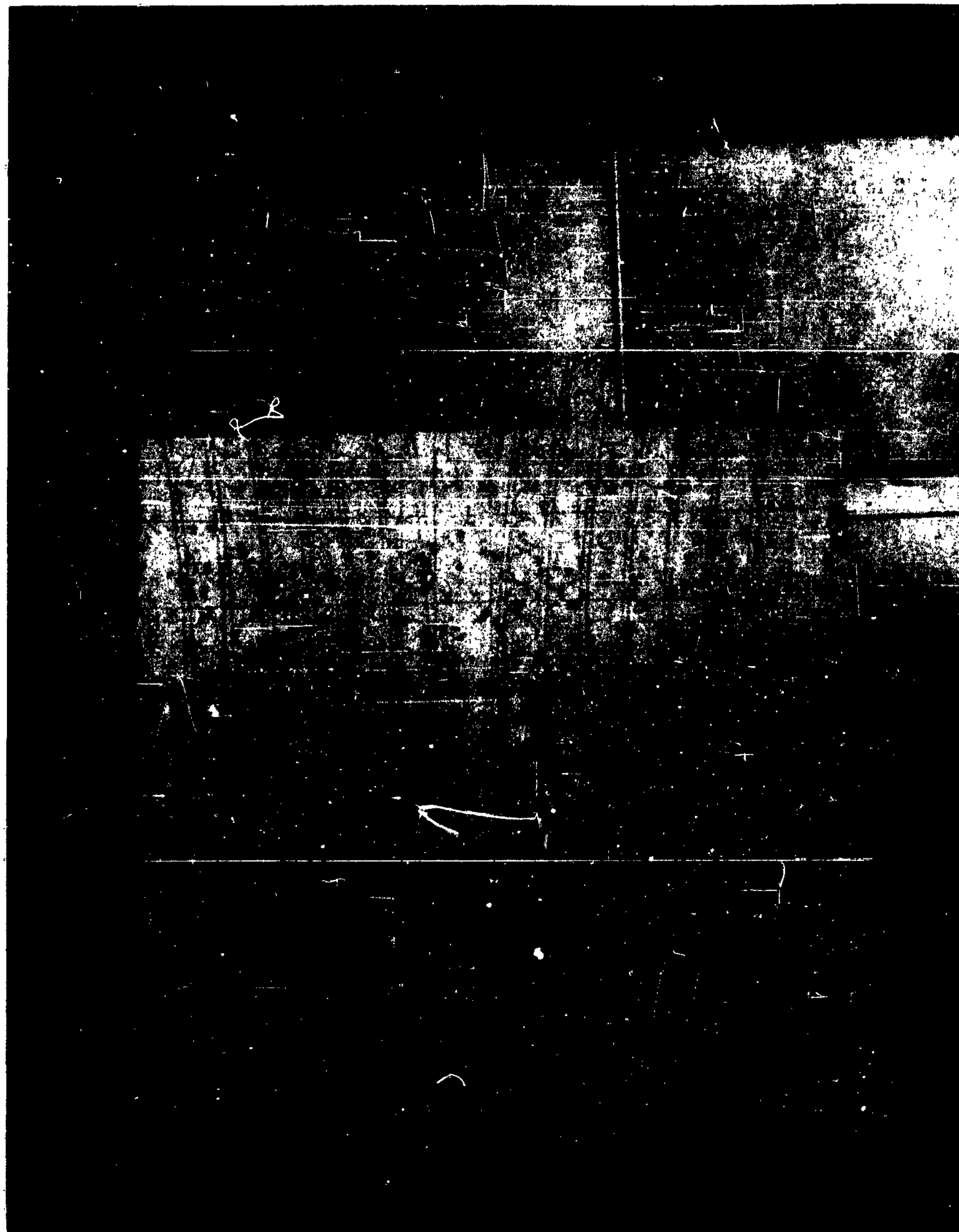

Figure 41. Impact Pattern, Round 95

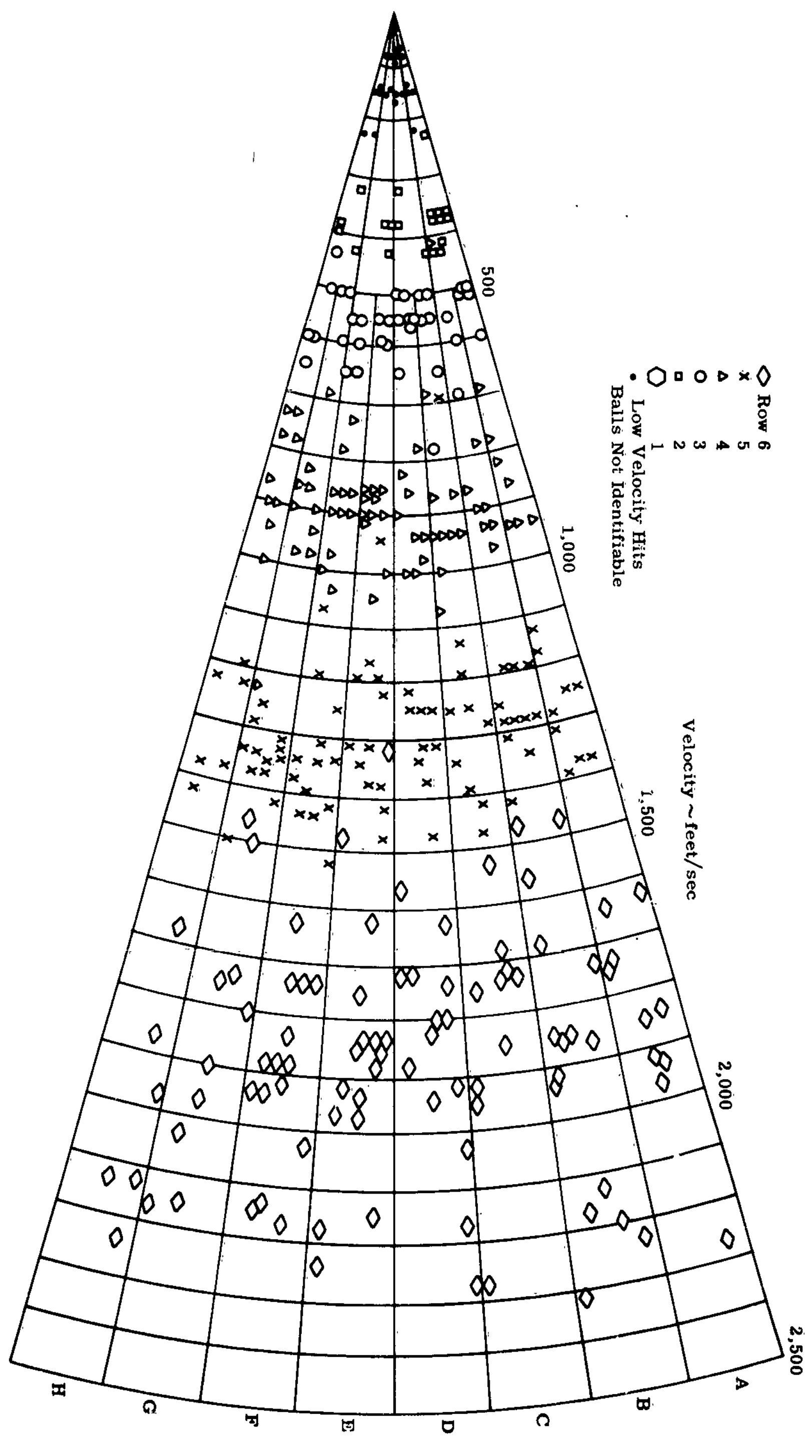

Figure 42. Velocity versus Radial Distribution, Round 95

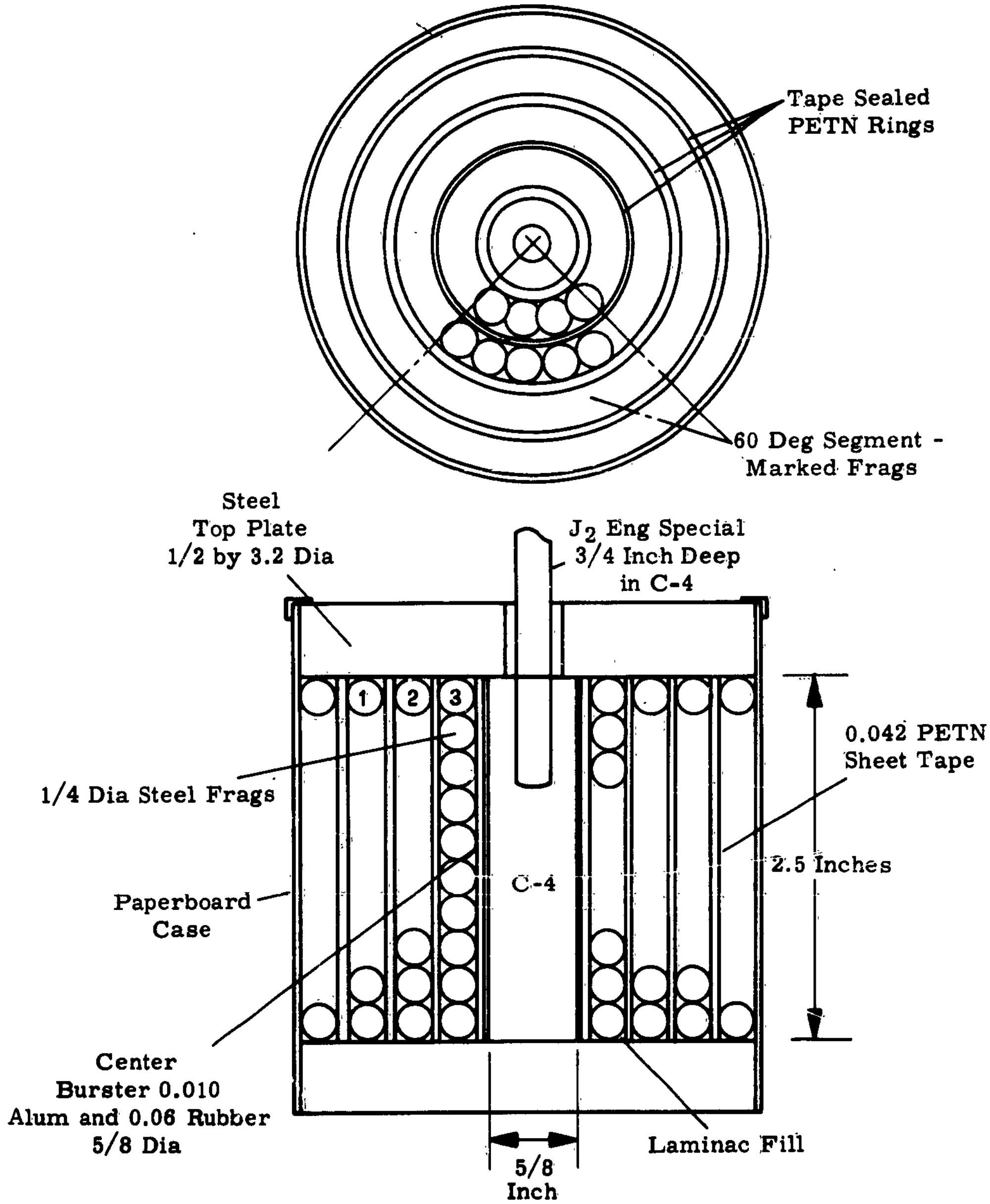

Figure 43. Test Model Design, Round 96

Rnd. No.	Round Description	Parameters Varied	Test Objective	Results and Comments
98	Type, Concentric Ring Fragment Nos., 4219 Fragment Wt. (Grams), 4732 Explosive Wt. (Grams), 157 End Plate Wt. (Grams), 2301 Inert Filler Wt. (Grams), 691 Total Wt. (Pounds), 17.4 C/M, 0.029 Figure No. 44	Double layers of fragments between explosive sheet 6 layers	Test feasibility for reduction of overall average fragment velocity.	Incomplete detonation frags moved as low-velocity group, approx. 350 FPS. Beam Spray - 8°.
99	Type, Concentric Ring Fragment Nos., 88.2 Fragment Wt. (Grams), 9693 Explosive Wt. (Grams), 357 End Plate Wt. (Grams), 3650 Inert Filler Wt. (Grams), 1382 Total Wt. (Pounds), 33.2 C/M, 0.032 Figure No. 44	Same as 98 except 8 layers	Same as 98	Confirmed results of Round 98. Beam Spray - 8°. Impact Pattern Figure 45.
100	Type, Spiral Cylinder Fragment Nos., 4840 Fragment Wt. (Grams), 5566 Explosive Wt. (Grams), 342 End Plate Wt. (Grams), 2582 Inert Filler Wt. (Grams), 525 Total Wt. (Pounds), 20 C/M, 0.056 Figure No. 46	Double layers of fragments between spiral explosive sheet - 6 layers	Test feasibility of double fragment layers for reduction of overall average fragment velocity	Feasibility Demonstrated, gradient from less than 100 to 1200 FPS.
101	Type, Spiral Cylinder Fragment Nos., 9080 Fragment Wt. (Grams), 9988 Explosive Wt. (Grams), 426 End Plate Wt. (Grams), 3649 Inert Filler Wt. (Grams), 1509 Total Wt. (Pounds), 34.3 C/M, 0.037 Figure No. 46	Repeat of Round 100 - 8 layers	Test of velocity reduction with additional double fragment layer.	Gradient same as 100, with max. velocity about 1300 FPS. Impact Pattern Figure 47.

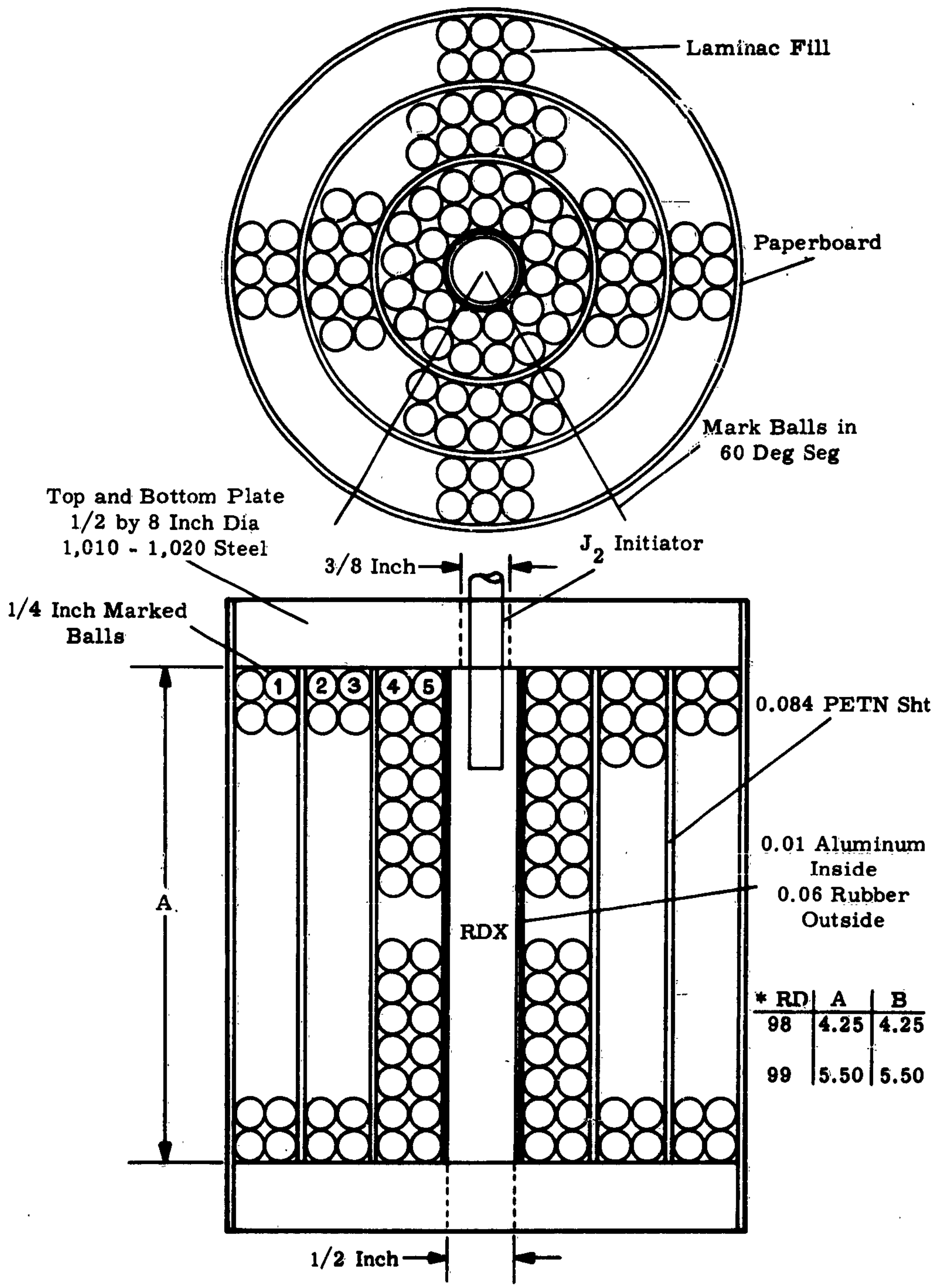

* RD	A	B
98	4.25	4.25
99	5.50	5.50

Figure 44. Test Model Design, Rounds 98 and 99

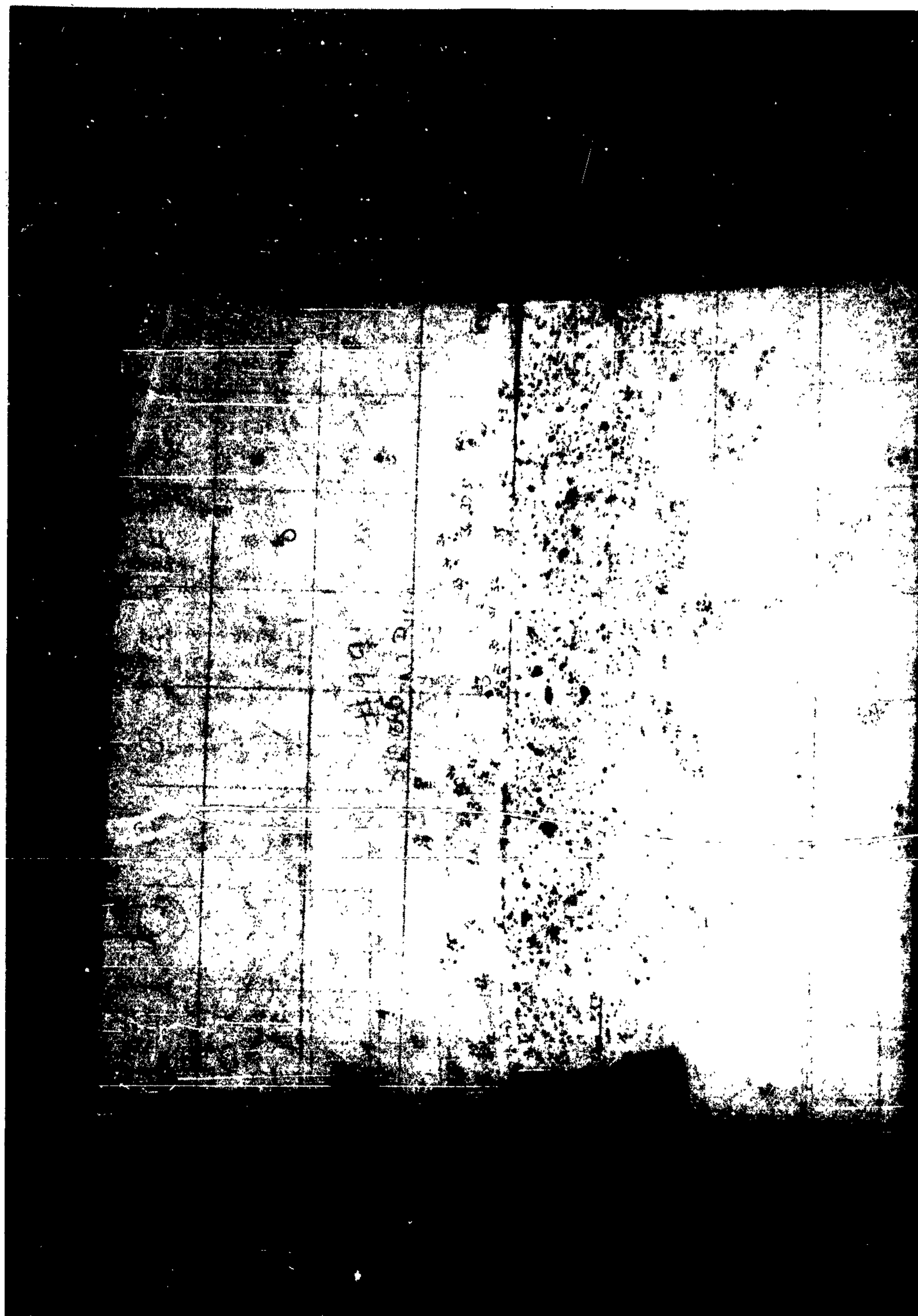

Figure 45. Impact Pattern, Round 99

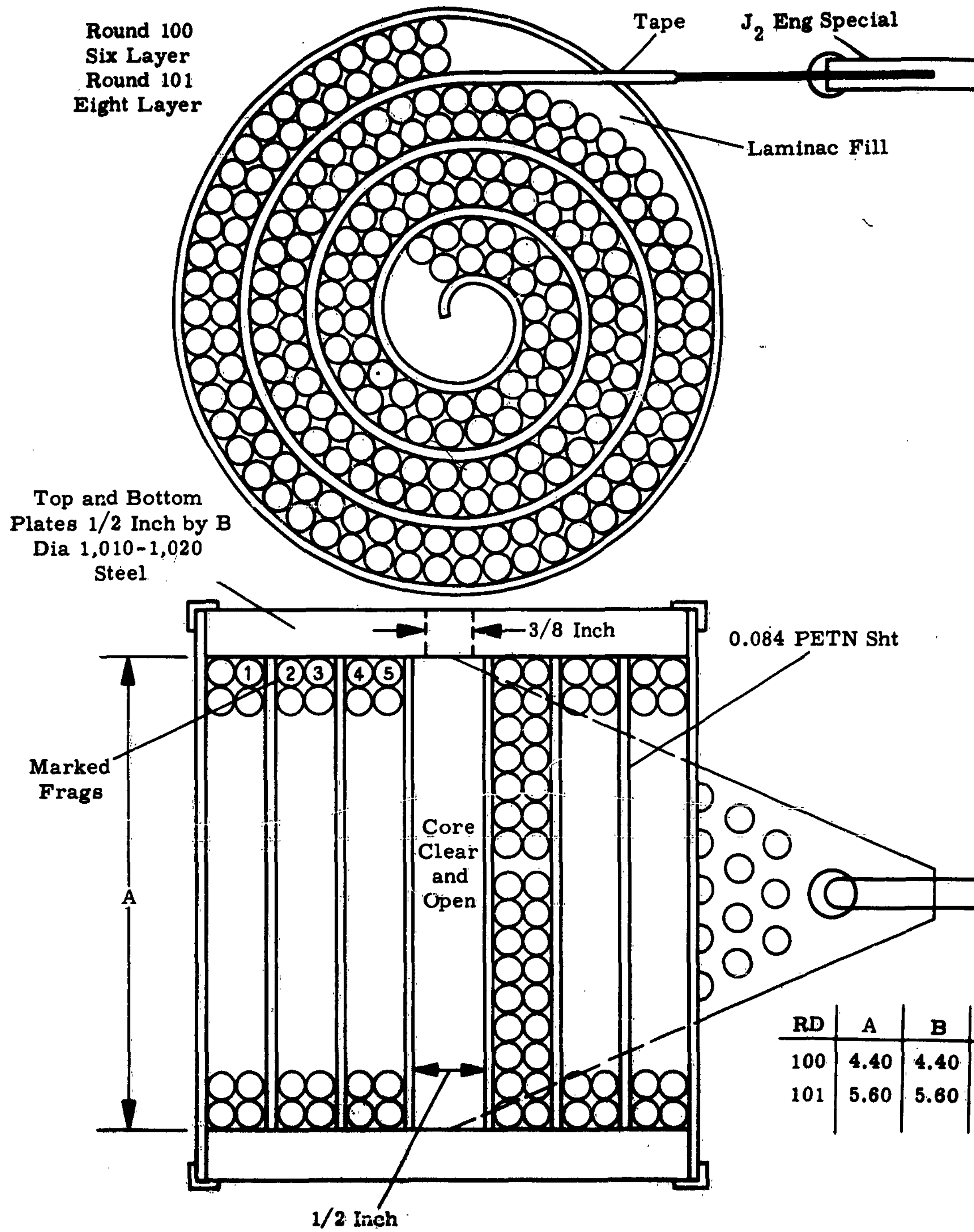

Figure 46. Test Model Design, Rounds 100 and 101

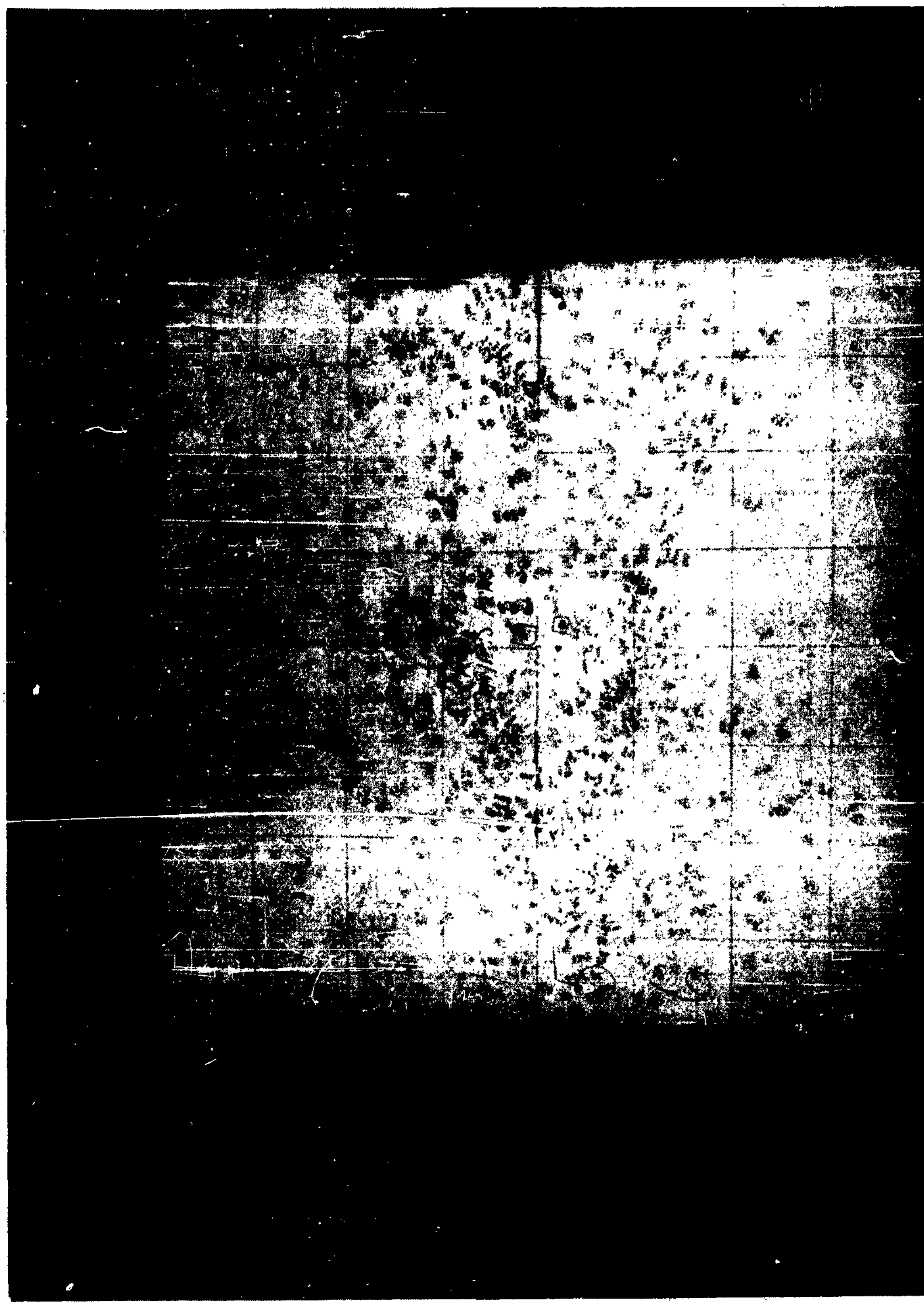

Figure 47. Impact Pattern, Round 101

Rnd. No.	Round Description	Parameters Varied	Test Objective	Results and Comments
102	Type, Concentric Hyperboloid Fragment Nos., 5464 Fragment Wt. (Grams), 6010 Explosive Wt. (Grams), 637 End Plate Wt. (Grams), 3340 Inert Filler Wt. (Grams), 1154 Total Wt. (Pounds), 24.5 C/M, 0.089 Figure No., 48	Increased hyperboloid curvature to 1/2"	Test effect of increased hyperboloid curvature.	Beam Spray - 12° Radiograph of expanding round, Figure 49.
103	Type, Concentric Hyperboloid Fragment Nos., 5646 Fragment Wt. (Grams), 6211 Explosive Wt. (Grams), 618 End Plate Wt. (Grams), 3304 Inert Filler Wt. (Grams), 725 Total Wt. (Pounds), 24 C/M, 0.89 Figure No., 48	Same as Round 102	Confirm Round 102 results, confirm pattern continuity over 360°, determine velocity and space distributions, confirm beam spray control.	Impact Pattern Figure 50. Polar Plot, Figure 51. Results similar to 102, continuous pattern, velocities 225 - 1540 FPS 90% of frags within 15°
104	Type, Spiral Cylinder Fragment Nos., 4020 Fragment Wt. (Grams), 4422 Explosive Wt. (Grams), 210 End Plate Wt. (Grams), 2302 Inert Filler Wt. (Grams), 834 Total Wt. (Pounds), 17.1 C/M, 0.040 Figure No., 52	Filled center void with frags, used explosive adhesive on sheet explosive splices.	Test initiation with increased confinement in frag pack. Increase density distribution of center fragments. Determine velocity and space distributions.	Complete detonation large No. low velocity frags in ground plane, velocity < 225-1250 ft/sec.
105	Type, Spiral Cylinder Fragment Nos., 6205 Fragment Wt. (Grams), 6825 Explosive Wt. (Grams), 305 End Plate Wt. (Grams), 2692 Inert Filler Wt. (Grams), 1093 Total Wt. (Pounds), 24 C/M, 0.039 Figure No., 53	Repeat of Round 100 except center void filled with frags-8 layers of frags.	Investigate effects of double fragment layers. Increase density of low velocity frags. Determine velocity and space distributions Test initiation.	Improved distribution of low velocity frags. Flash radiography confirms high density of low velocity frags. Vel. < 150-1440 ft/sec. Complete detonation. Impact Pattern Figure 54.

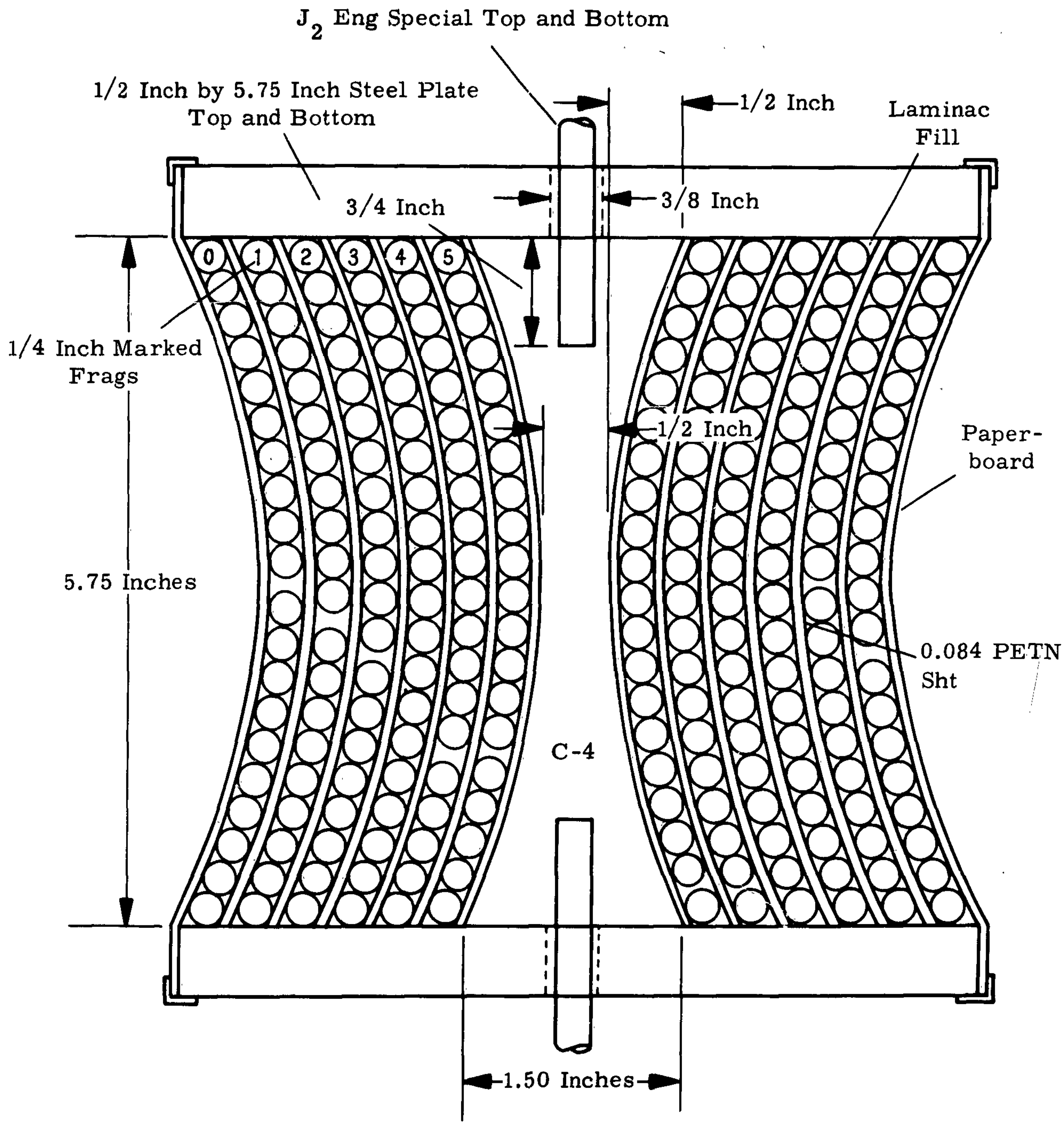

Figure 48. Test Model Design, Rounds 102 and 103

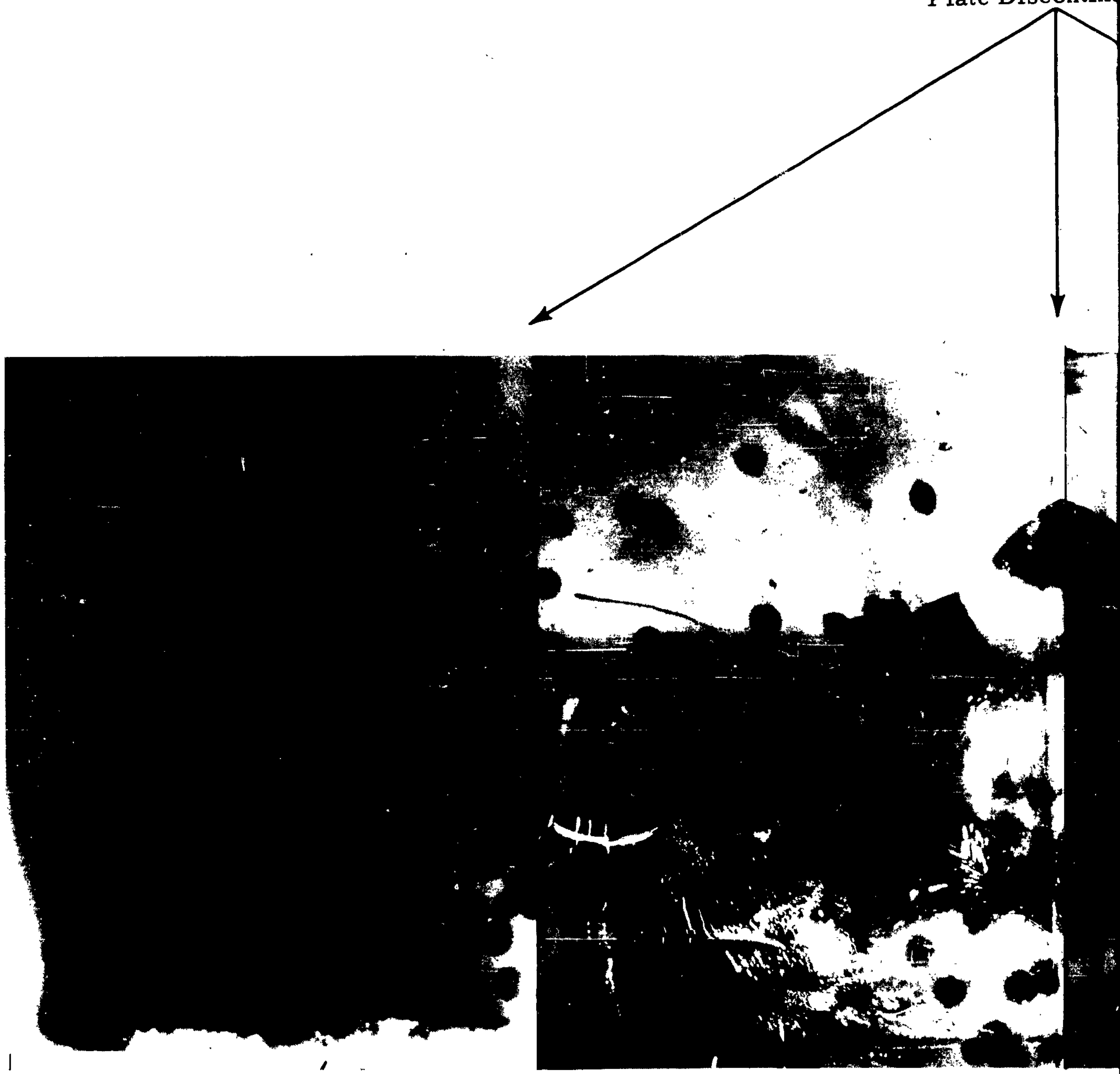

Figure 49. Flash Radiography of

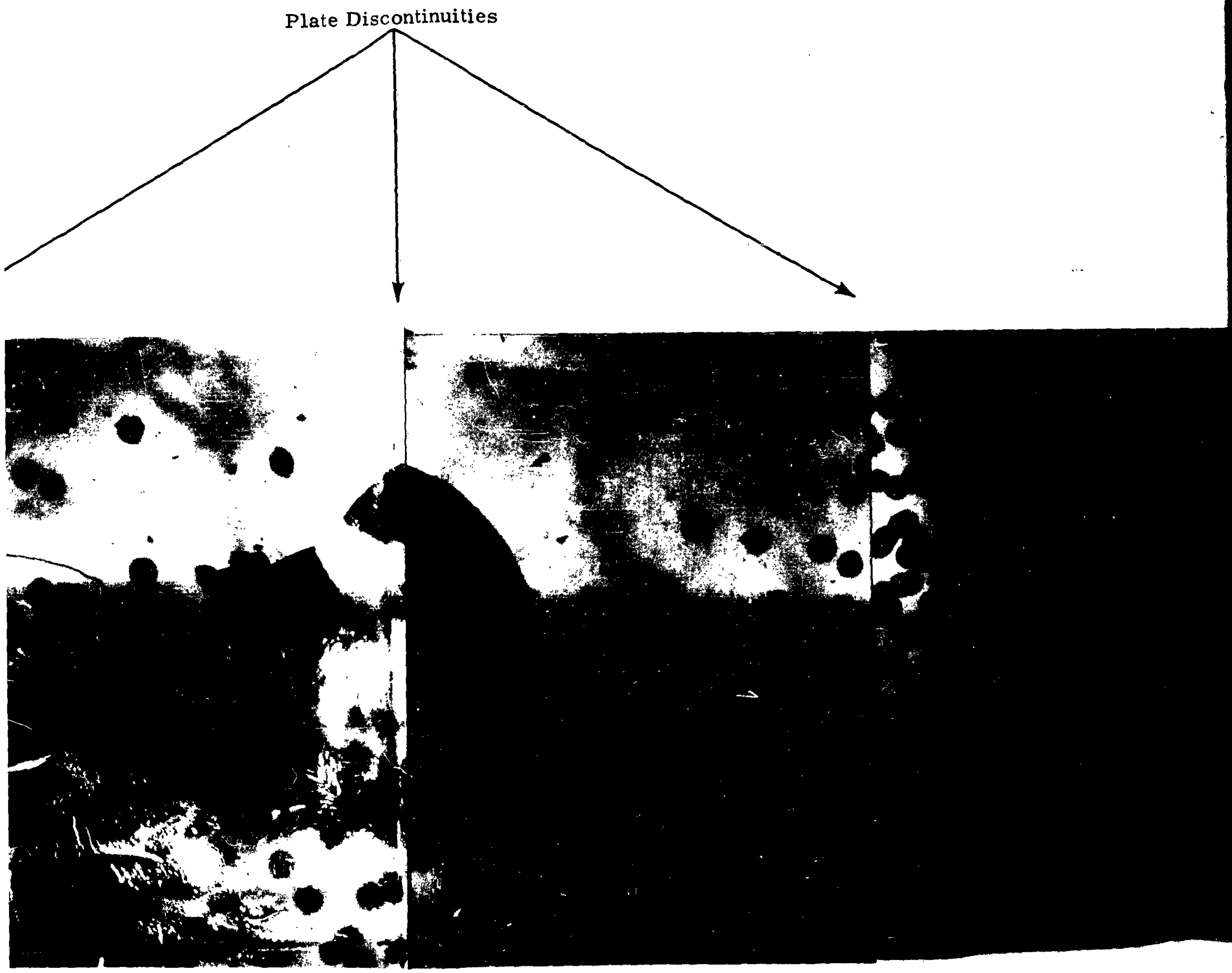

Figure 49. Flash Radiography of Test, Round 102

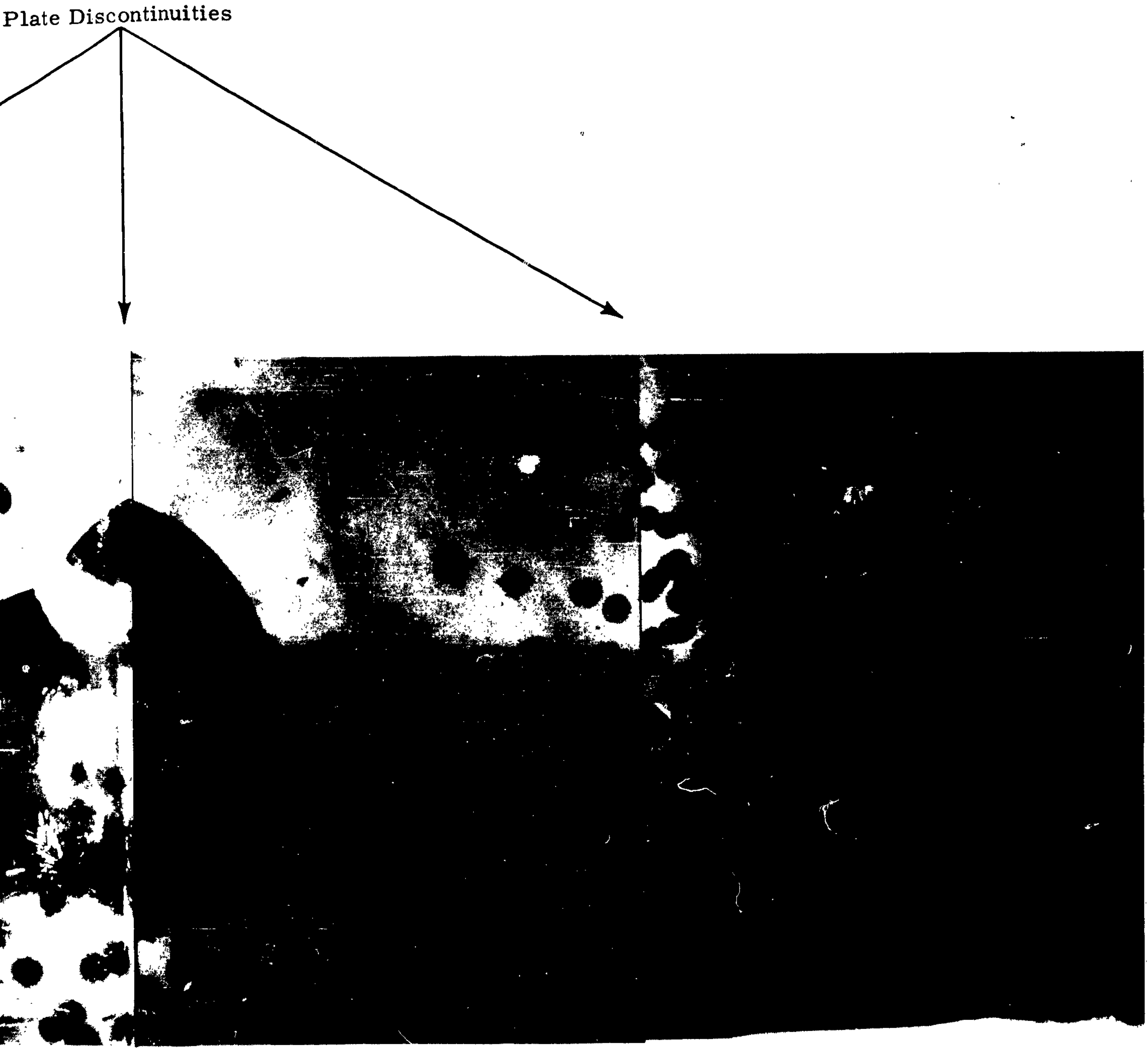

h Radiography of Test, Round 102

Figure 50. Impact Pattern, Round 103

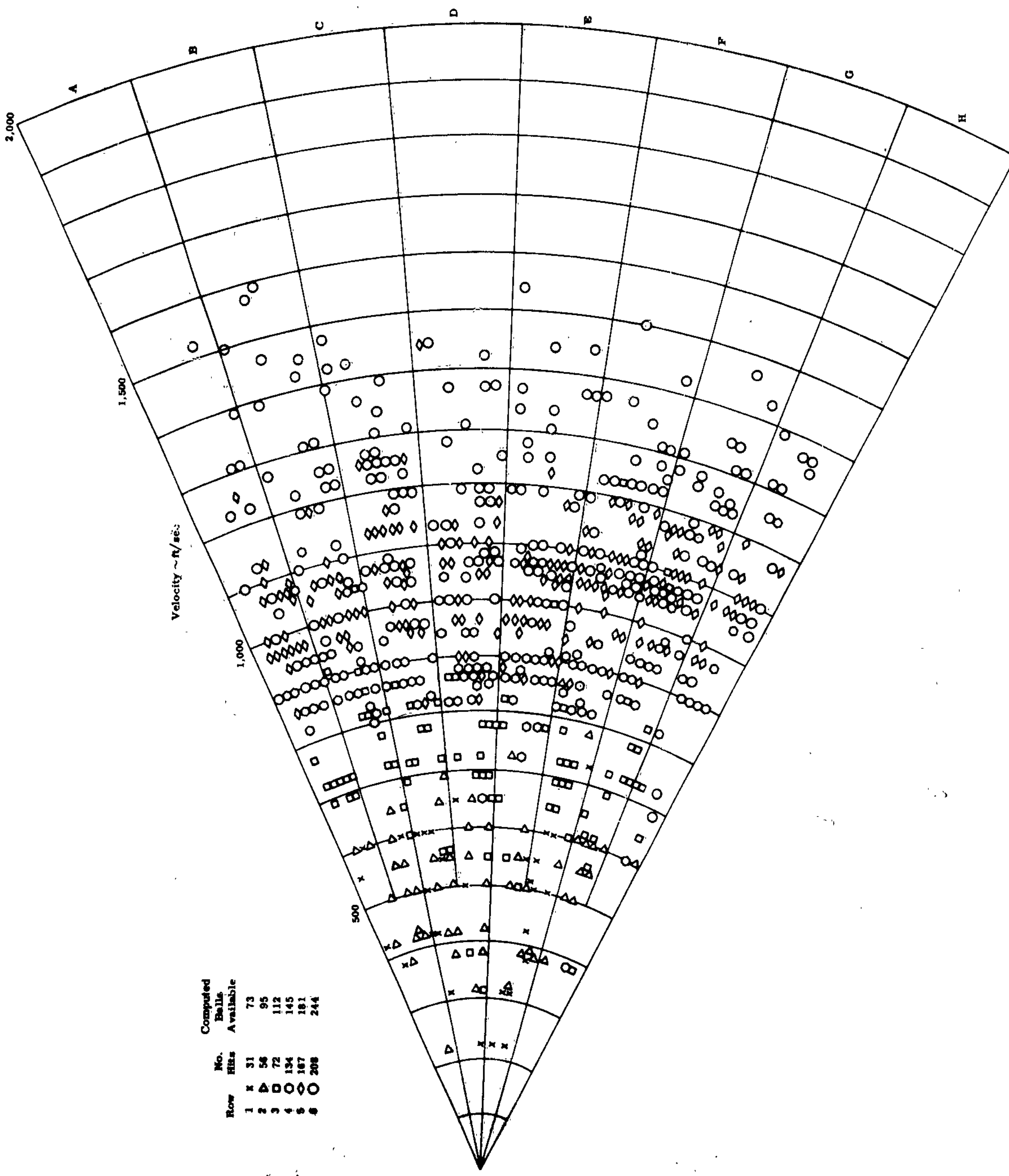

Figure 51. Velocity versus Radial Distribution, Round 103

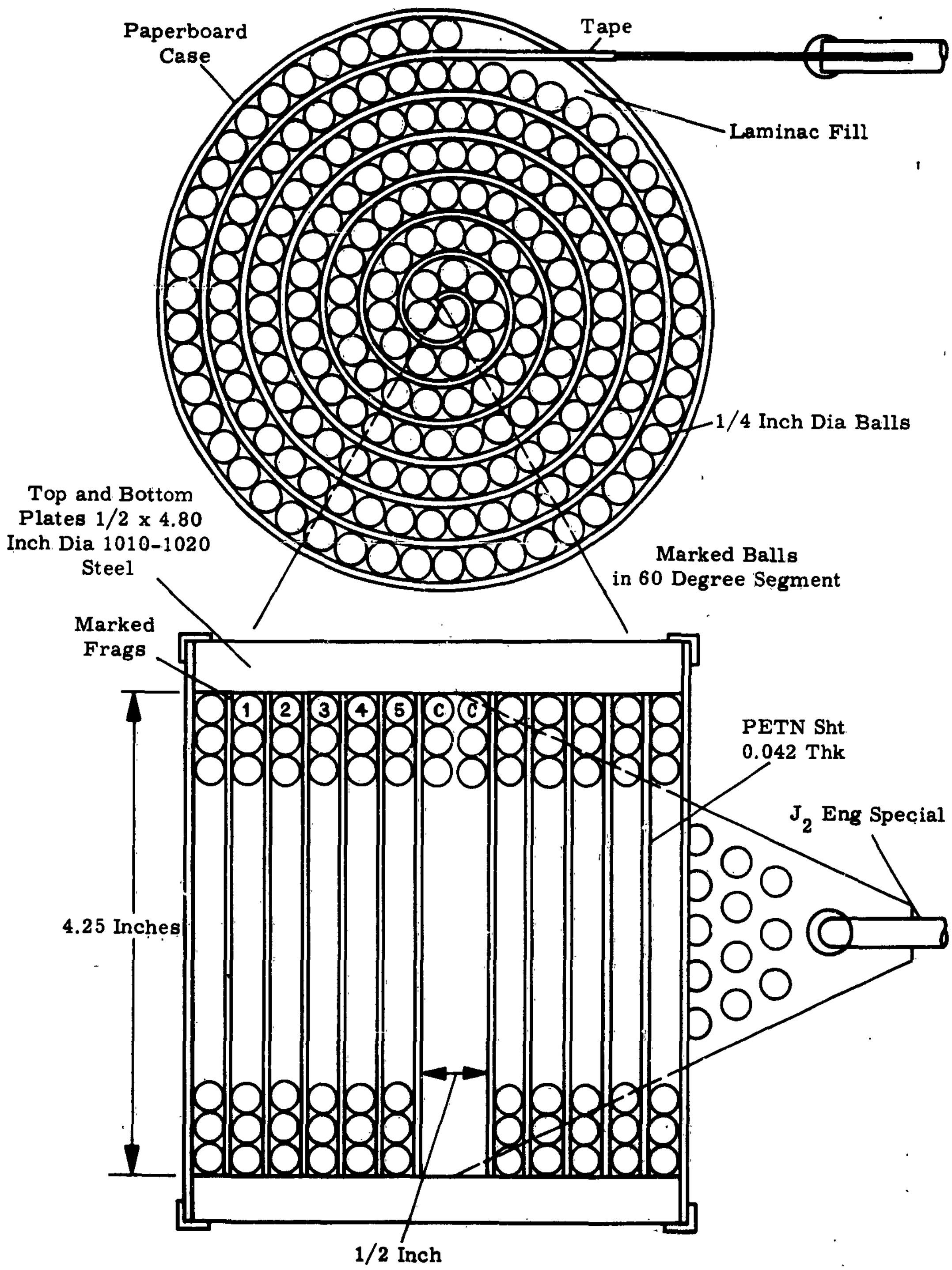

Figure 52. Test Model Design, Round 104

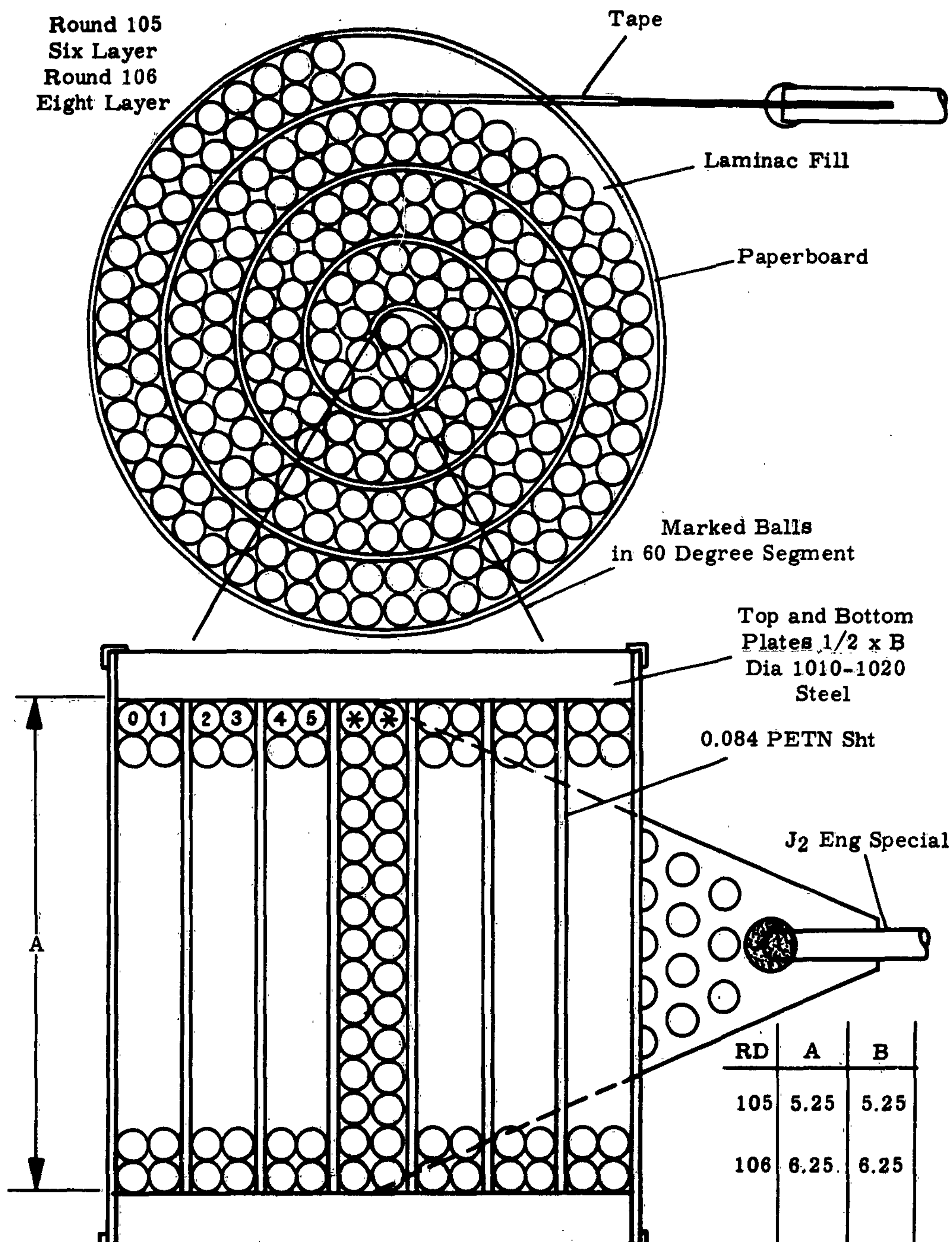

RD	A	B
105	5.25	5.25
106	6.25	6.25

Figure 53. Test Model Design, Rounds 105 and 106

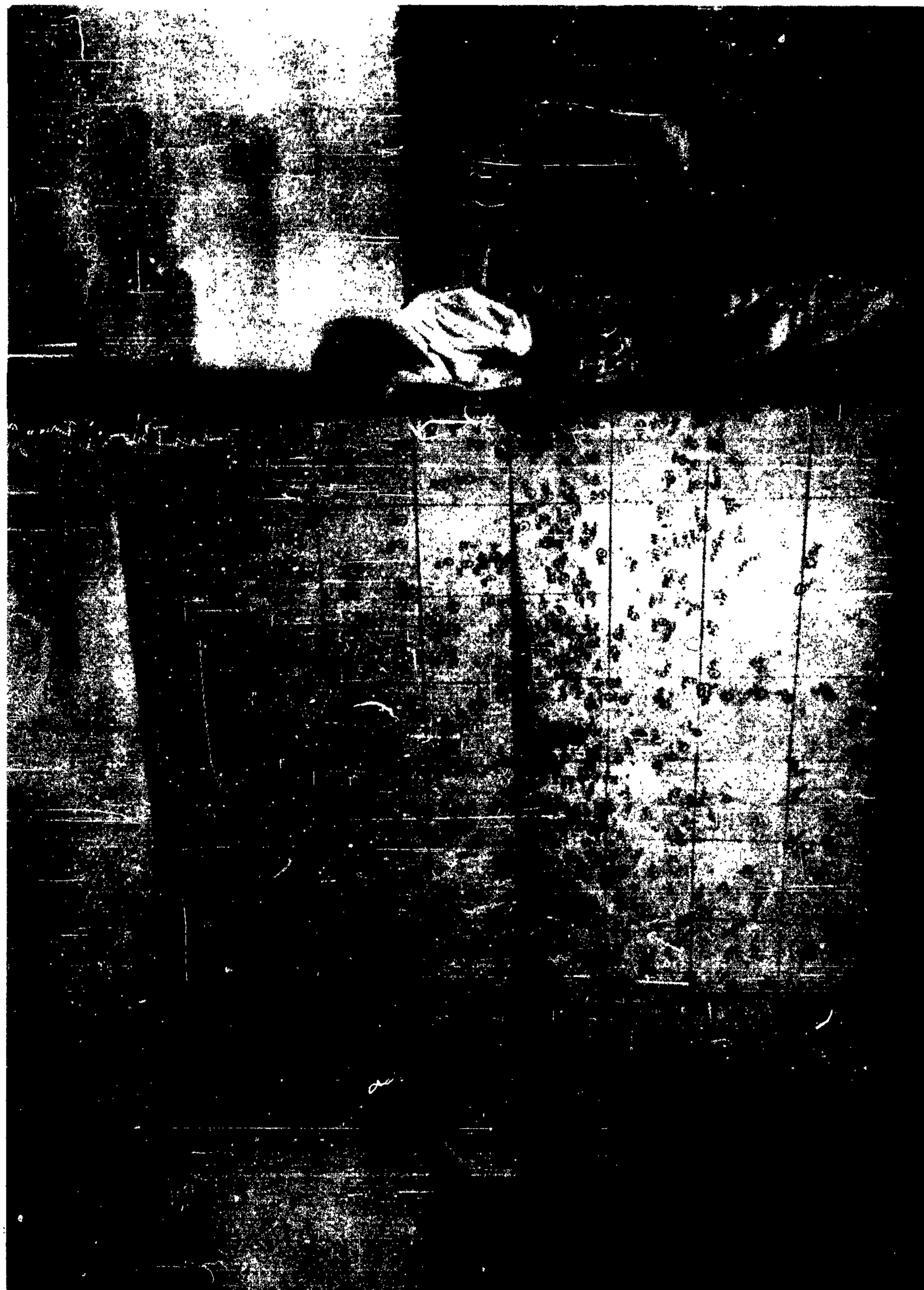

Figure 54. Impact Pattern, Round 105

Rnd. No.	Round Description	Parameters Varied	Test Objective	Results and Comments
106	Type, Spiral Cylinder Fragment Nos., 10,826 Fragment Wt. (Grams), 11,909 Explosive Wt. (Grams), 552 End Plate Wt. (Grams), 4232 Inert Filler Wt. (Grams), 2358 Total Wt. (Pounds), 42 C/M, 0.039 Figure No., 53	Same as 105 except 10 layers of frags.	Same as 105	Confirmed results of Round 105. Velocity 150-1540 ft/sec. Polar Plot Figure 55.
107	Type, Concentric Hyperboloid Fragment Nos., 2049 Fragment Wt. (Grams), 2254 Explosive Wt. (Grams), 287 End Plate Wt. (Grams), 94 Inert Filler Wt. (Grams), 484 Total Wt. (Pounds), 6.9 C/M, 0.105 Figure No., 56	Explosive end plates; 0.084" sheet explosive. 1/4" curvature; 4 layers.	Fragment beam spray control. Determine velocity and space distributions.	Velocity 150-1880 ft/sec. Flash radiography confirms velocity distributions. 87% of fragments within 12°
108	Type, Concentric Hyperboloid Fragment Nos., 2032 Fragment Wt. (Grams), 2235 Explosive Wt. (Grams), 225 End Plate Wt. (Grams), 1087 Inert Filler Wt. (Grams), 479 Total Wt. (Pounds), 8.9 C/M, 0.083 Figure No., 57	Same as 107 except using fragmenting end plates instead of exploding.	Fragment beam spray control. Determine velocity and space distribution effects of fragmenting end plates.	82% of frags within 12°. Impact Pattern Fig. 58 Vel. 225 to 1480 ft/sec. Hvy frag concentration in end plate panel, velocity approx. 1000 FPS.
109	Type, Spiral Cylinder Fragment Nos., 3772 Fragment Wt. (Grams), 4149 Explosive Wt. (Grams), 131 End Plate Wt. (Grams), 2224 Inert Filler Wt. (Grams), 697 Total Wt. (Pounds), 15.9 C/M, 0.027 Figure No., 59	0.025" sheet explosive same as 104 except for above.	Test initiation. Determine velocity and space distribution. Reduce overall avg. velocities.	Complete detonation 150-879 ft/sec. Polar Plot Fig. 60. Impact Pattern Fig. 61. 82% of hits within 12°.

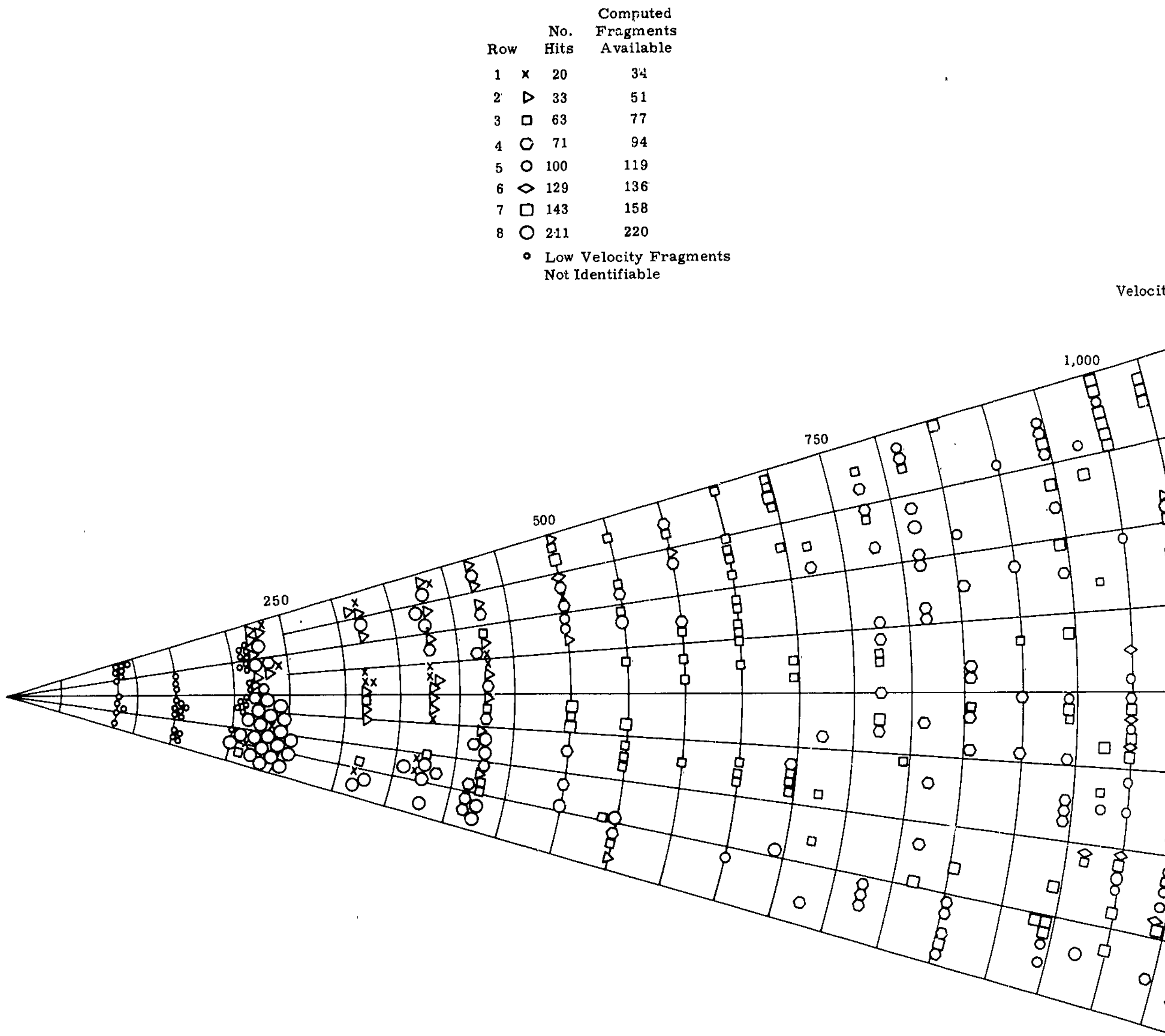

Figure 55. Velocity versus F

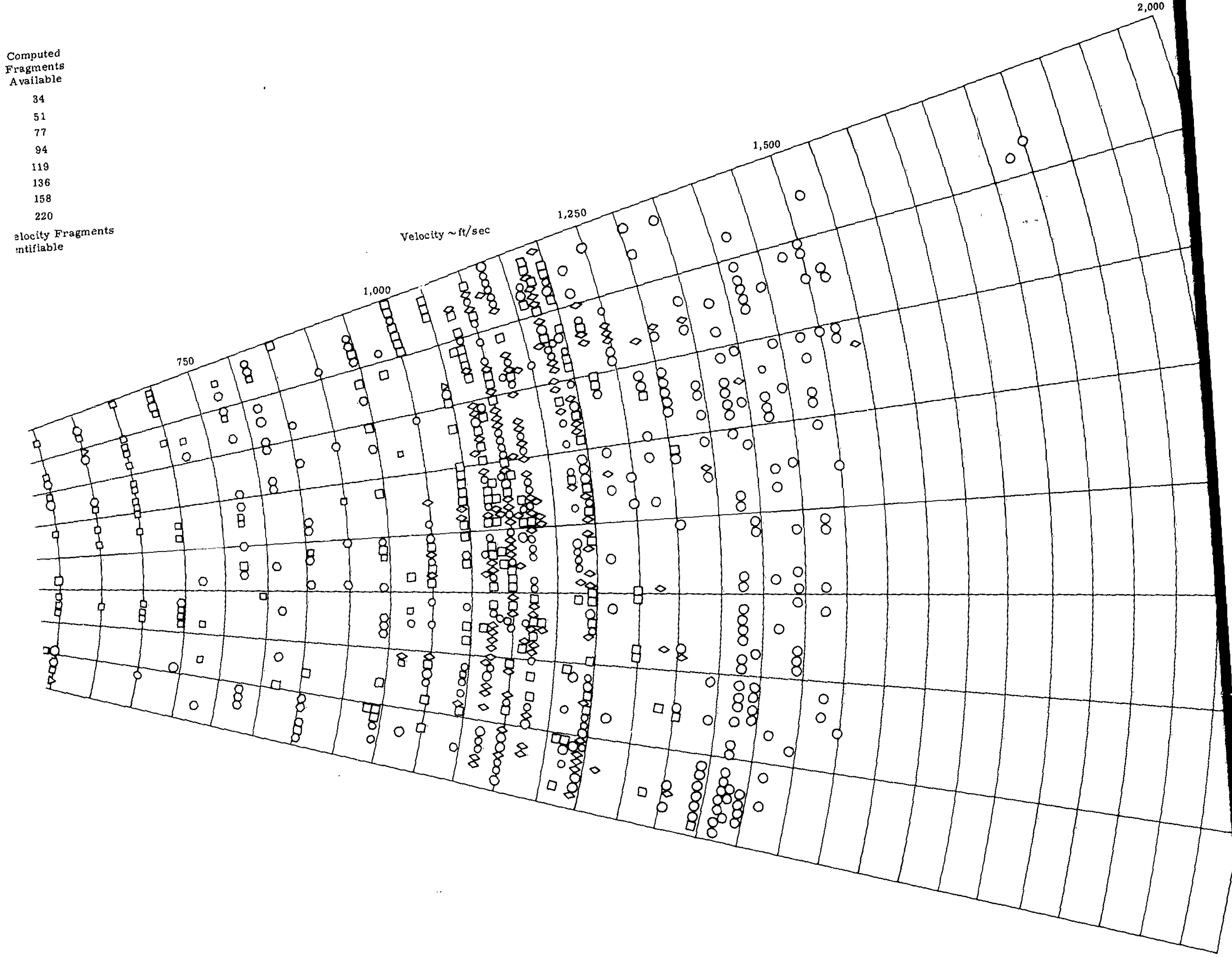

Figure 55. Velocity versus Radial Distribution, Round 106

CONFIDENTIAL

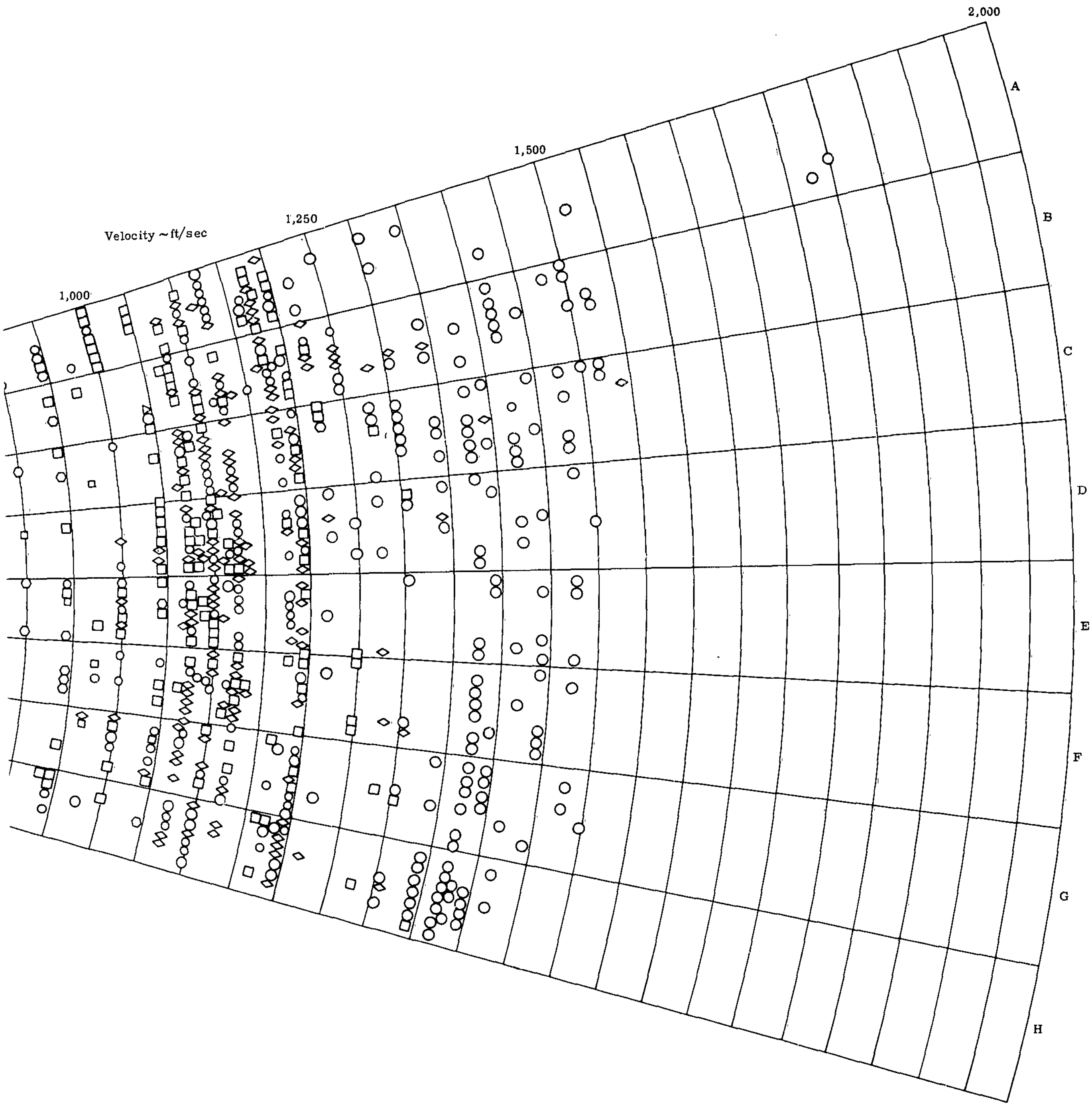

ɔcity versus Radial Distribution, Round 106

CONFIDENTIAL

3

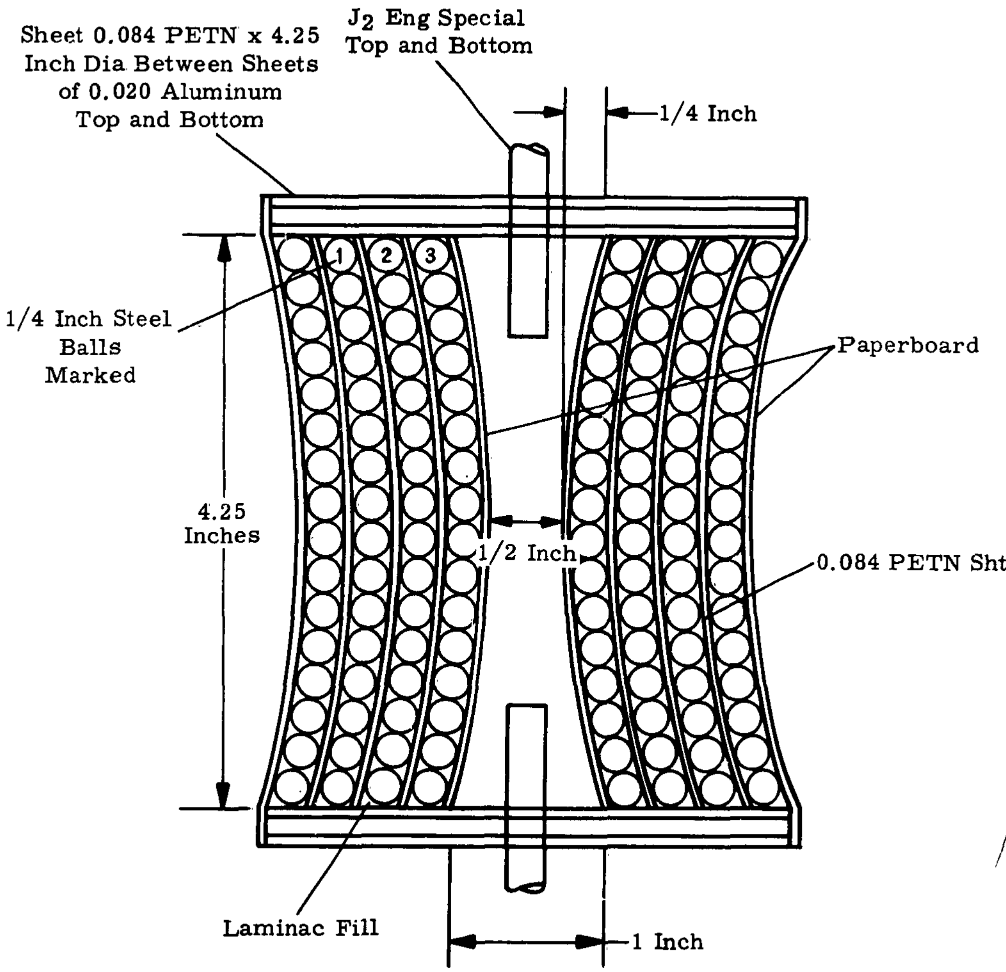

Figure 56. Test Model Design, Round 107

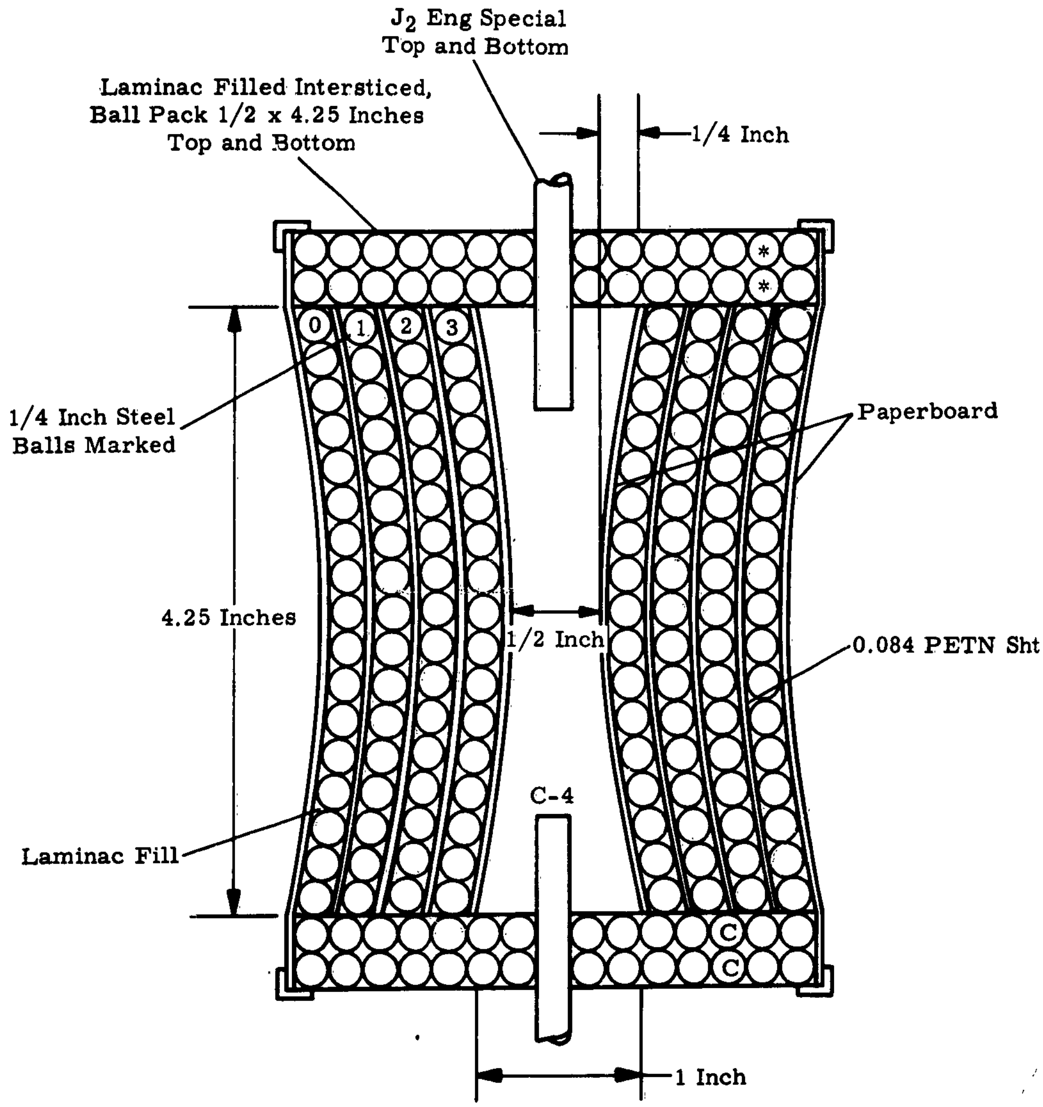

Figure 57. Test Model Design, Round 108

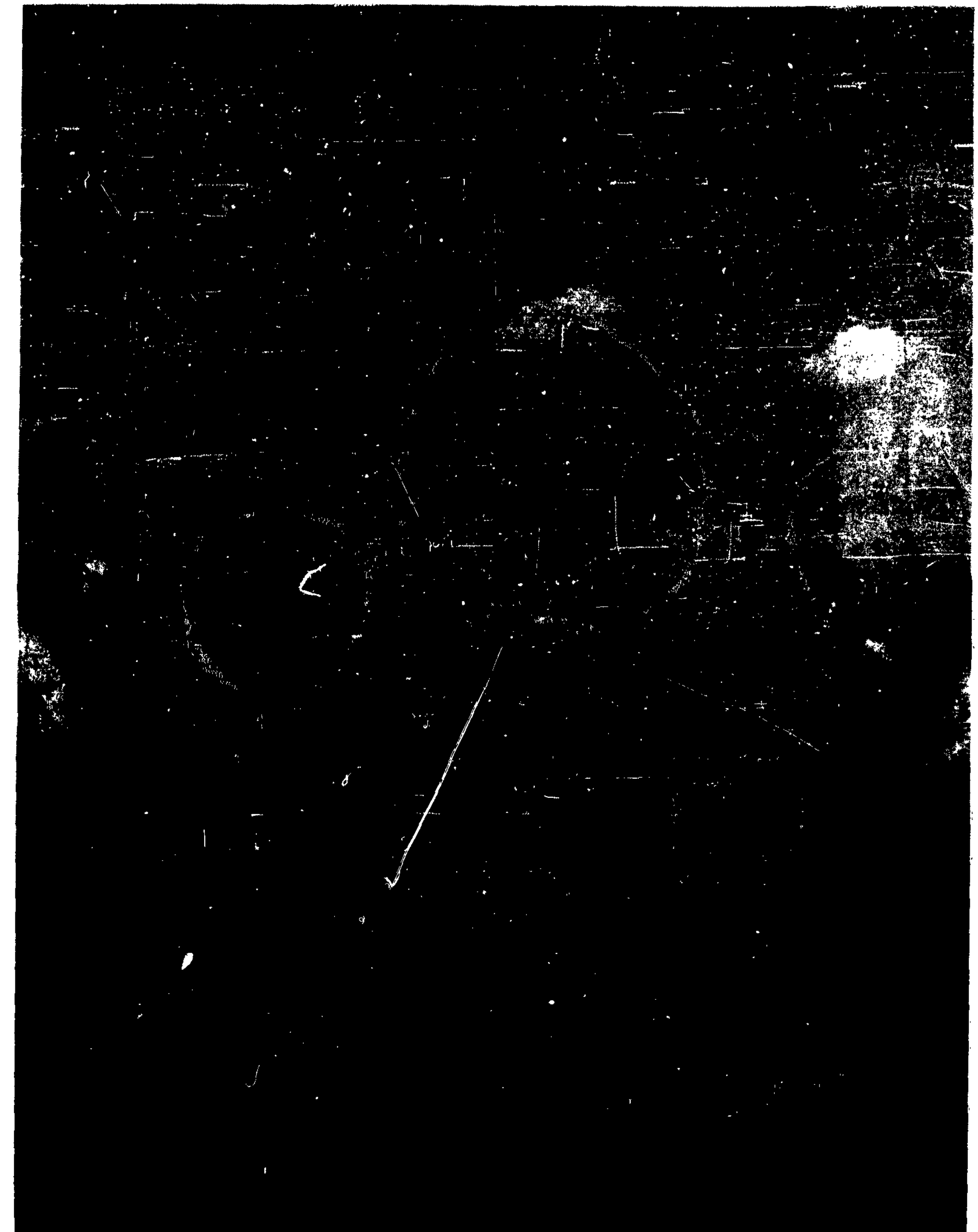

Figure 58. Impact Pattern, Round 108

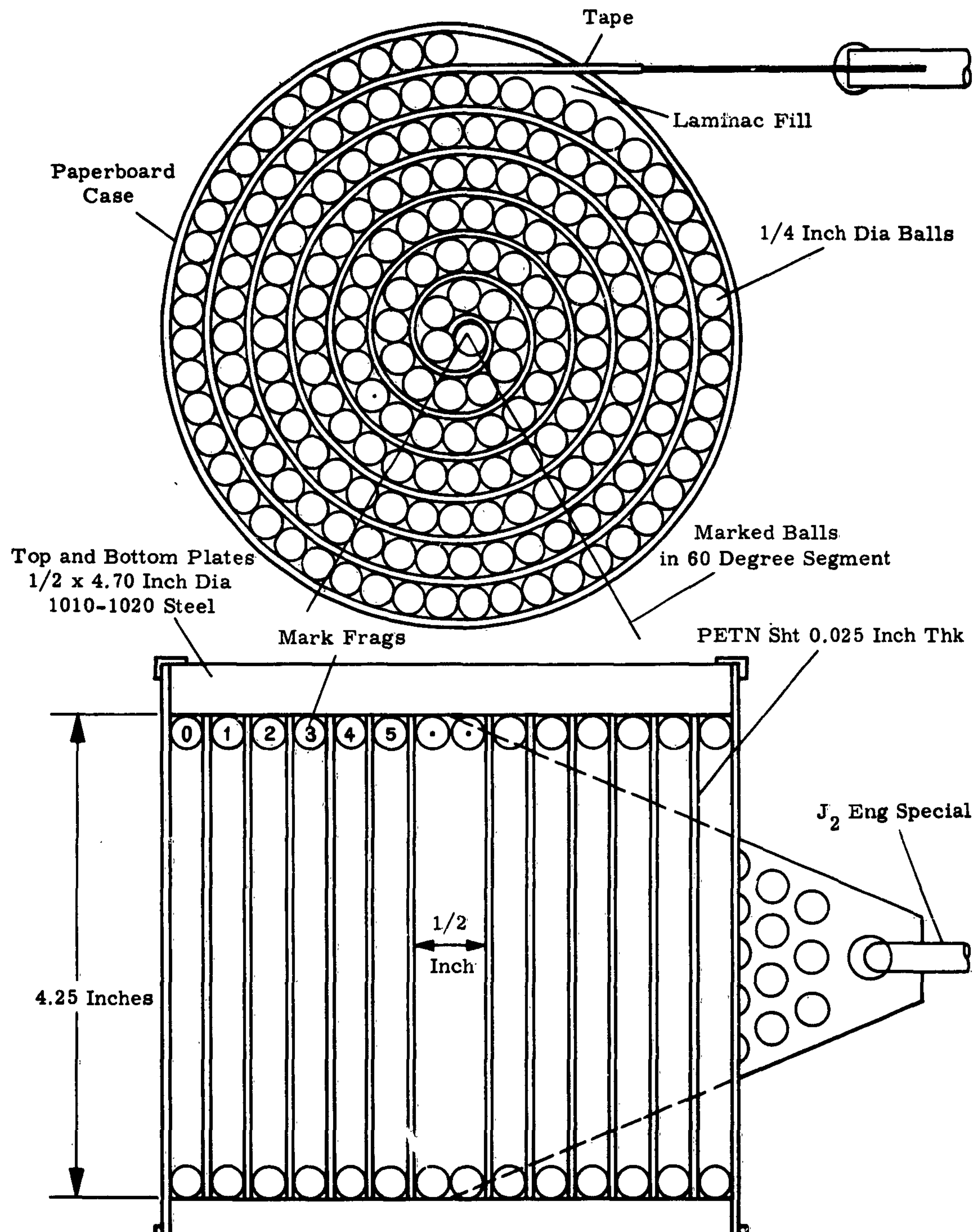

Figure 59. Test Model Design, Round 109

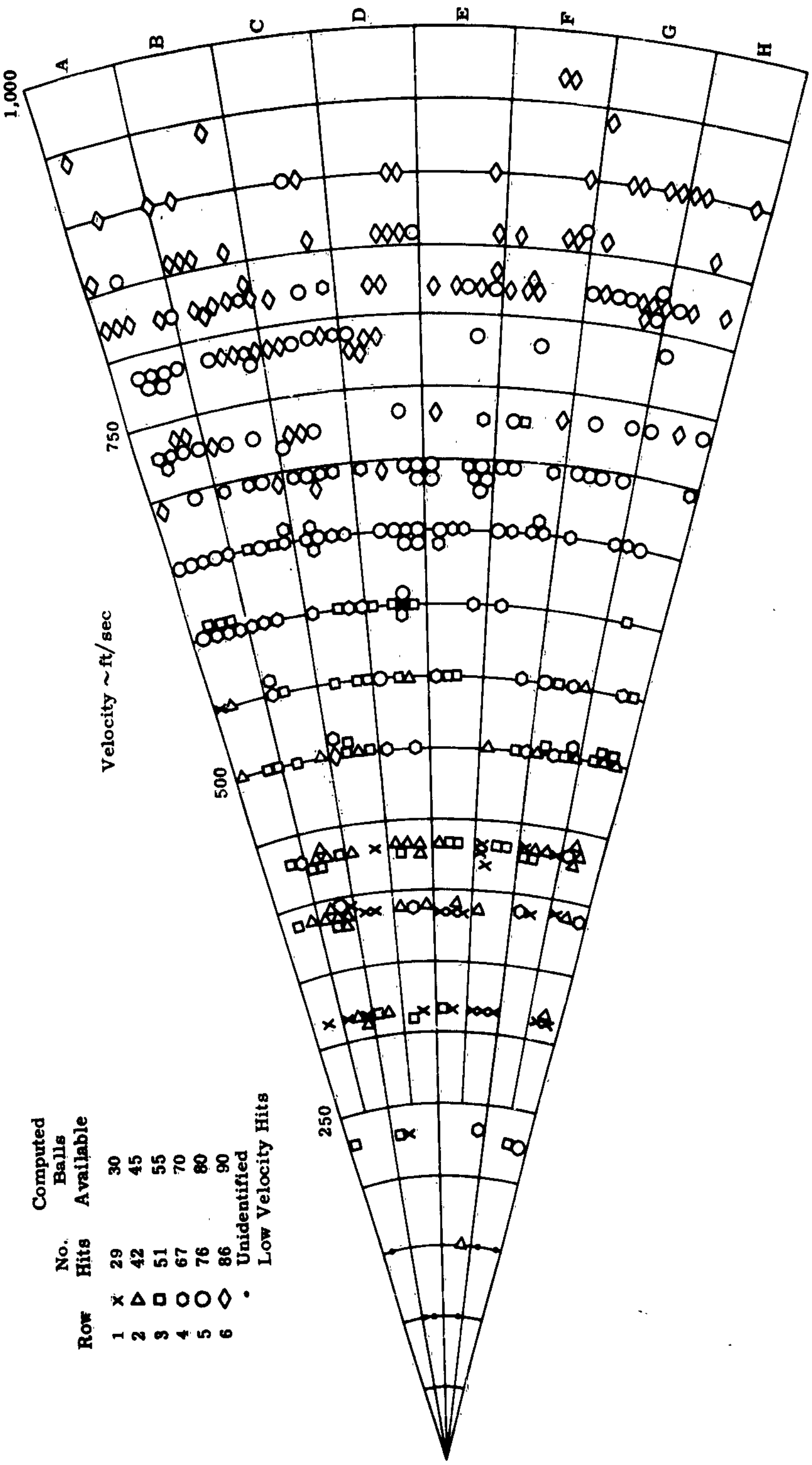

Figure 60. Velocity versus Radial Distribution, Round 109

Figure 61. Impact Pattern, Round 109

Rnd. No.	Round Description	Parameters Varied	Test Objective	Results and Comments
RE-1	Type, Spiral Cylinder Fragment Nos., 23,716 Fragment Wt. (Grams), 26,109 Explosive Wt. (Grams), 714 End Plate Wt. (Grams), 13,733 Inert Filler Wt. (Grams), Unknown Total Wt. (Pounds), Unknown C/M, 0.027 Figure No., 62	Increased number of fragment layers - 14. Thin gaged explosive - 0.042 and 1 inch thick steel end plates.	Determine feasibility of projecting 14 layers of fragments. Determine beam spray control achievable with massive end plates. Determine fragment space and velocity distribution.	14 layers projected. Maximum velocity 750 ft/sec., min. velocity 200 ft/sec. Impact pattern too dense for recovery. Impact Pattern Fig. 63. 75% fragment hits within 25°.
RE-2	Type, Concentric Hyperboloid Fragment Nos., 11,269 Fragment Wt. (Grams), 12,396 Explosive Wt. (Grams), 1103 End Plate Wt. (Grams), 2983 Inert Filler Wt. (Grams), Unknown Total Wt. (Pounds), Unknown C/M, 0.102 Figure No., 64	L/D = 2	Basic data for beam spray control L/D scaling effects	Low order; excellent beam spray control - 90% of hits within 25°. Impact Pattern Fig. 65.
RE-3	Type, Concentric Hyperboloid Fragment Nos., 11,127 Fragment Wt. (Grams), 12,240 Explosive Wt. (Grams), 828 End Plate Wt. (Grams), 101 Inert Filler Wt. (Grams), Unknown Total Wt. (Pounds), Unknown C/M, 0.067 Figure No., 66	Explosive end plates; 0.042" explosive layers.	Explosive end plates; control of beam spray and feasibility of initiating multiple layers of thin gaged sheet explosive.	Excellent beam spray control, 83% of hits within 20°. Space distribution between fragment layers uniform. Impact Pattern Figure 67.

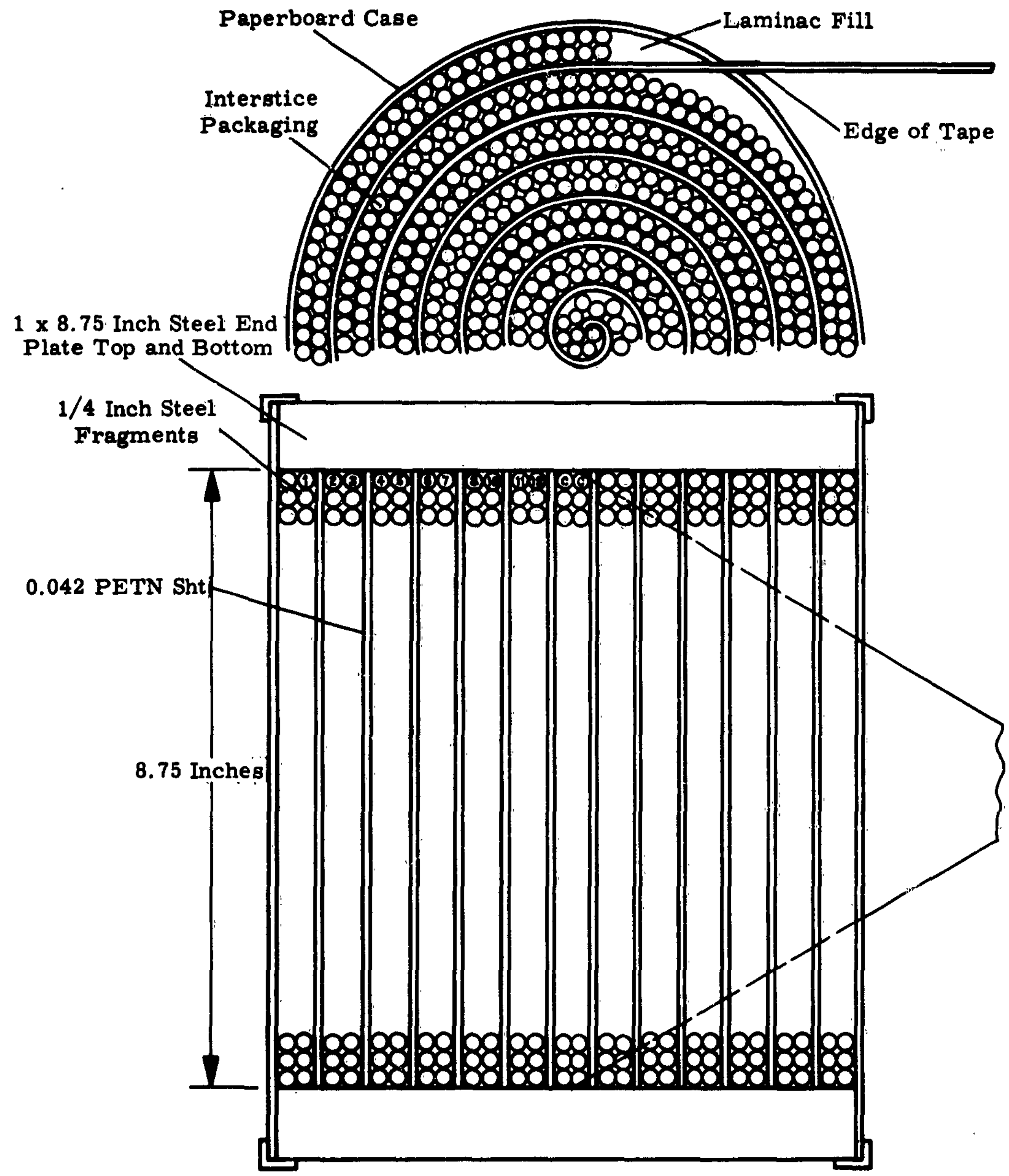

Figure 62. Test Model Design, Round RE-1

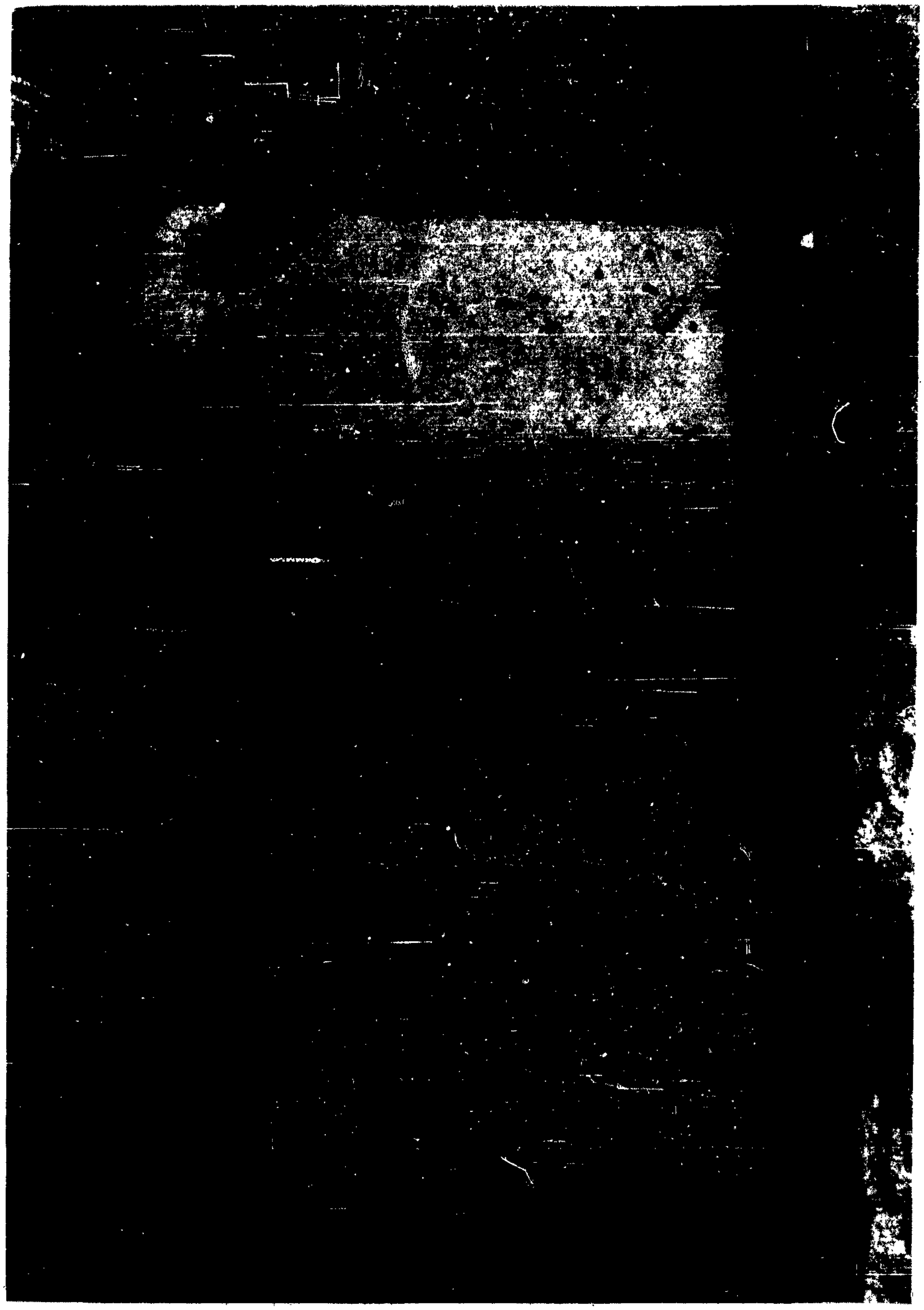

Figure 63. Impact Pattern, Round RE-1

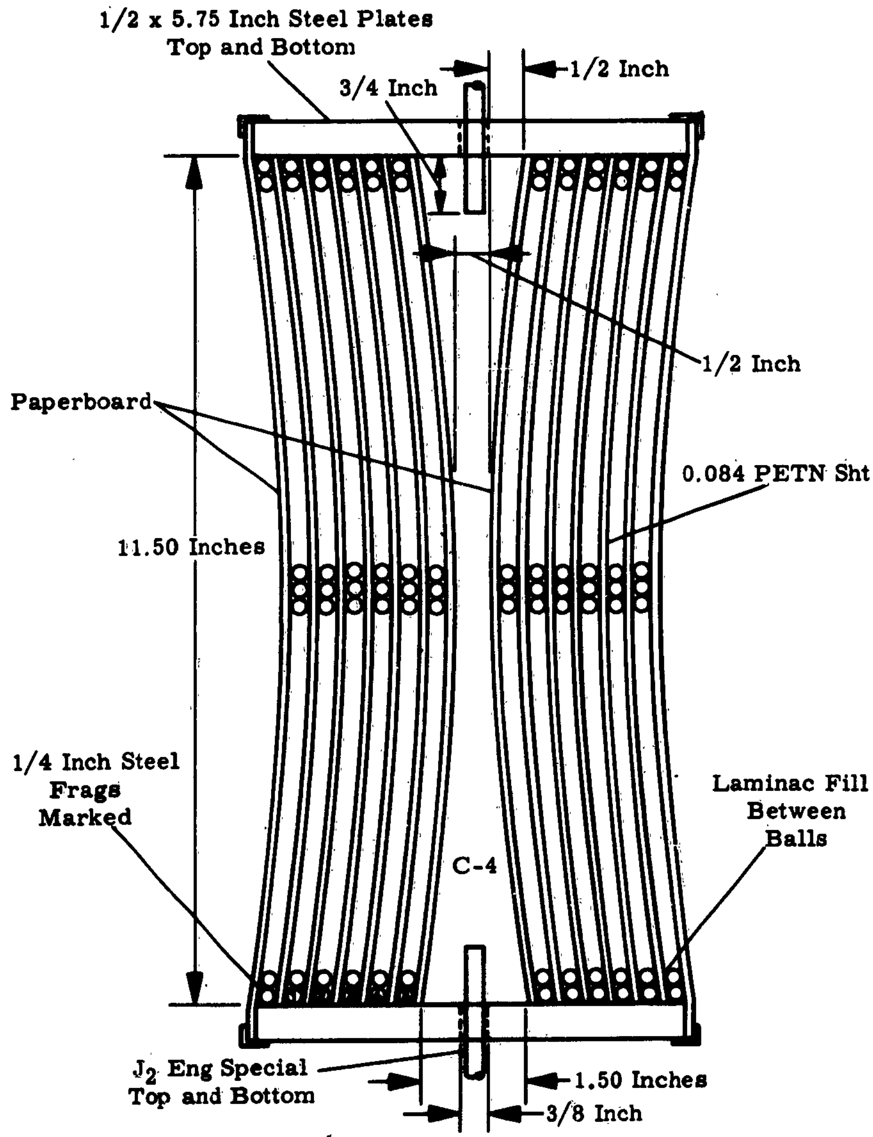

Figure 64. Test Model Design, Round RE-2

Figure 65. Impact Pattern, Round RE-2

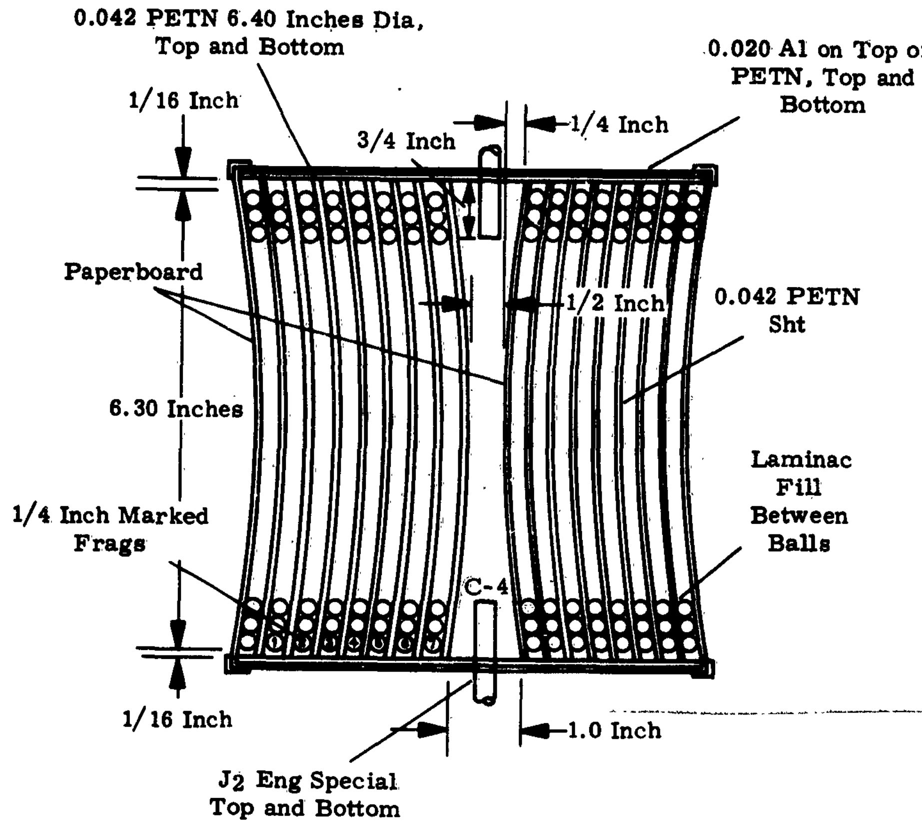

Figure 66. Test Model Design, Round RE-3

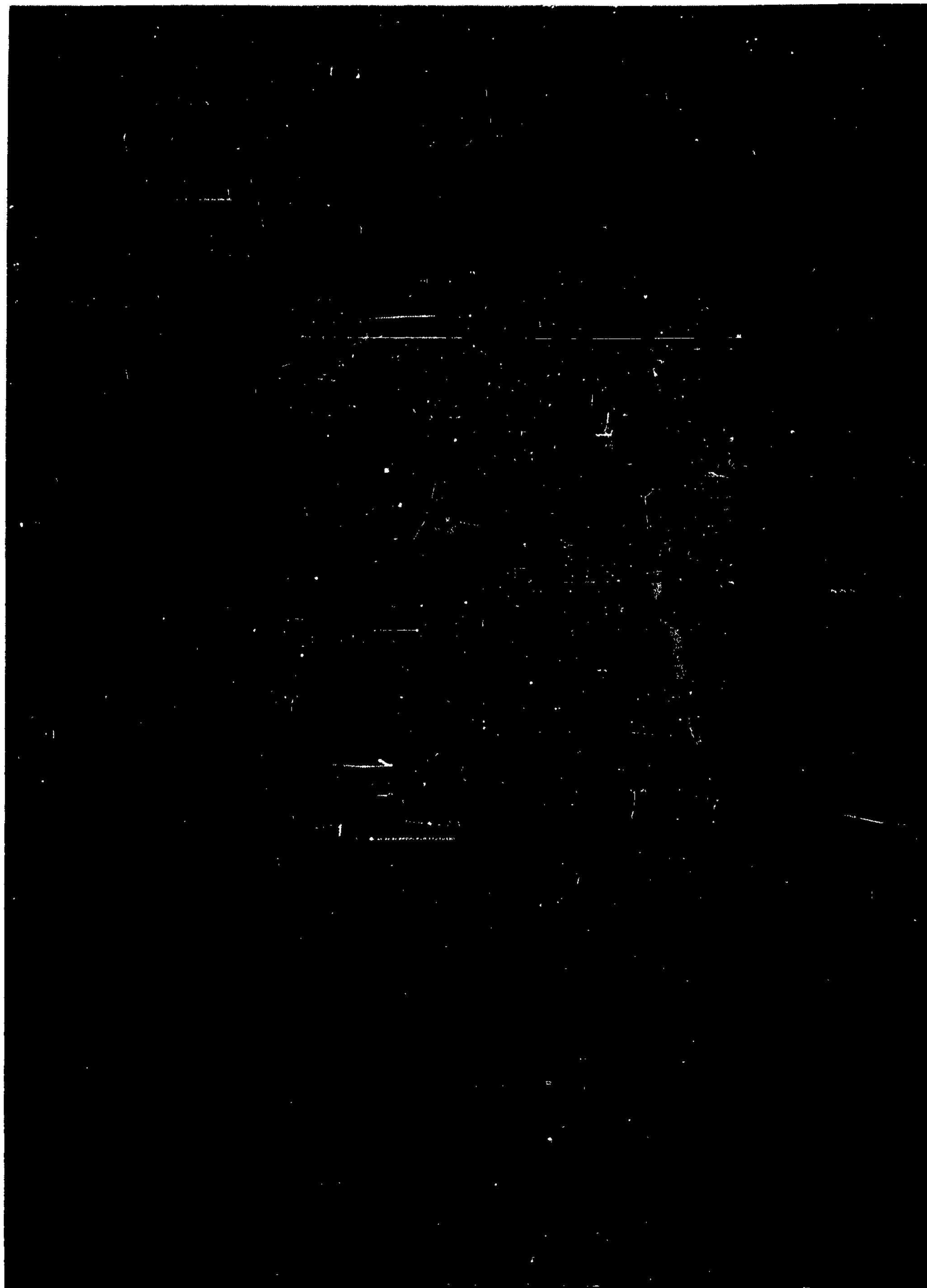

Figure 67. Impact Pattern, Round RE-3

Rnd. No.	Round Description	Parameters Varied	Test Objective	Results and Comments
RE-4	Type, Concentric Hyperboloid Fragment Nos., 6137 Fragment Wt. (Grams), 6751 Explosive Wt. (Grams), 388 End Plate Wt. (Grams), 1989 Inert Filler Wt. (Grams), Total Wt. (Pounds), C/M, 0.056 Figure No., 68	Fragmenting end plates (double layer 1/4" steel spheres)	Beam spray control by fragmenting double end plates. Initiation of thin gaged sheet exp. by center burster.	Frag. end plates combined with hyperboloid shape provides 80% hits in 20° - and can fill center of disc with frags. Max. velocity of end frags. 1000 ft/sec. Impact Pattern Fig. 69.
RE-5	Type, Spiral Cylinder Fragment Nos., 4372 Fragment Wt. (Grams), 4809 Explosive Wt. (Grams), 104 End Plate Wt. (Grams), 2116 Inert Filler Wt. (Grams), 717 Total Wt. (Pounds), 17.1 C/M, 0.019 Figure No., 70	0.025 thick explosive	Basic data for velocity reduction	Max. vel. - 600 ft/sec. Min. vel. 200 ft/sec. Thin gaged explosive can reduce expansion rate. Impact Pattern Fig. 71. Polar Plot Fig. 72.
RE-6	Type, Concentric Hyperboloid Fragment Nos., 1597 Fragment Wt. (Grams), 1757 Explosive Wt. (Grams), 159 End Plate Wt. (Grams), 1214 Inert Filler Wt. (Grams), 181 Total Wt. (Pounds), 7.2 C/M, 0.082 Figure No., 73	Standard	Control round for basic scaling data on fragment mass effects.	Linear velocity gradient; 96% of hits in 36° - uniform space distribution.
RE-7	Type Fragment Nos., 4990 Fragment Wt. (Grams), 5489 Explosive Wt. (Grams), 284 End Plate Wt. (Grams), 3169 Inert Filler Wt. (Grams), 917 Total Wt. (Pounds), 21.7 C/M, 0.044 Figure No. 74	Fragmenting end plates (4 layers of 1/4" steel spheres)	Beam spray control by large fragmenting end plates.	90% of hits in 30° Unable to recover large number of low vel. because of high impact pattern density. End plates did not fragment completely. Center in large mass. Impact Pattern Fig. 75.

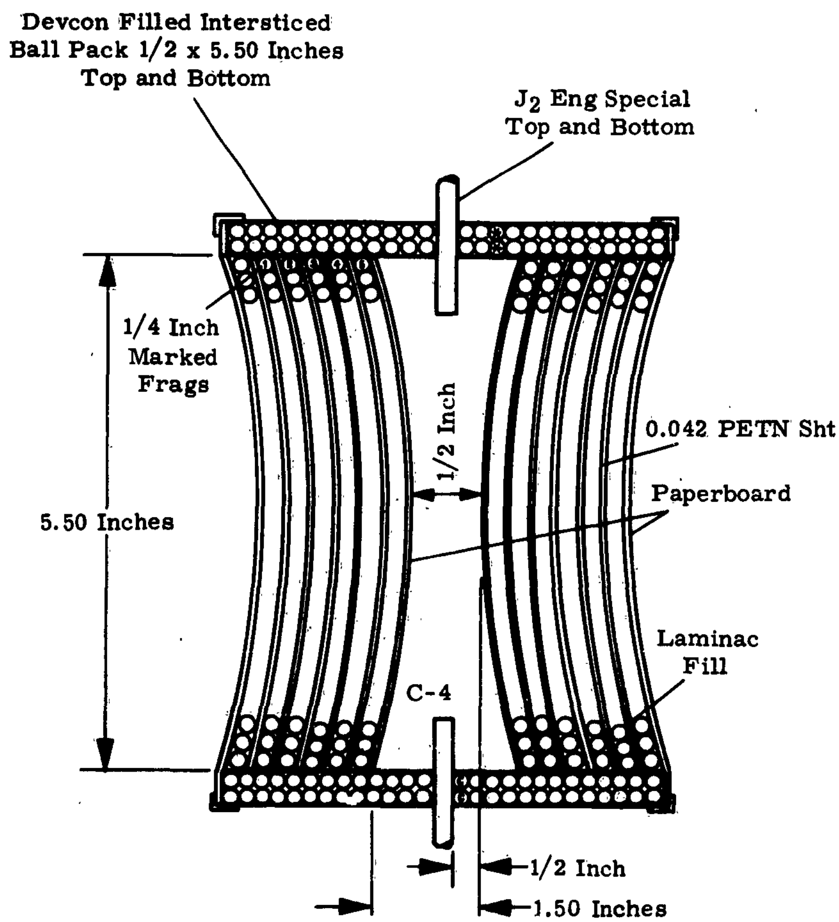

Figure 68. Test Model Design, Round RE-4

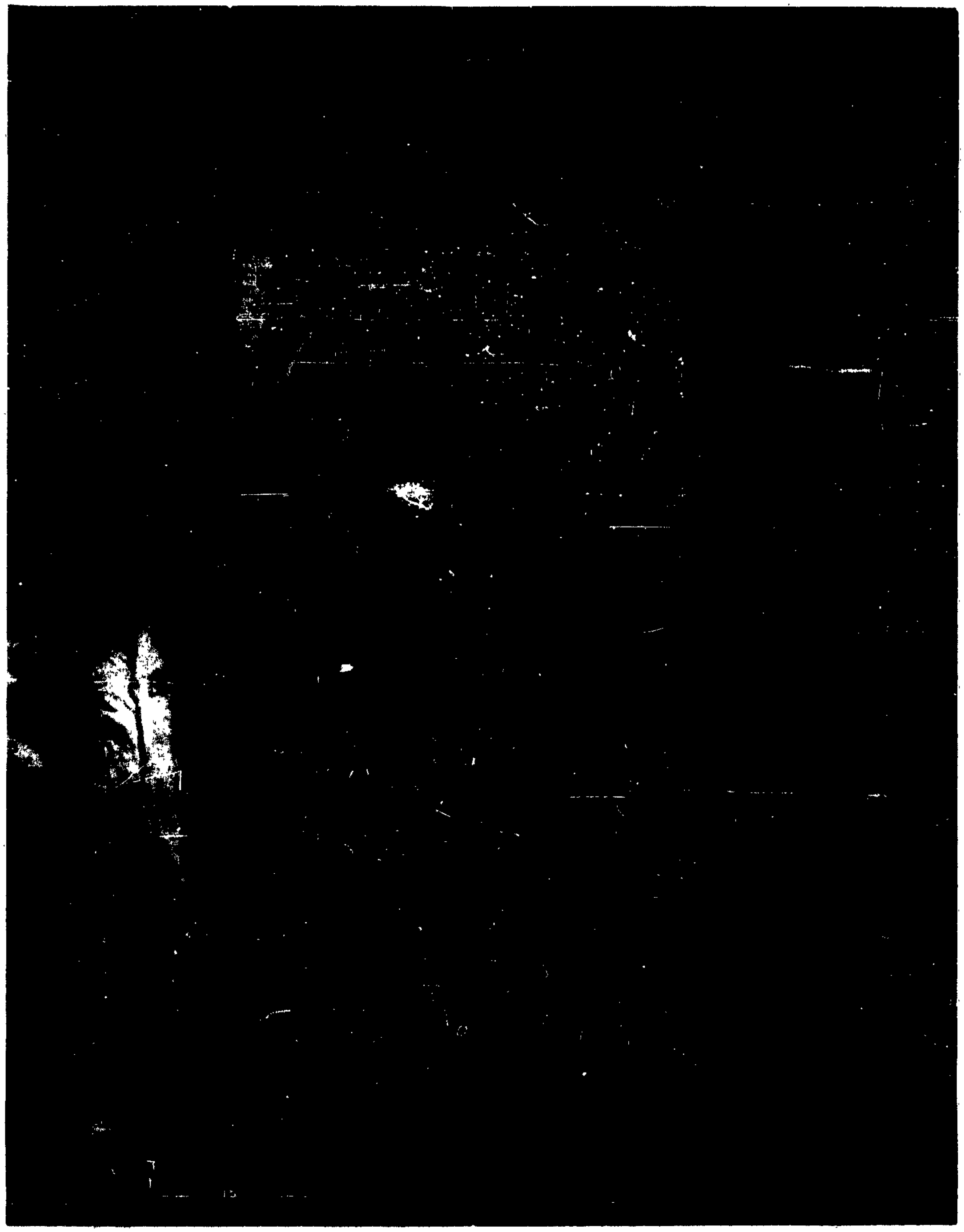

Figure 69. Impact Pattern, Round RE-4

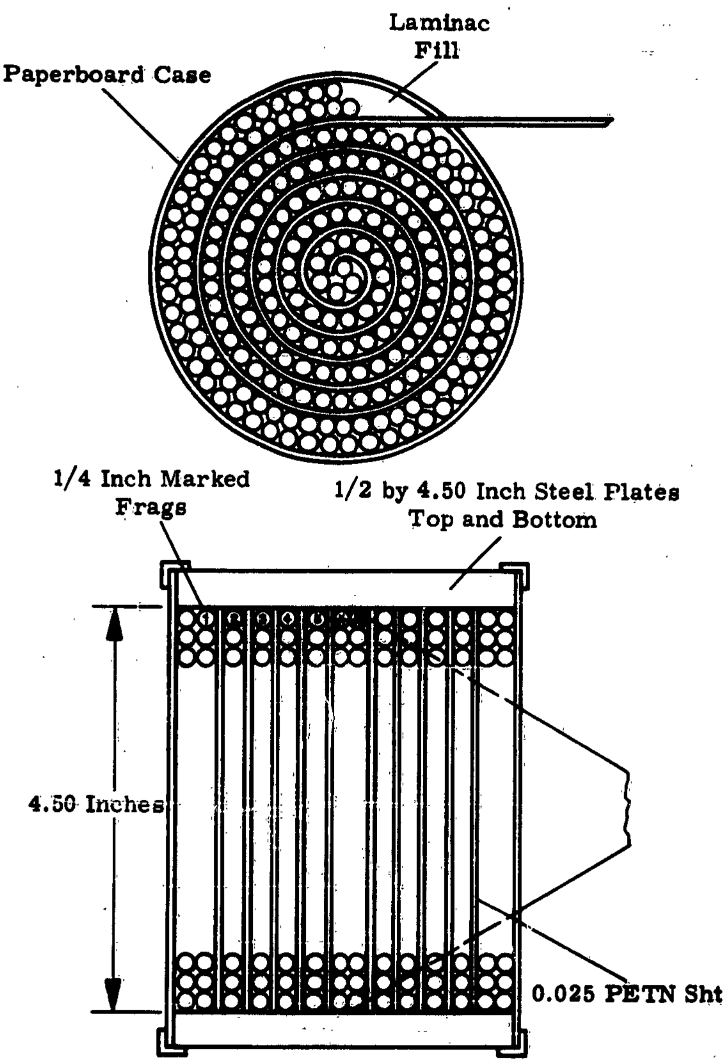

Figure 70. Test Model Design, Round RE-5

Figure 71. Impact Pattern, Round RE-5

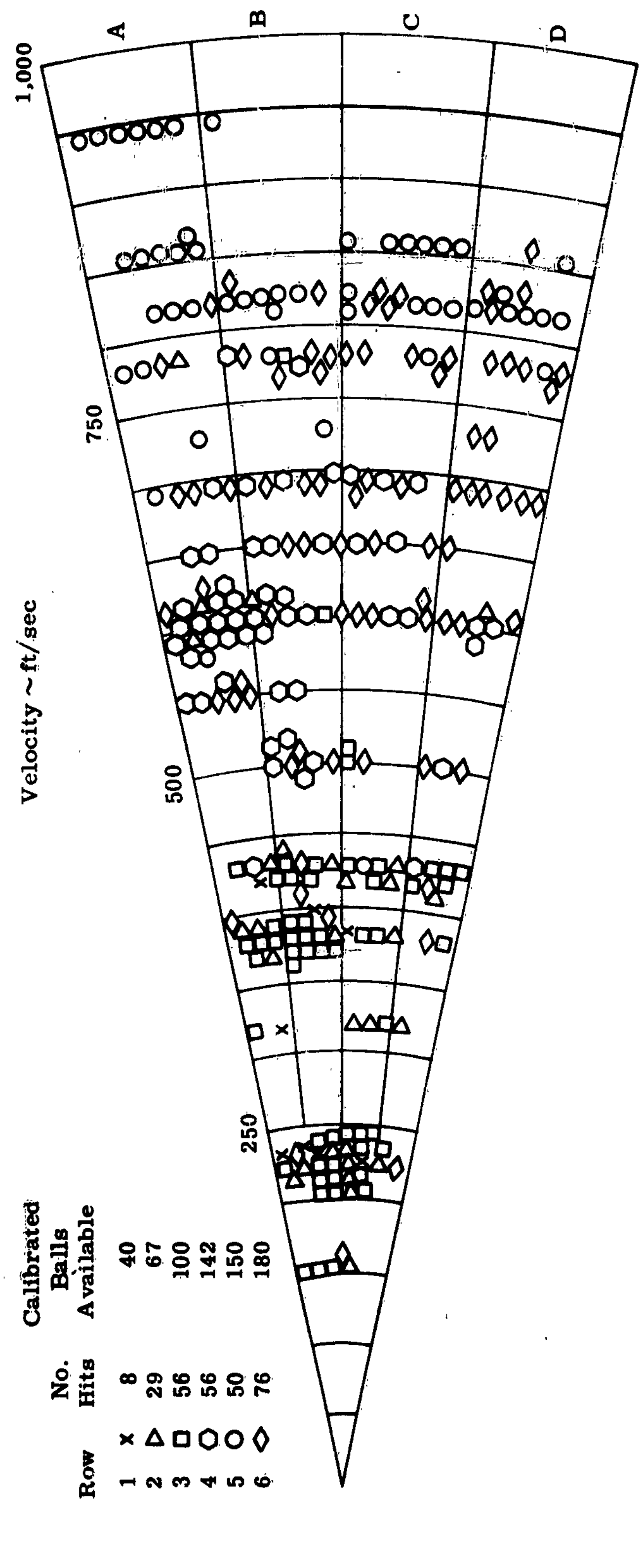

Figure 72. Velocity versus Radial Distribution, Round RE-5

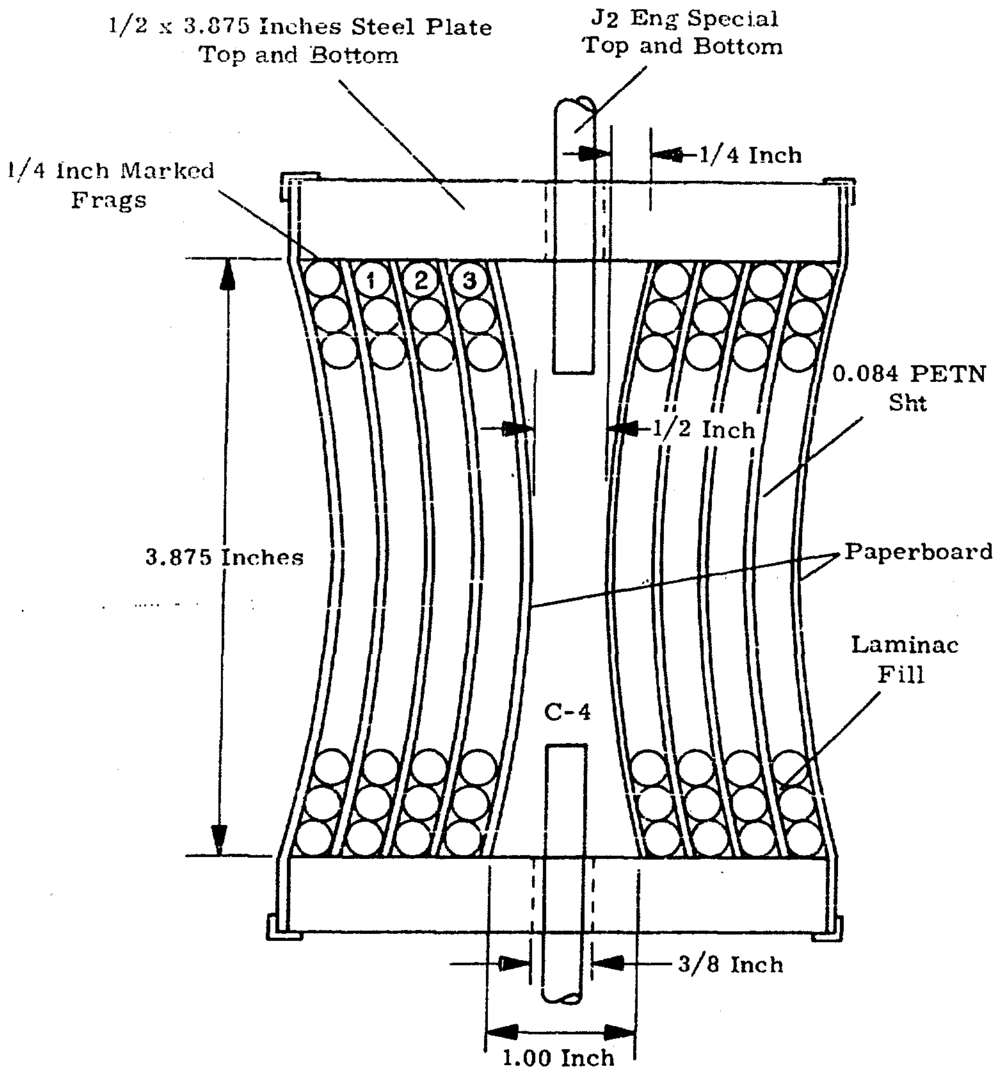

Figure 73. Test Model Design, Round RE-6

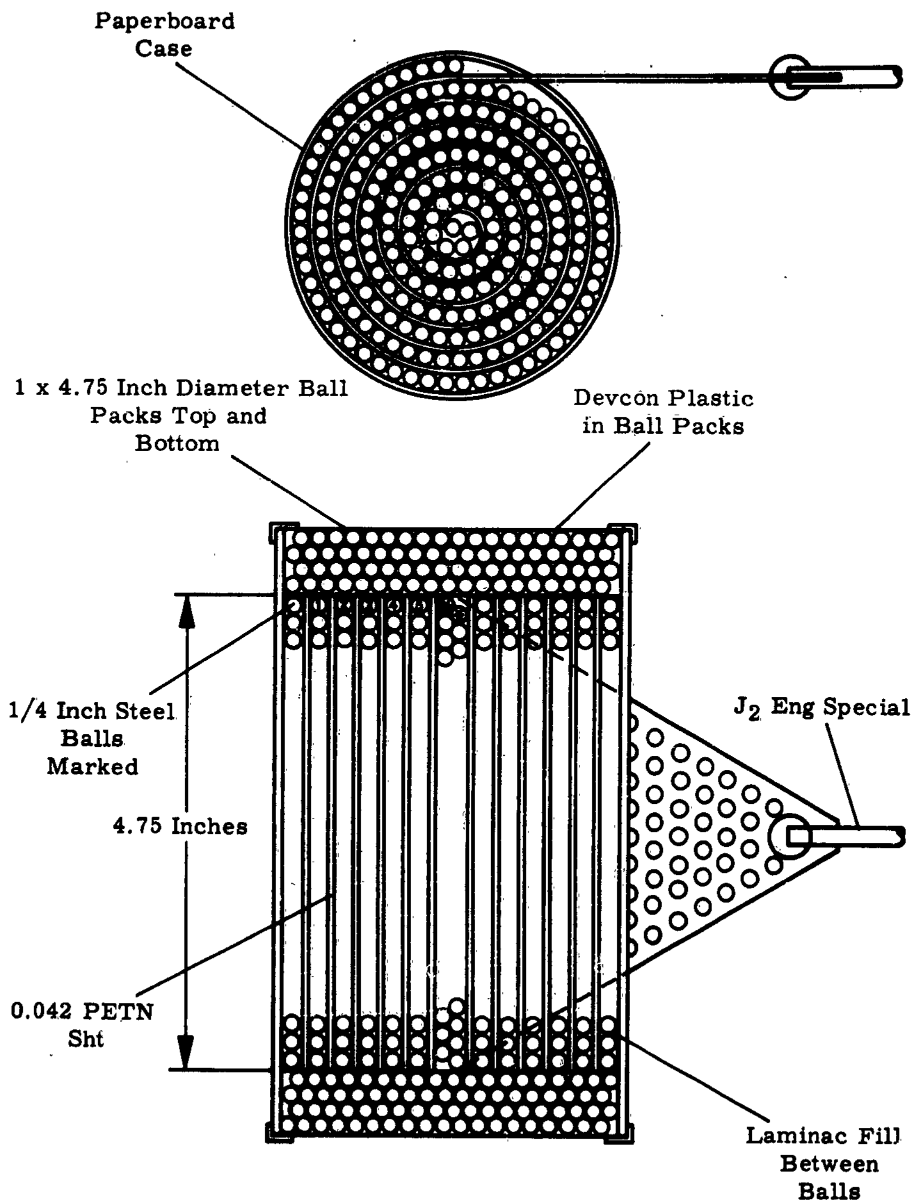

Figure 74. Test Model Design, Round RE-7

Figure 75. Impact Pattern, Round RE-7

Rnd. No.	Round Description	Parameters Varied	Test Objective	Results and Comments
RE-8	Type, Concentric Hyperboloid Fragment Nos., 25,710 Fragment Wt. (Grams), 28,281 Explosive Wt. (Grams), 1277 End Plate Wt. (Grams), 143 Inert Filler Wt. (Grams), Total Wt. (Pounds), C/M, 0.045 Figure No., 76	13 layers multiple fragment layers between outer explosive layers.	Design concept feasibility and effects of double pressure tape.	(Pattern too dense for recovery). Max. vel. ≈ 1350 ft/sec. Min. vel. < 100 ft/sec. (est.) No evidence of tape affecting performance 80% of hits in 30°
RE-9	Type, Concentric Hyperboloid Fragment Nos., 737 Fragment Wt. (Grams), 6173 Explosive Wt. (Grams), 293 End Plate Wt. (Grams), 3318 Inert Filler Wt. (Grams), 881 Total Wt. (Pounds), 23.5 C/M, 0.042 Figure No., 77	Use of 1/2" steel spheres.	Fragment size scaling data.	Low order det. Max. vel. = 760 ft/sec. min. vel. = 100 ft/sec unsymmetrical impact pattern. showed need for explosive end plates to propagate detonation to subsequent layers.
RE-10	Type, Concentric Hyperboloid Fragment Nos., 620 Fragment Wt. (Grams), 5193 Explosive Wt. (Grams), 248 End Plate Wt. (Grams), 3300 Inert Filler Wt. (Grams), 859 Total Wt. (Pounds), 21.1 C/M, 0.041 Figure No., 77	Same as RE-9	Same as RE-9	Max. vel. = 500 ft/sec. Min. vel. = 100 ft/sec. Unsymmetrical impact pattern. Low order - same results as RE-9.
RE-11	Type, Concentric Hyperboloid Fragment Nos., 5976 Fragment Wt. (Grams), 6574 Explosive Wt. (Grams), 795 End Plate Wt. (Grams), 3360 Inert Filler Wt. (Grams), 1974 Total Wt. (Pounds), 28.0 C/M, 0.093 Figure No., 78	1/4" nickel fragments used.	Gross effects resulting from use of nickel fragments.	Max. vel. = 1100 ft/sec - Frags. deformed in innermost layers. Beam spray unsymmetrical.

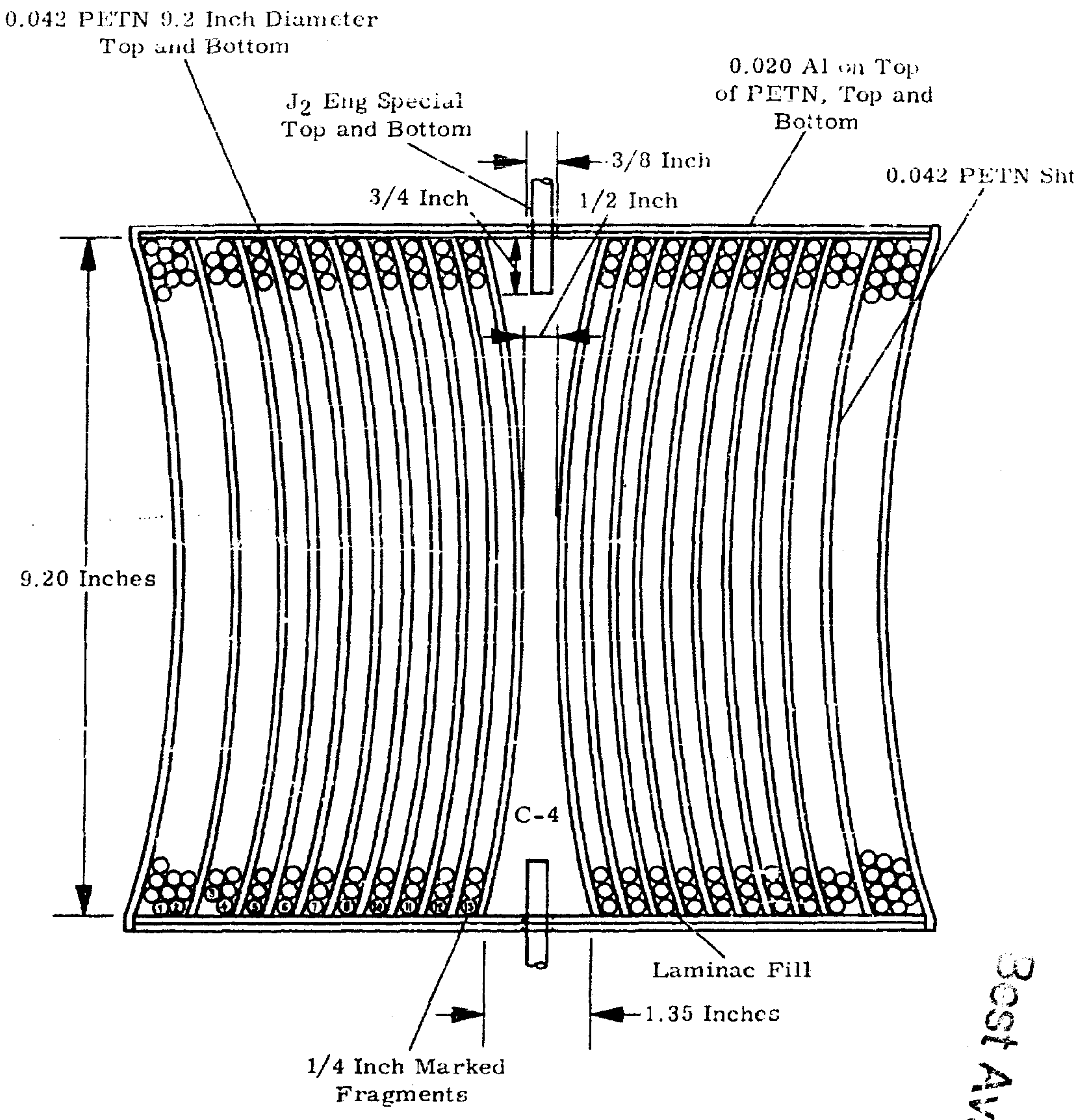

Figure 76. Test Model Design, Round RE-8

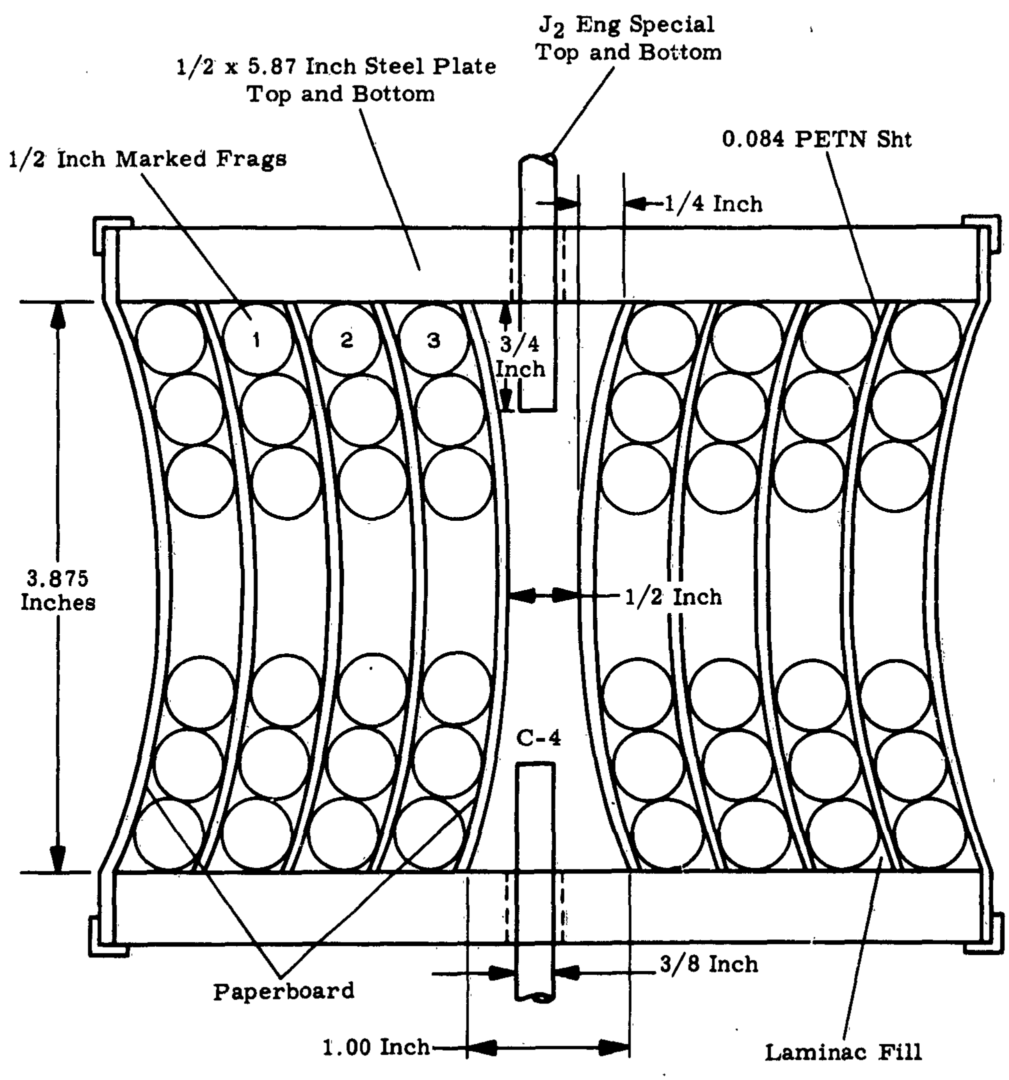

Figure 77. Test Model Design, Rounds RE-9 and RE-10

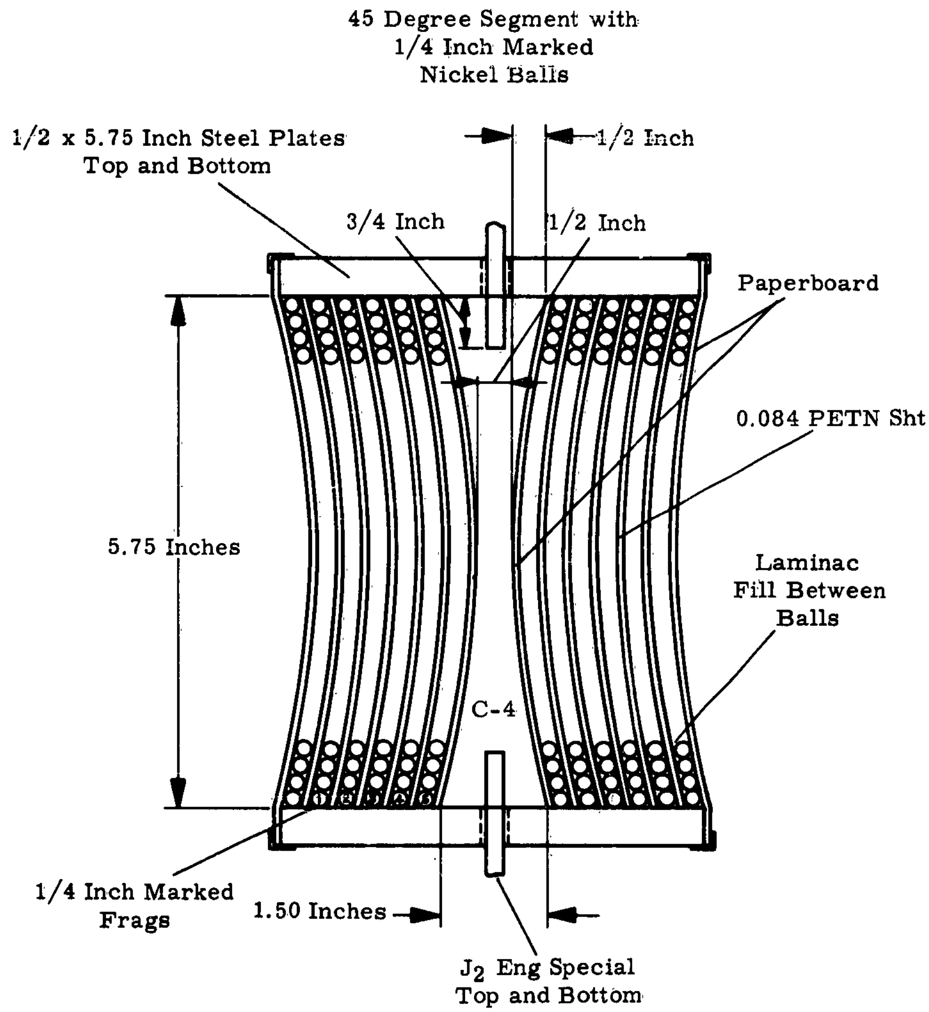

Figure 78. Test Model Design, Round RE-11

Rnd. No.	Round Description	Parameters Varied	Test Objective	Results and Comments
RE-12	Type, Spiral Cylinder Fragment Nos., 4900 Fragment Wt. (Grams), 5390 Explosive Wt. (Grams), 270 End Plate Wt. (Grams), 2969 Inert Filler Wt. (Grams), Total Wt. (Pounds), C/M, 0.051 Figure No., 79	Use of silicone rubber for packaging fragments.	Gross effects resulting from packaging fragments in silicone rubber.	Max. vel. = 950 ft/sec. No evidence of silicone rubber in arena. Impact pattern unaffected by matrix material. (frags. moved as group) 90% in 30°.
RE-13	Type, Concentric Hyperboloid Fragment Nos., 12,080 Fragment Wt. (Grams), 13,288 Explosive Wt. (Grams), 1462 End Plate Wt. (Grams), 3232 Inert Filler Wt. (Grams), Unknown Total Wt. (Pounds), Unknown C/M, 0.110 Figure No., 80	L/D = 2	L/D Scaling effects	Max Fastax Vel = 1365 ft/sec. Max. Radiograph Vel. = 1355 ft/sec. Beam Spray opened to 40° curvature must be increased with larger L/D to maintain beam spray control.
RE-14	Type, Concentric Hyperboloid Fragment Nos., 28,500 Fragment Wt. (Grams), 31,350 Explosive Wt. (Grams), 1085 End Plate Wt. (Grams), 5306 Inert Filler Wt. (Grams), 6456 Total Wt. (Pounds), 97.4 C/M, 0.029 Figure No., 81	14 layers, exp. and fragmenting end plates	Design concept feasibility	Max. Vel. = 850 ft/sec. Min. Vel. = 200 ft/sec. Max. beam spray = 70° Heavy concentration within 15°. Complete det. end plate frag. vel. 200 to 1000 ft/sec. Uniform impact dist. of end plate frags. Impact Pattern Fig. 80.

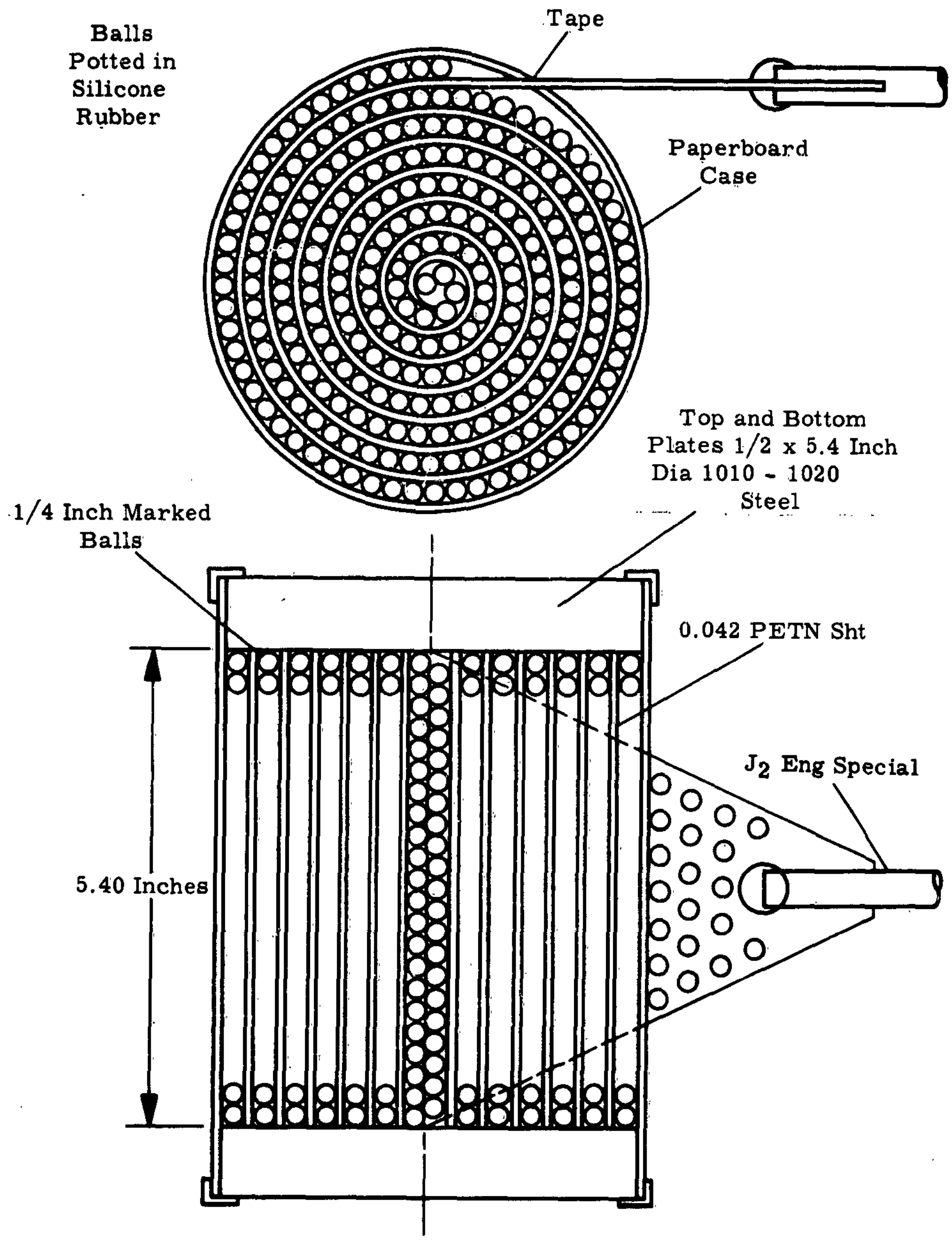

Figure 79. Test Model Design, Round RE-12

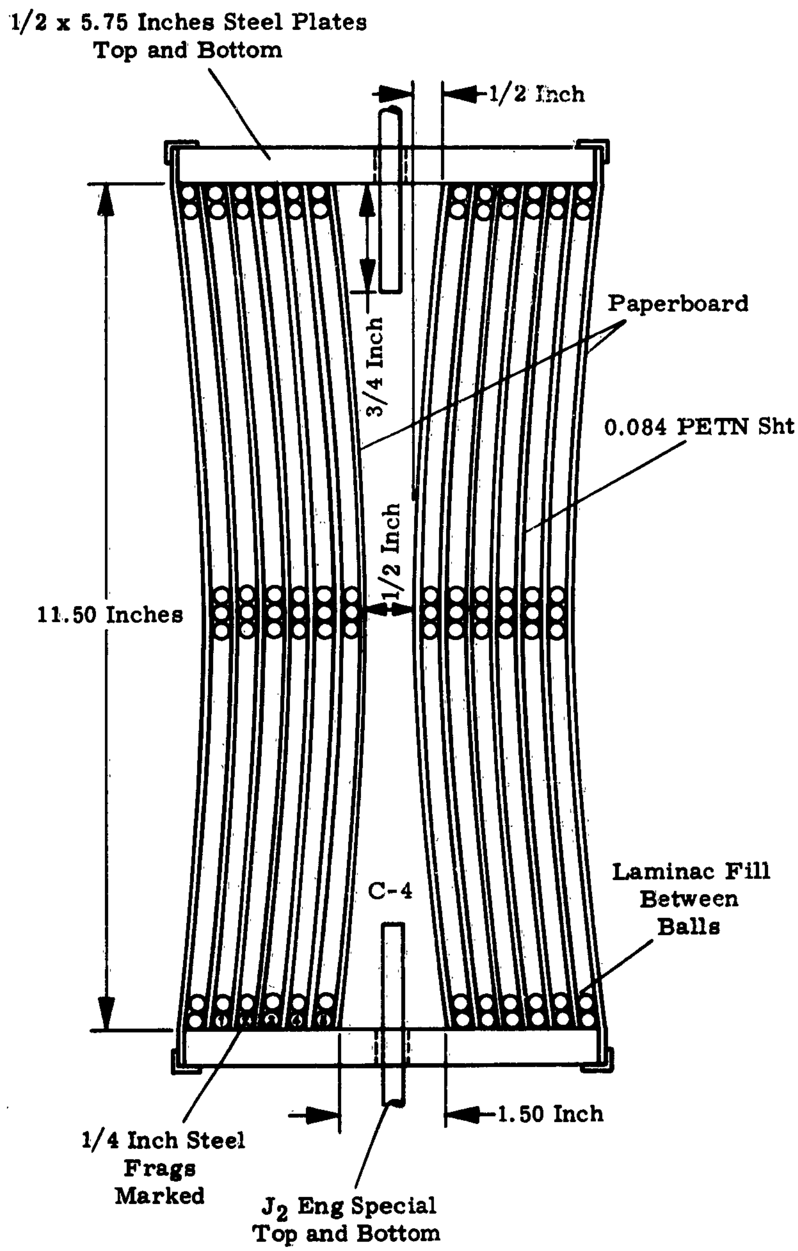

Figure 80. Test Model Design, Round RE-13

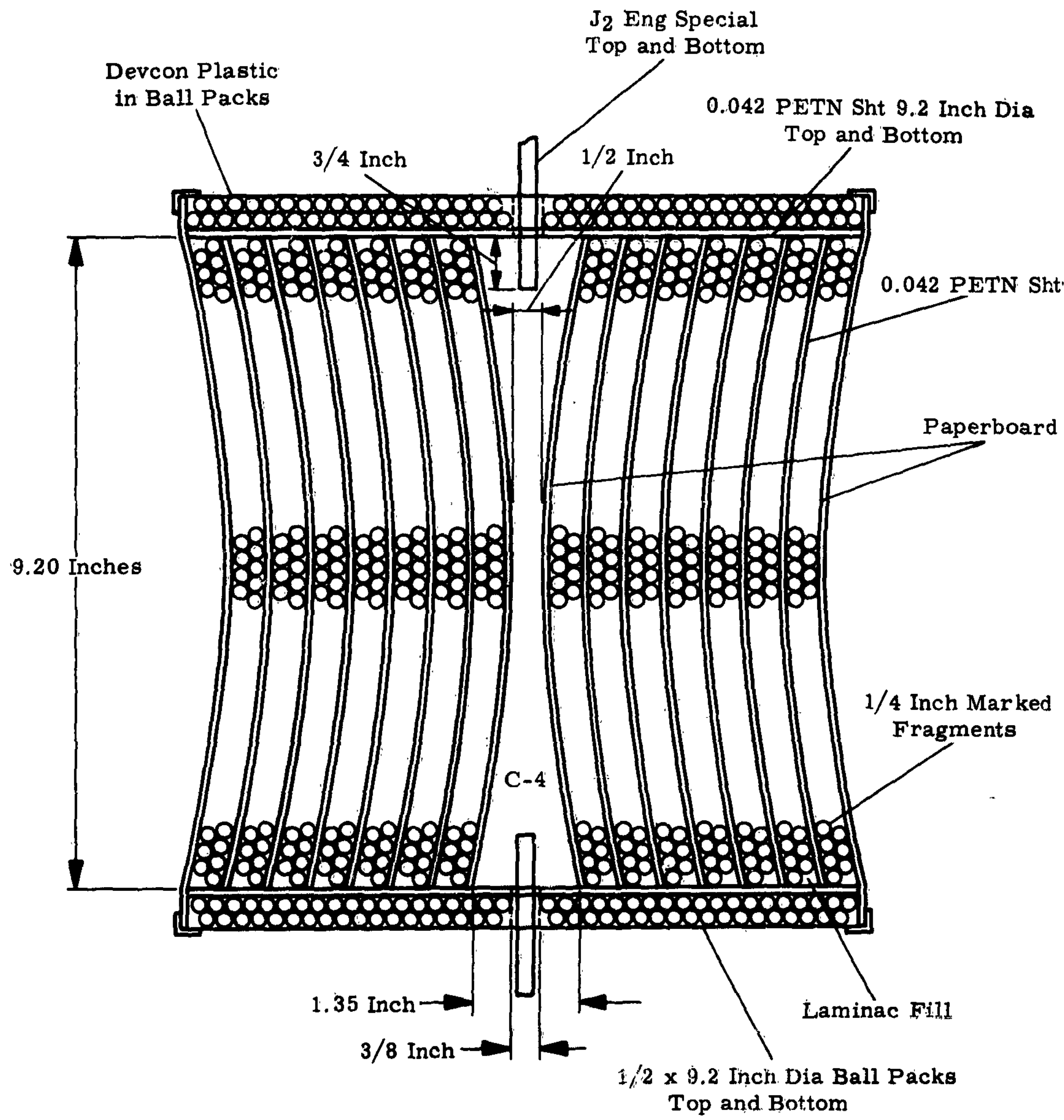

Figure 81. Test Model Design, Round RE-14

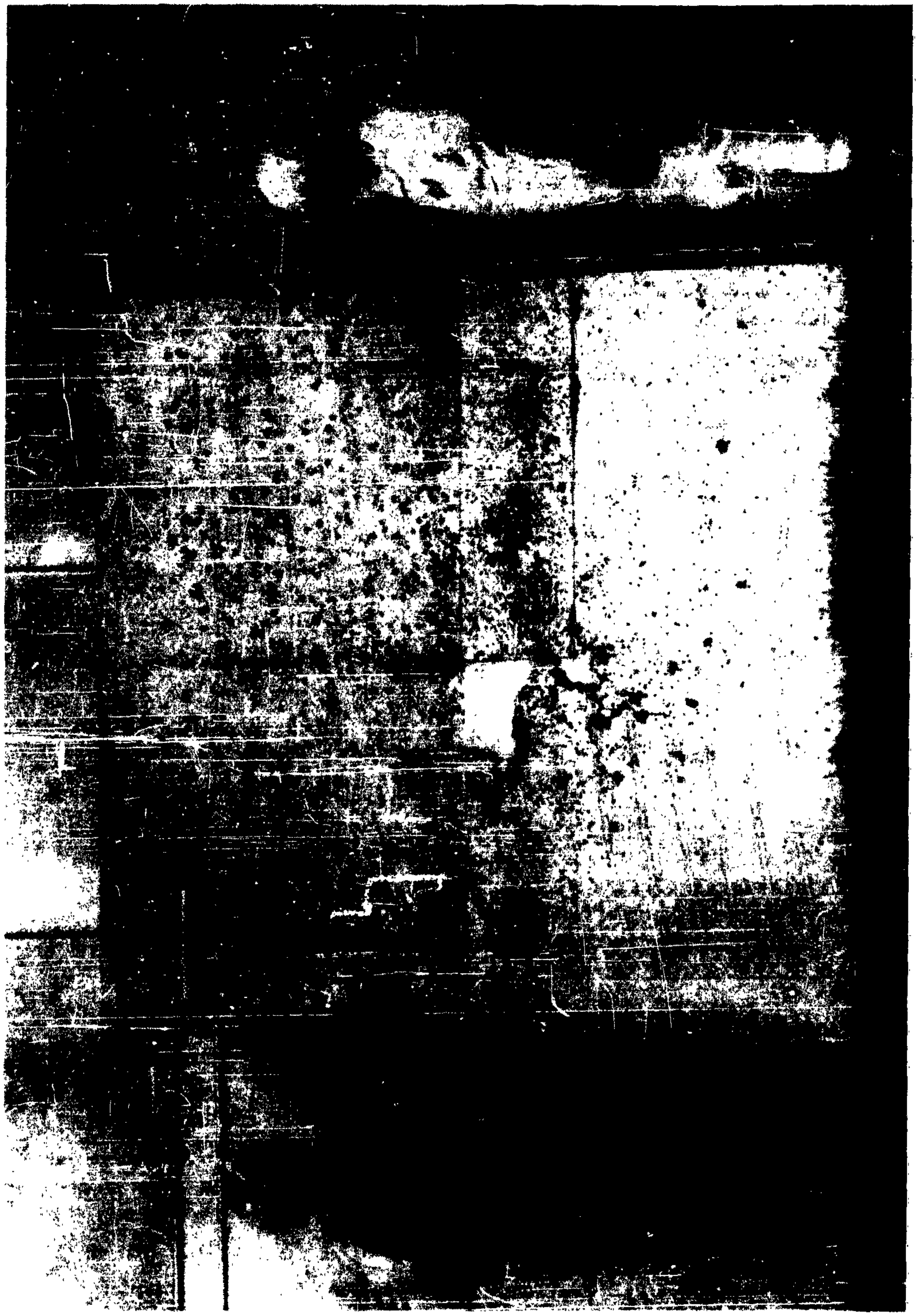

Figure 82. Impact Pattern, Round RE-14

Rnd. No.	Round Description	Parameters Varied	Test Objective	Results and Comments
RE-15	Type, Concentric Cylinder Fragment Nos., 28,900 Fragment Wt. (Grams), 31,790 Explosive Wt. (Grams), 1061 End Plate Wt. (Grams), 5650 Inert Filler Wt. (Grams), 3645 Total Wt. (Pounds), 92.8 C/M, 0.030 Figure No., 83	14 layers cylinder with hyperboloid center burster.	Design concept feasibility	Max Vel. = 1125 ft/sec Min Vel. = 200 ft/sec. Beam spray similar to RE-14. Polar Plot Fig. 84.
RE-16	Type, Spiral Hyperboloid Fragment Nos., 34,132 Fragment Wt. (Grams), 37,545 Explosive Wt. (Grams), 1,465 End Plate Wt. (Grams), 8,626 Inert Filler Wt. (Grams), 2,455 Total Wt. (Pounds), 115.75 C/M, 0.037 Figure No., 85	Spiral-Hyperboloid with sled mounting hardware. Case on Round-fiberglass Epon inert filler	Determine feasibility of projecting 14 layers of fragments using hyperboloid concept and spiral wrap	Beam spray 70° max. with 62% within 30°. velocity gradient 100 to 1000 ft/sec.
RE-17	Type, Spiral Hyperboloid Fragment Nos., 31,859 Fragment Wt. (Grams), 35,045 Explosive Wt. (Grams), 2,512 End Plate Wt. (Grams), 9,265 Inert Filler Wt. (Grams), 2,455 Total Wt. (Pounds), 120.5 C/M, 0.067 Figure No., 86, 87, 88.	Wrap of explosive around outside of round before case is put on. Configuration shaping mold used on this round.	To further reduce fragment radial velocities through the use of an external layer of sheet explosive.	Several lg. chunks of frag. pkg. found in arena and also shown by flash radiography vel. gradient 100-1000 ft/sec. Beam spray 45° max. 97% on 32° Impact Pattern Fig.89
RE-18	Type, Spiral Hyperboloid Fragment Nos., 28,943 Fragment Wt. (Grams), 31,837 Explosive Wt. (Grams), 1,343 End Plate Wt. (Grams), 9,321 Inert Filler Wt. (Grams), 6,100 Total Wt. (Pounds), 111.4 C/M, 0.035 Figure No., Identical to RE-17	Use of laminac inert filler.	Same as RE-17	Vel. Grad. 100-930 ft/sec. 90% vel. below 750 ft/sec. 30° beam spray angle; 180° witness panel configuration of pattern dist. continuity. Polar Plot Fig. 90.

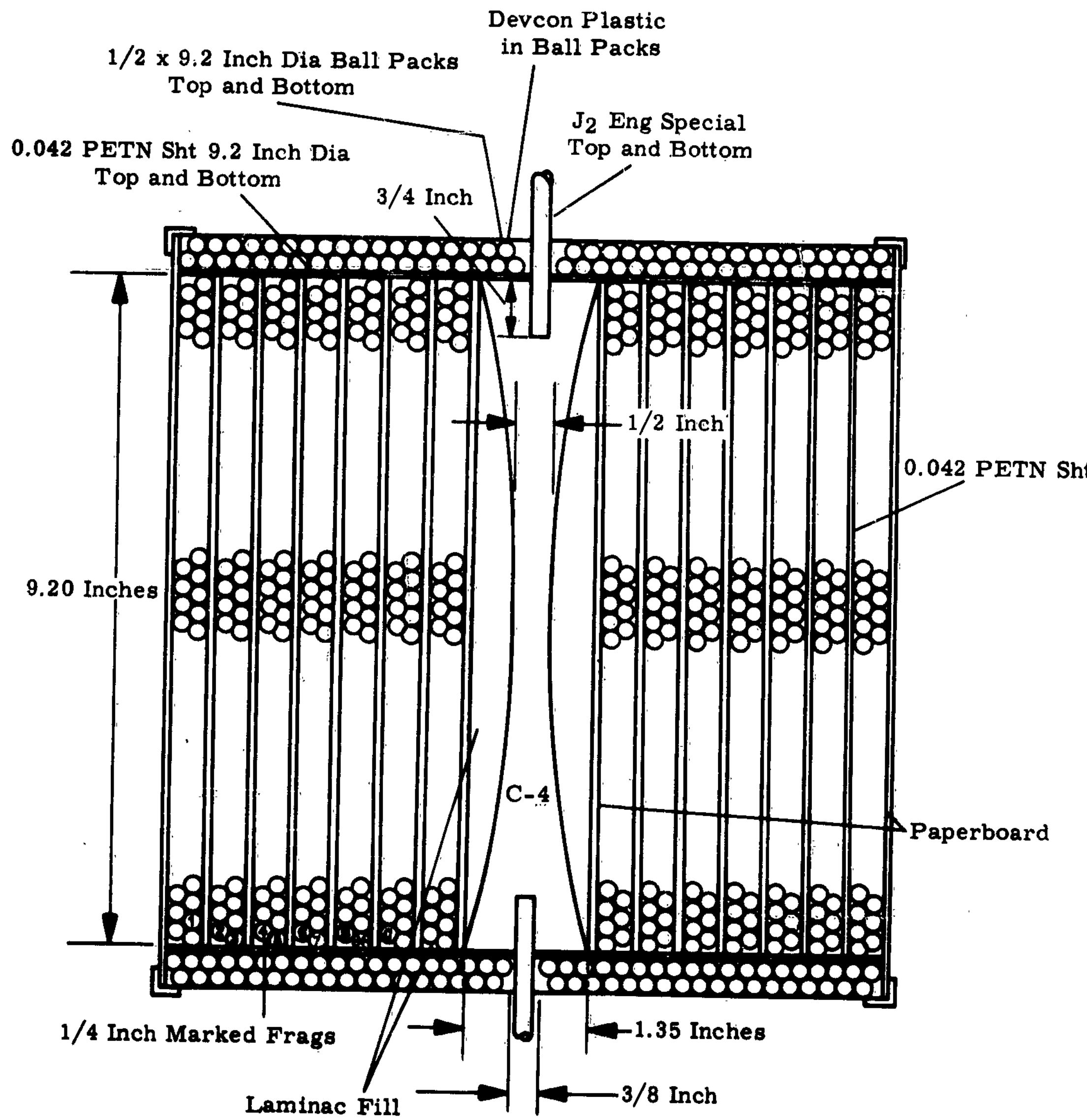

Figure 83. Test Model Design, Round RE-15

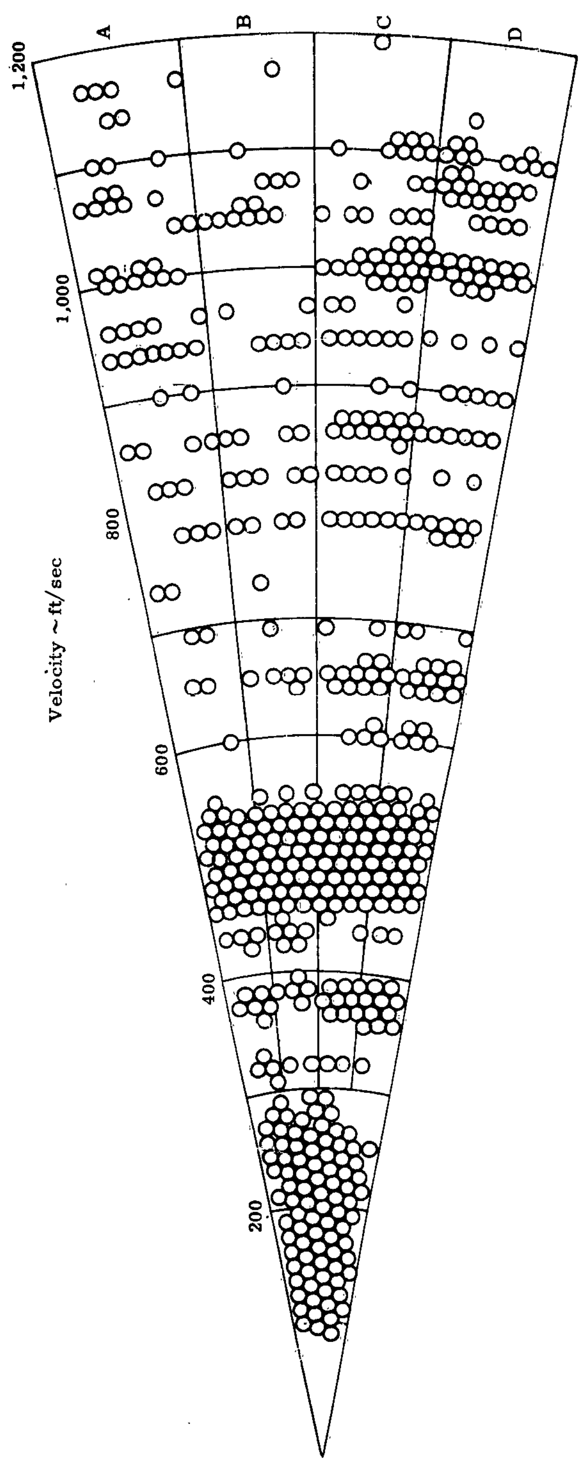

Figure 84. Velocity versus Radial Distribution, Round RE-15

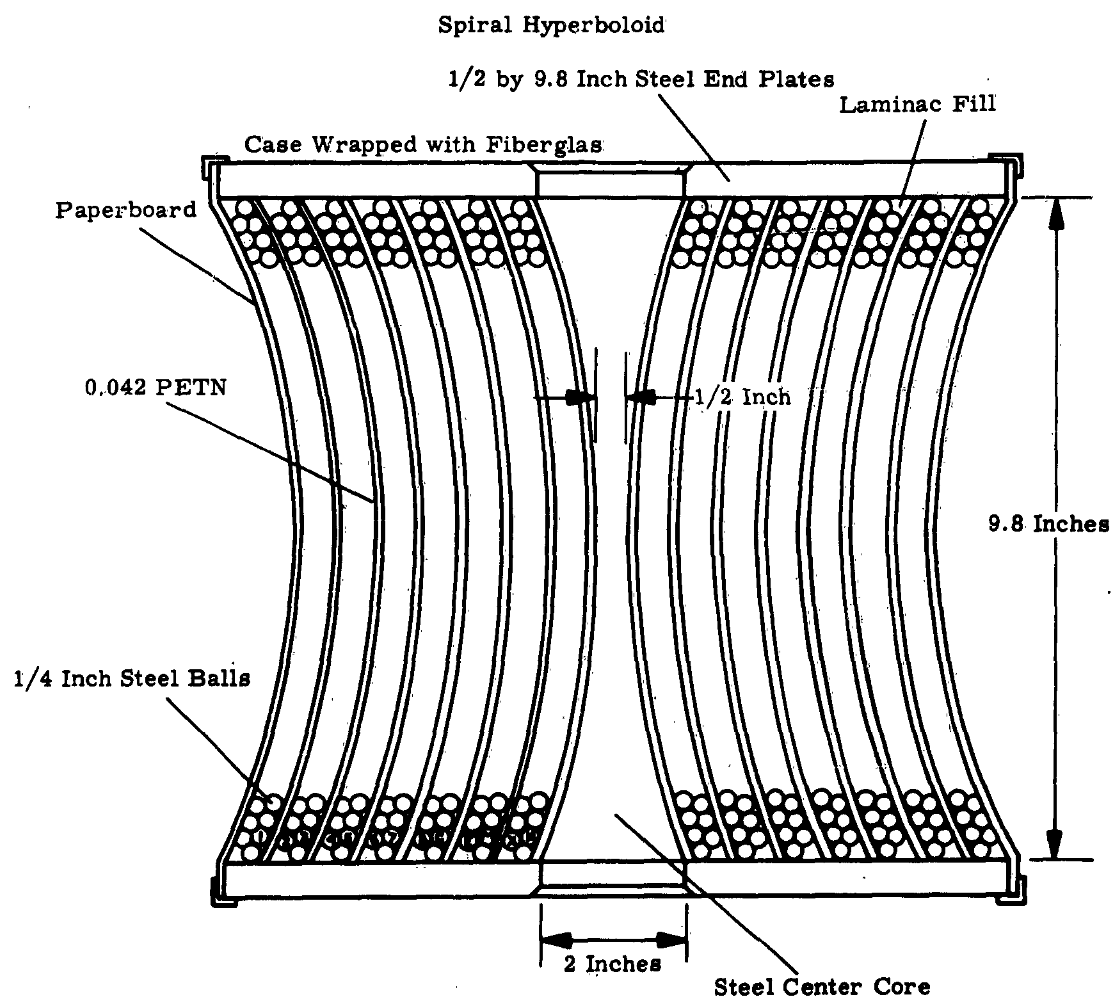

Figure 85. Test Model Design, Round RE-16

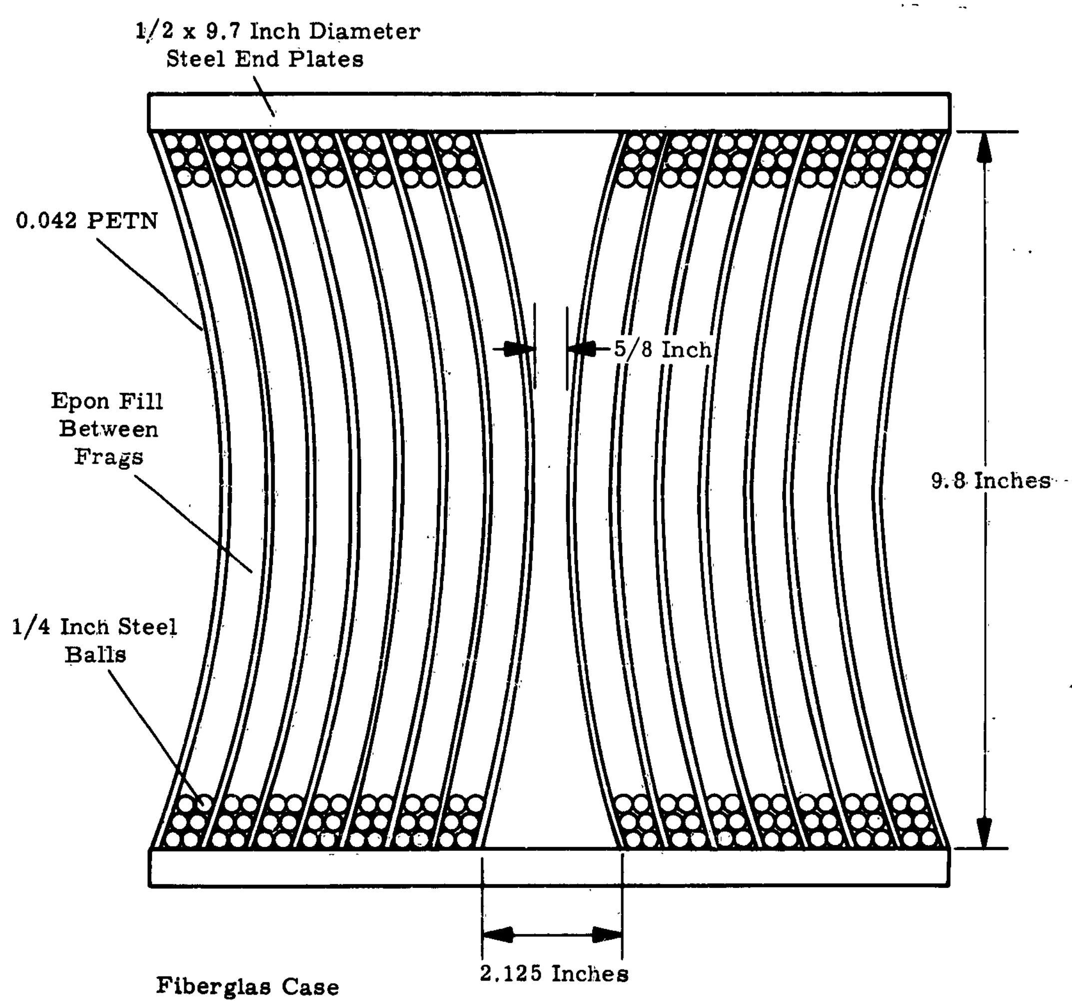

Figure 86. Test Model Design, Round RE-17

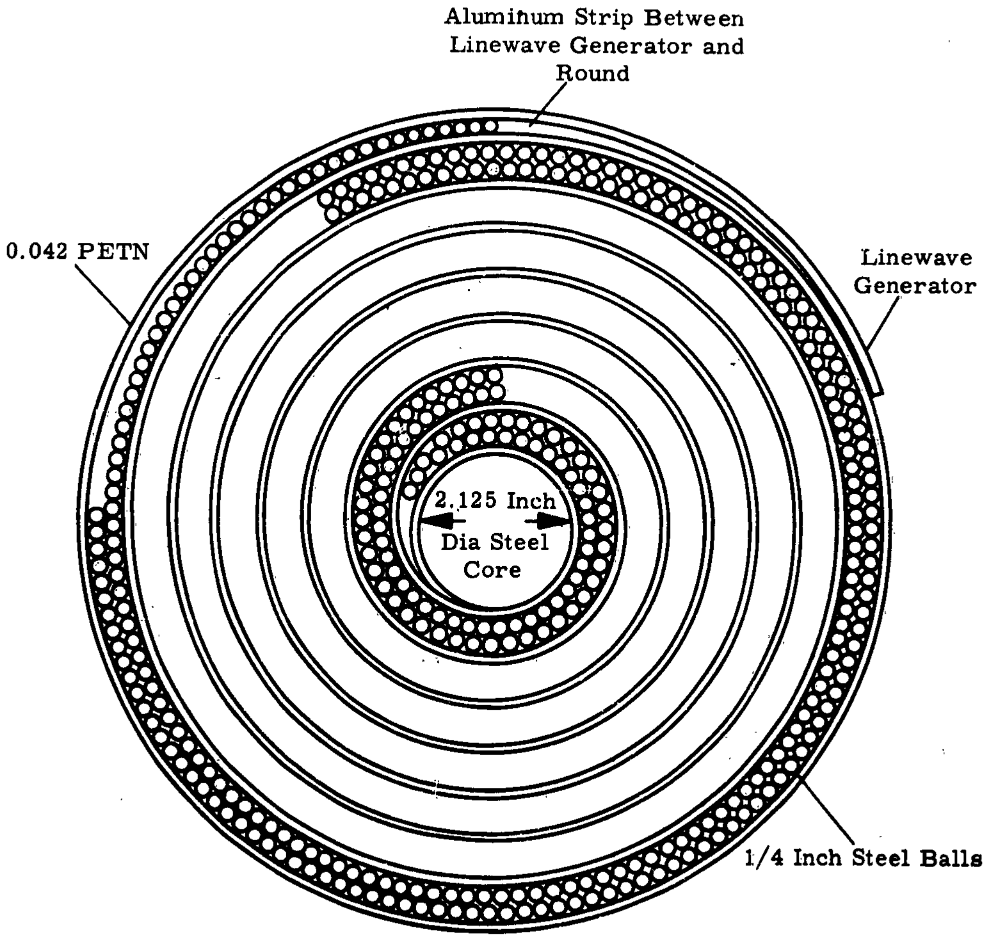

Figure 87. Test Model Design, Round RE-17

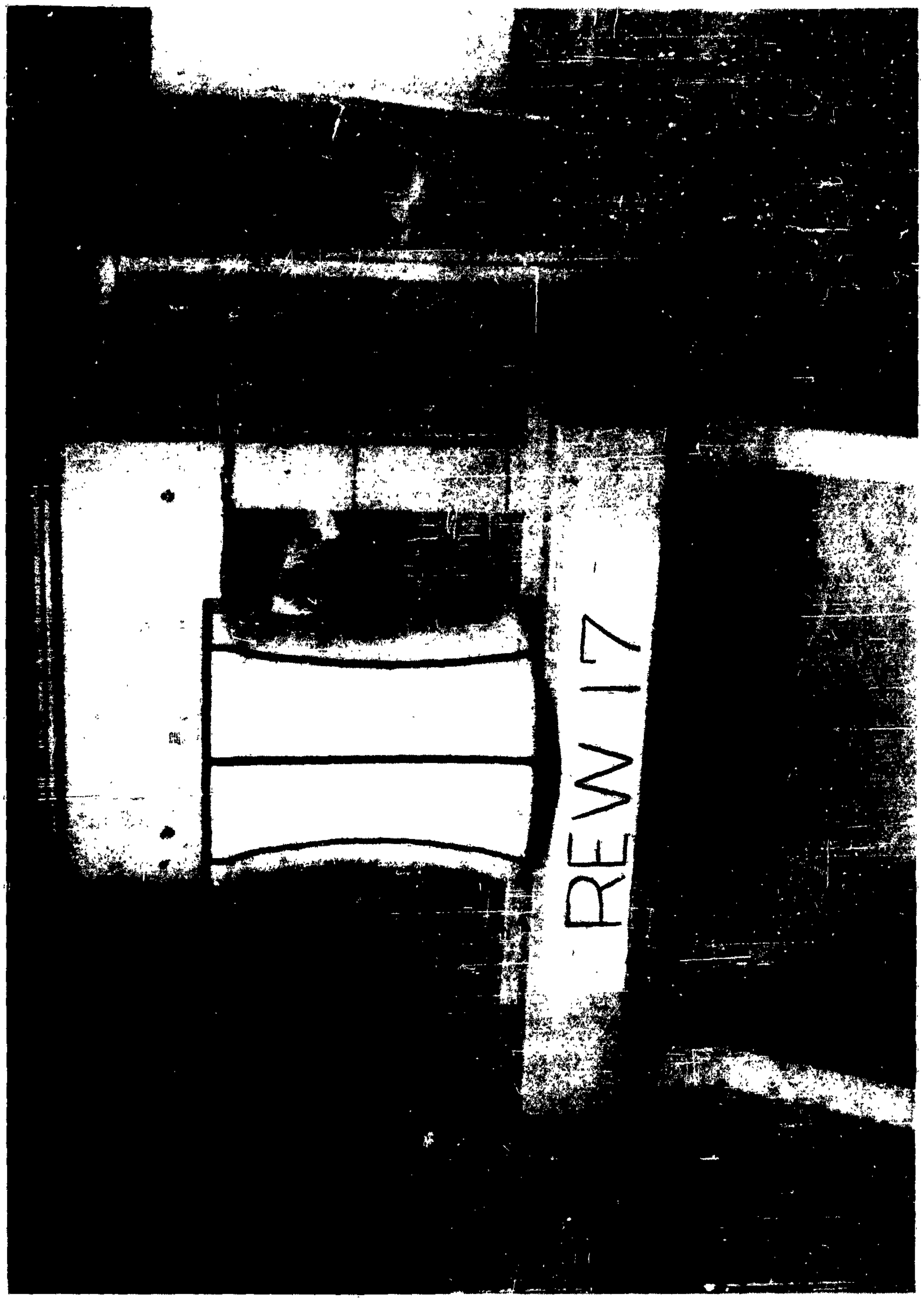

Figure 88. Warhead Test Model RE-17

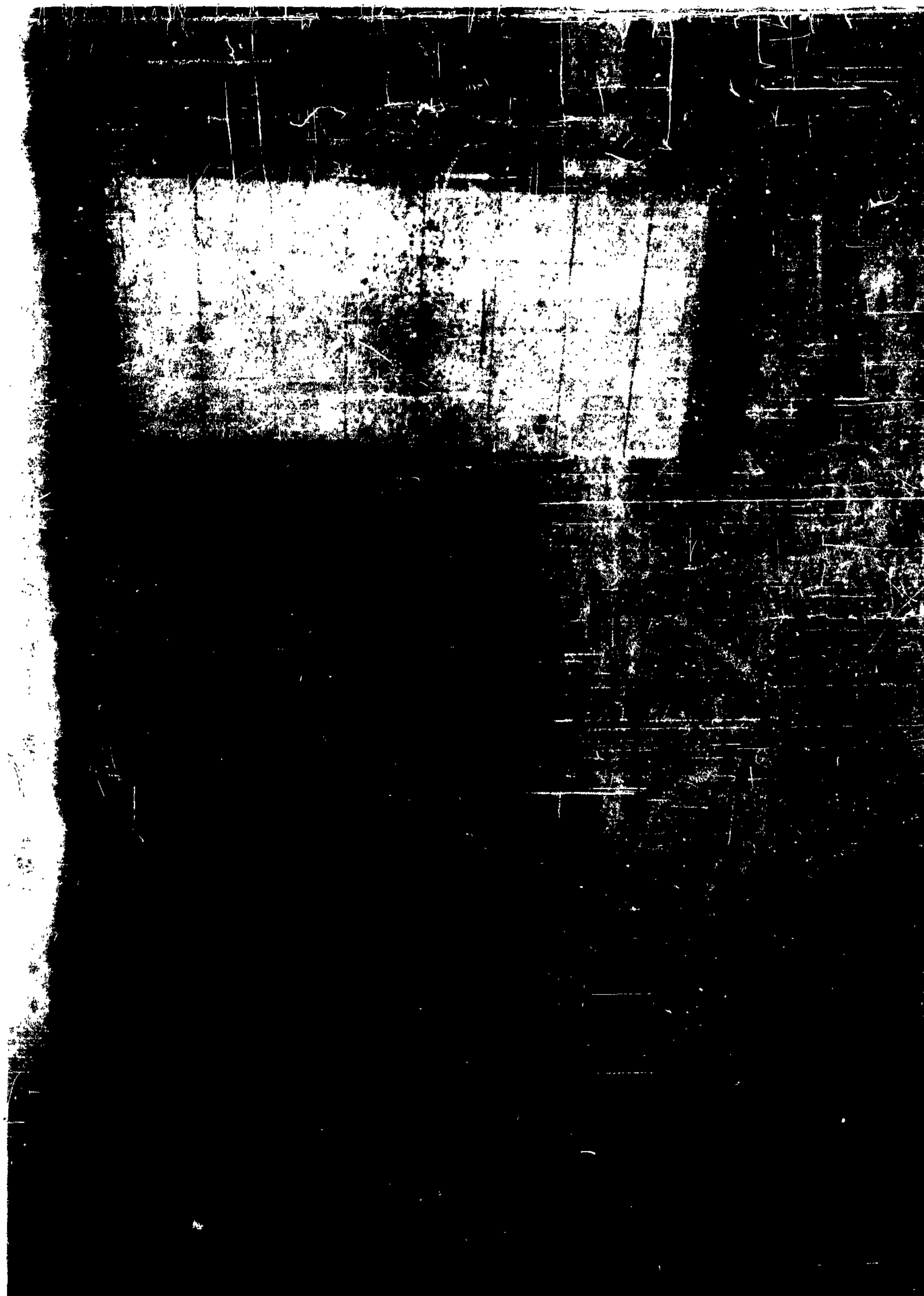

Figure 89. Impact Pattern, Round RE-17

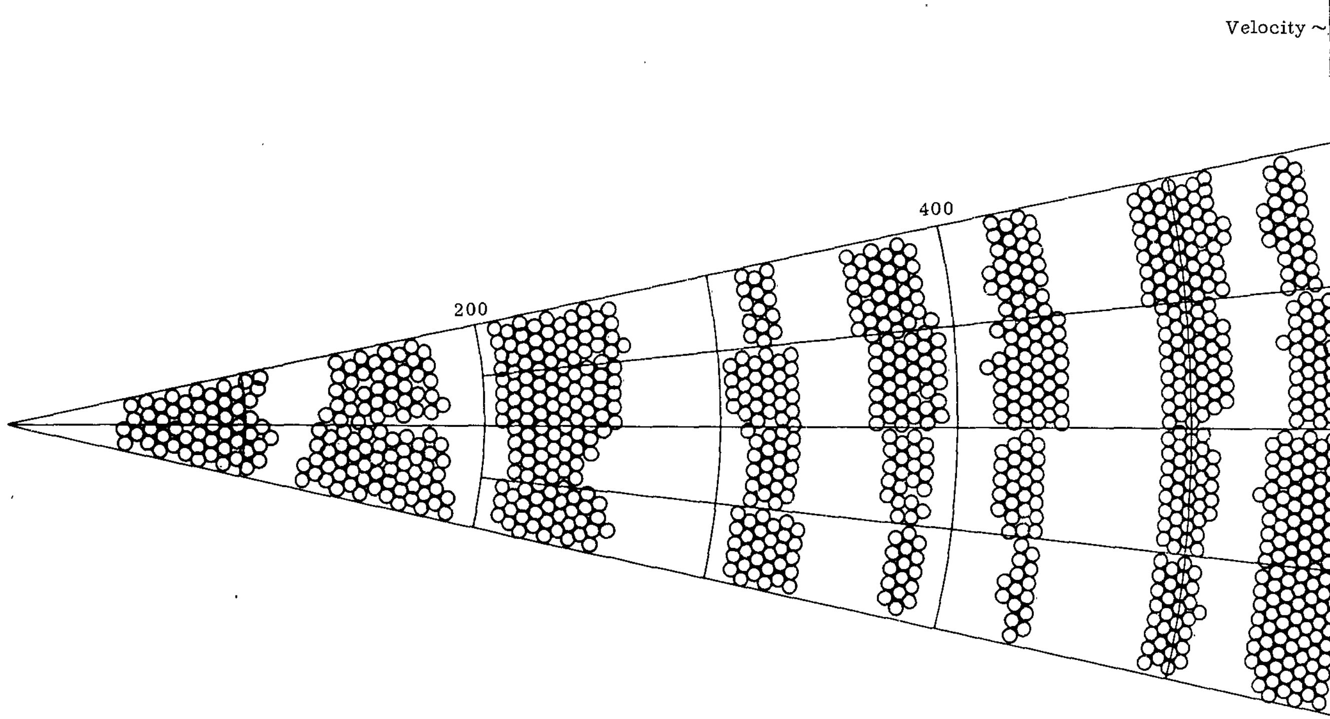

Note: Apparent banding of fragments results from multiplicity of hits within same area and accuracy with which recovery can be related to impact velocity.

Figure 90. Velocity versus Radial D

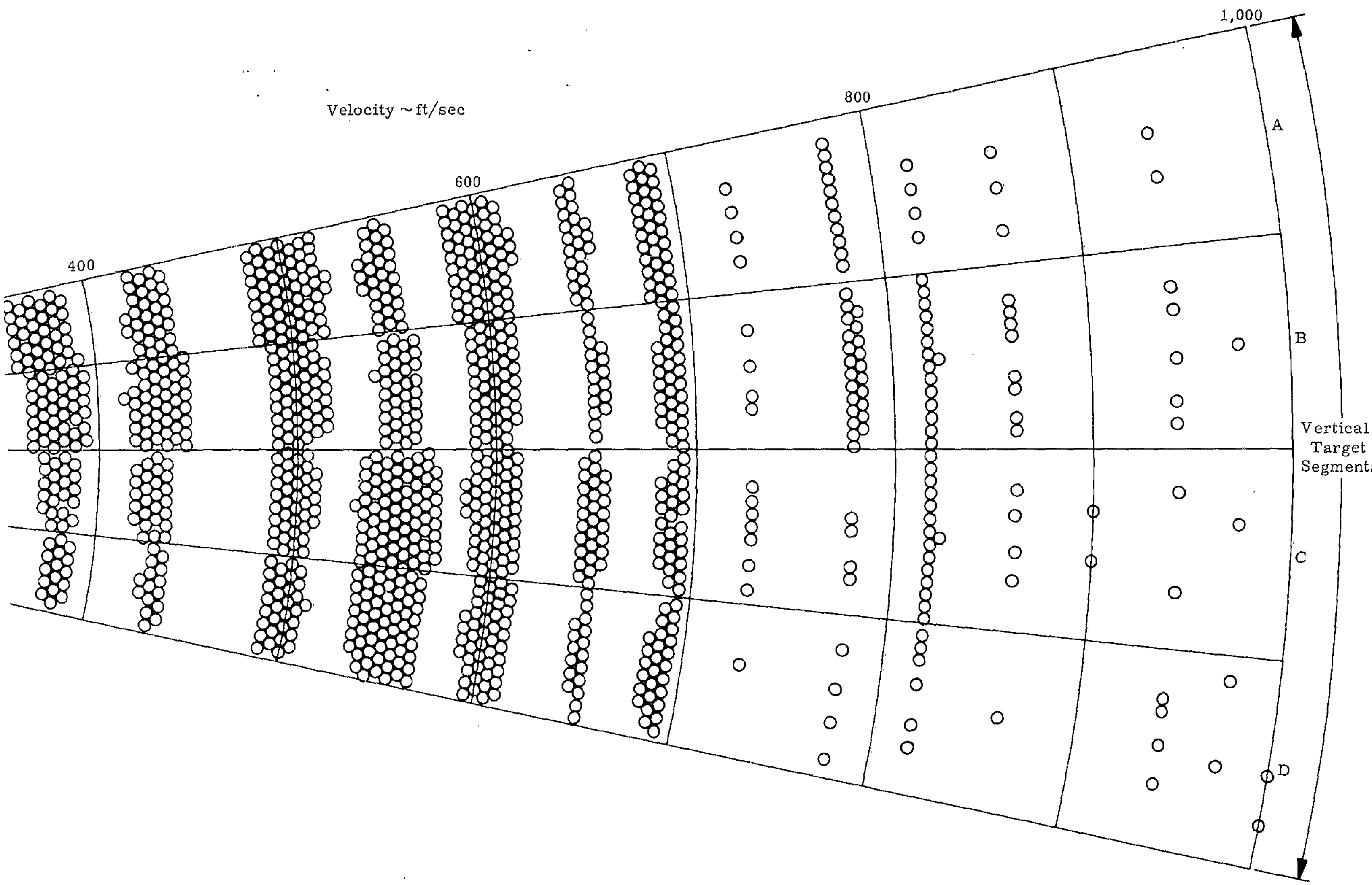

gure 90. Velocity versus Radial Distribution, Round RE-18

2

Rnd. No.	Round Description	Parameters Varied	Test Objective	Results and Comments
RE-19	Type, Spiral Hyperboloid Fragment Nos., 30,077 Fragment Wt. (Grams), 33,085 Explosive Wt. (Grams), 1354 End Plate Wt. (Grams), 9,120 Inert Filler Wt. (Grams), 4,521 Total Wt. (Pounds), 111.3 C/M, 0.036 Figure No., Identical to RE-17	Same as RE-18	Fabricated for Eglin rocket sled functional feasibility demonstrations.	Uniform frag. dist. pattern with 15-20 frag. hits per sq. ft. over a radial dist. of approx. 20 ft. These data agree with calculations using a detonation distance of 28 ft. from target and sled vel. of approx. 1300 ft/sec.
RE-20	Type, Spiral Hyperboloid Fragment Nos., 30,737 Fragment Wt. (Grams), 33,811 Explosive Wt. (Grams), 1,378 End Plate Wt. (Grams), 9,099 Inert Filler Wt. (Grams), 3,121 Total Wt. (Pounds), 109.8 C/M, 0.037 Figure No., Identical to RE-17	Same as RE-18 & 19	Same as RE-19	Warhead detonation occurred 24 ft. in front of target thus cutting radial dispersion down to 15 ft. Other data equivalent to RE-19
RE-21	Type, Concentric Hyperboloid Fragment Nos., 1,698 Fragment Wt. (Grams), 14,222 Explosive Wt. (Grams), 845 End Plate Wt. (Grams), 107 Inert Filler Wt. (Grams), 1,848 Total Wt. (Pounds), 37.3 C/M, 0.060 Figure No., 91	1/2" steel spheres 0.084 sheet explosive	To obtain scaling data on frag. size and shape effects.	Increasing frag size from a 1/4" to 1/2" diameter steel sphere, while retaining an equivalent charge to mass ratio, provides essentially the same frag velocities - max. velocity 1200 FPS.

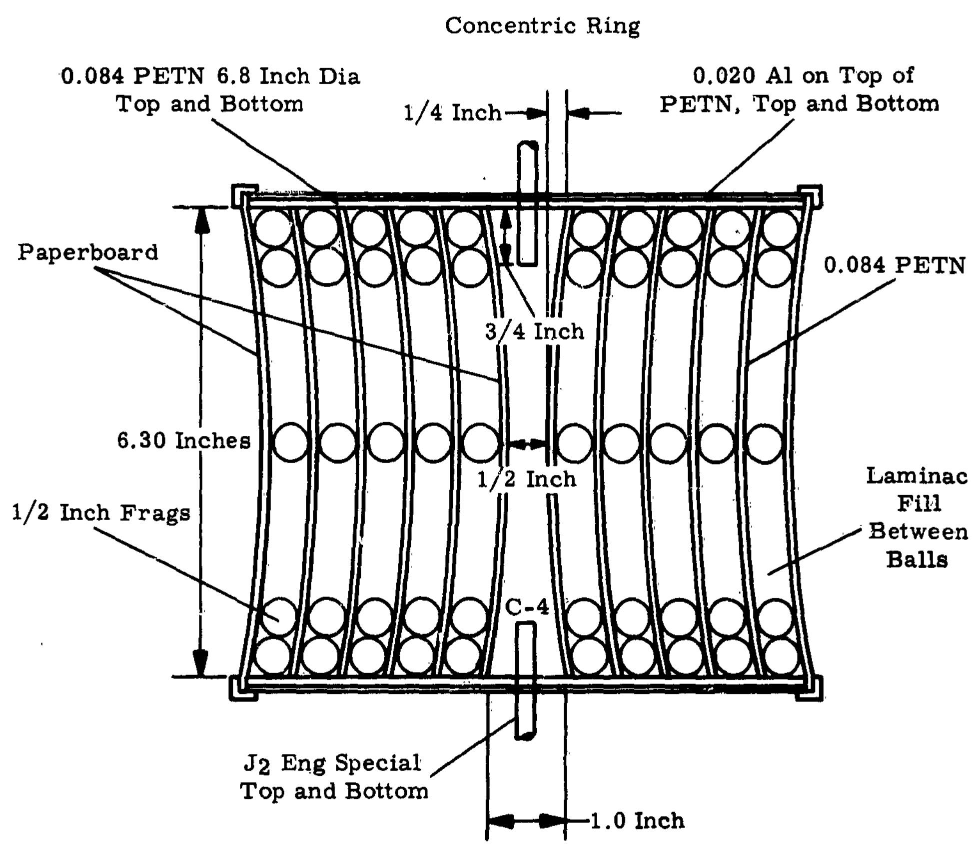

Figure 91. Test Model Design, Round RE-21

Rnd. No.	Round Description	Parameters Varied	Test Objective	Results and Comments
RE-22	Type, Concentric Hyperboloid Fragment Nos., 5,325 Fragment Wt. (Grams), 10,118 Explosive Wt. (Grams), 704 End Plate Wt. (Grams), 91 Inert Filler Wt. (Grams), 1660 Total Wt. (Pounds), 27.5 C/M, 0.070 Figure No. 92	1/4" steel cubes 0.084 sheet explosive	Same as RE-21	Use of cubical frag. as opposed to spherical frags. while retaining an equivalent charge to mass ratio, provides a more concentrated impact pattern and approx. a 20% increase in frag. velocities - max. velocity 1800 FPS
RE-23	Type, Spiral Hyperboloid Fragment Nos., 27,880 Fragment Wt. (Grams), 33,456 Explosive Wt. (Grams), 1,330 End Plate Wt. (Grams), 9,502 Inert Filler Wt. (Grams), 8,243 Total Wt. (Pounds), 120.2 C/M, 0.040 Figure No., Identical to RE-17	1/4" nickel spheres in round	Project 14 layers of nickel frags without deformation of fragments.	Velocities approx. same as steel spheres; no deformation of fragments. Uniform distribution pattern.

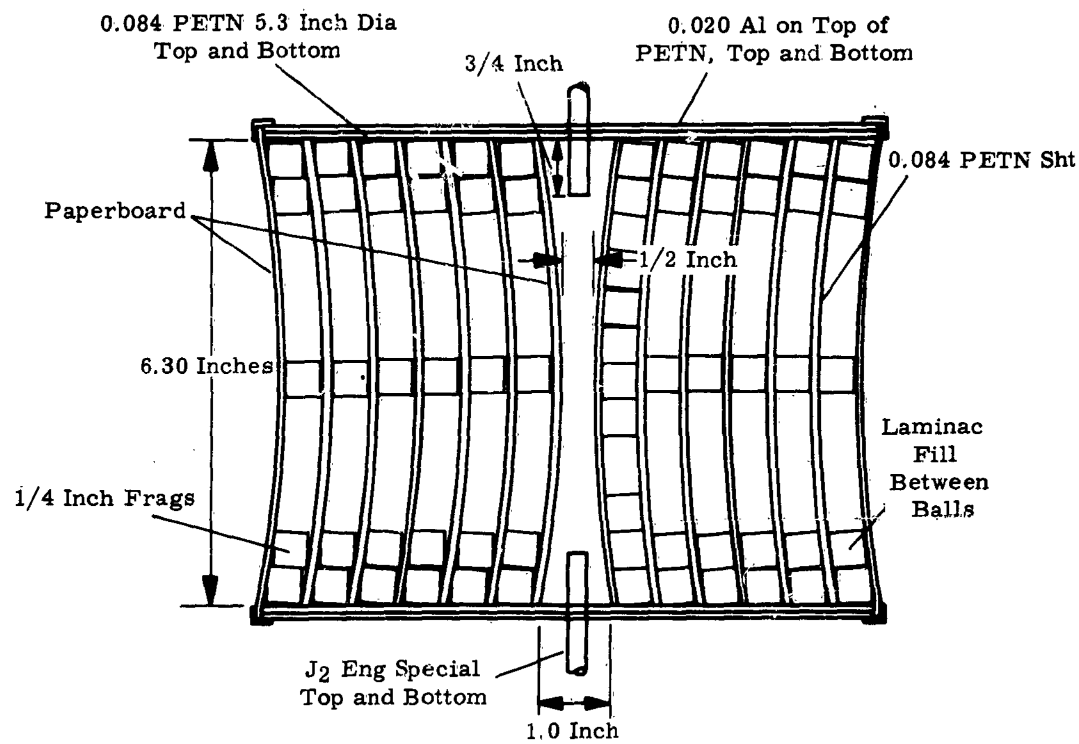

Figure 92. Test Model Design, Round RE-22

The reverse side of this page is blank.

DISTRIBUTION LIST

1	DOD R&E
3	ADVANCED RSCH PROJ AGENCY (Mr. Koether)
1	WPNS SYS EVAL GP
1	HQ USAF (AFOCE)
1	HQ USAF (AFRDP)
1	HQ USAF (AFCIN)
1	HQ USAF (AFRSTB)
1	HQ USAF (AFORQ-Q1)
1	HQ USAF (AFRSTE)
1	AFSC (MSFA)
1	AFSC (SCSA)
1	ASD (ASJ)
2	AFAL (AVNS)
1	AFML (MAA)
1	AFML (MAY)
2	AFFDL (FDTS)
1	FTD (TDFA)
1	FTD (TDFS)
1	FTD (TDBTL)
1	FTD (TDEA)
2	FTD (TDEWA)
1	SEG
1	SEG (SEAF)
1	SEG (SEBA)
1	SEG (SEPRR)
1	RTD (RTTW)
2	RTD (TECH LIB)
2	SSD (SSTAS/Capt Hayford)
1	SSD (SSTDS)
2	SSD (SSTRT/Capt Gavcus)
1	SSD (SSTRT/Capt K.R.Hughey)
1	SAFSP (SP6/Maj Sherline)
2	BSD (BSVDA/Capt W.H.Black)
1	BSD (BSVDA/Capt Baker)
1	BSD (BS4DV/Capt Dickison)
1	ESD (ESTI)
1	AFCRL (CRXL)
1	RADC (RAALD)
2	AEDC (TECH LIB)
1	AFWL (WLDC/Mr O'Haver)
1	AFWL (WLRPT/Capt Gillespie)
1	AFWL (WLAX)
2	AFWL (WLIL)
1	SAC (OA)
1	AU (AUL-9764)
1	DIRECTORATE OF R&D (Lt Col S.W.Josephson)
2	OFFICE OF NAVAL RESCH (Physics Div)
1	US NAVAL ORD LAB (Library)
1	US NAVAL WPNS EVAL FAC
1	US NAVAL WPNS LAB (Library)
3	NAVAL RESCH LAB (CODE 6240)
2	NAVAL RSCH LAB (Tech Lib)
1	US NAVAL ORD LAB
1	NAVAL ORDNANCE LAB (Mr. C. S. Chambre)
5	NAVAL ORDNANCE LAB (Mr. B. F. Huston)
1	NAVAL ORDNANCE TEST STN (Capt R.E. Jensen)
3	US NAV ORD LAB (Code 551, 552, 511)
1	AFSC (STLO/Maj H.B.Powell)
2	US ARMY ENGR R&D LABS (Stinfo Branch)
2	USA MSL COMD (Tech Lib)
1	ARMY MATERIEL COMMAND (AMCRD-DE-W)
2	PICATINNY ARSENAL (Tech Lib)
3	PICATINNY ARSENAL (SMUPA-DW8/S. Stein)
1	FRANKFORD ARSENAL (Lib)
1	US ARMY RESEARCH OFFICE-DURHAM (CRD-AA-IP)
2	BALLISTIC RESCH LAB (Tech Lib)
3	BALLISTIC RESCH LAB (AMXBR-T/Dr.F.E.Allison Dr.C.Glass)
20	DDC
2	DIR USAF PROJ RAND
5	MARTIN-MARIETTA CORP (Tech Lib/Mr.W.R. Porter)
1	RAYTHEON CO. (Msl Sys Div/W. Hurd)
1	RSCH INST - Illinois Inst of Tech (Mr. F. Zimmerman)
2	BATTELLE MEMORIAL INSTITUTE (Battelle-Defender)
1	SHOCK HYDRODYNAMIC INC. (Mr. B.J. Bjork)
1	PHYSICS INTERNATIONAL (Dr. C. Godfrey)
2	LOCKHEED AIRCRAFT CORP. (Tech Info Ctr)
1	GENERAL AMERICAN TRANS CORP. (Mr. P.A.Saigh)
1	AEROSPACE CORP (Mr. Tom Friedman)
1	BALLISTIC RESCH LAB (AMXBR-X/Dr.R.J.Eichelberger)

3 AEROSPACE CORP
(Mr. D. Singer)
2 AEROSPACE CORP
(Tech Lib)
2 AEROSPACE CORP
(Dr. J. Brown)
2 AEROSPACE CORP
(Mr. C. Kelley)
1 AEROSPACE CORP
(Mr. R. Farrin)
1 AEROSPACE CORP.
(Mr. V. Frost)
1 PGF
4 PGBPS-4
1 ATBT
1 ATG
4 ATWR
1 LTV ASTRONAUTICS DIV

CONFIDENTIAL (Gp-4) **CONFIDENTIAL**

Security Classification

DOCUMENT CONTROL DATA - R&D

(Security classification of title, body of abstract and indexing annotation must be entered when the overall report is classified)

1. ORIGINATING ACTIVITY (Corporate author) Armament Sciences Laboratory, Research Division Martin Company, Orlando, Florida	2a. REPORT SECURITY CLASSIFICATION CONFIDENTIAL 2b. GROUP 4

3. REPORT TITLE

Radially Expanding Fragmentation Warhead Study, Second Summary Report (March 1965)

4. DESCRIPTIVE NOTES (Type of report and inclusive dates)

Summary Technical Report for period ending January 1965

5. AUTHOR(S) (Last name, first name, initial)

PORTER, WILLIAM R.

6. REPORT DATE	7a. TOTAL NO. OF PAGES	7b. NO. OF REFS
May 1965	144	5

8a. CONTRACT OR GRANT NO. AF 08(635)-4263 b. PROJECT NO. 9850 c. Task No. 985001 d.	9a. ORIGINATOR'S REPORT NUMBER(S) ATL-TR-65-35 9b. OTHER REPORT NO(S) (Any other numbers that may be assigned this report)

10. AVAILABILITY/LIMITATION NOTICES

Qualified requesters may obtain copies of this report from the Defense Documentation Center

11. SUPPLEMENTARY NOTES	12. SPONSORING MILITARY ACTIVITY Detachment 4, RTD Advanced Technology Branch Eglin AFB, Fla

13. ABSTRACT

(C) Work has been continued on the experimental evolution and analytical confirmation of an explosive layered warhead design capable of projecting 14 layers of fragments into a slowly expanding radial pattern. Major accomplishments leading to the evolved design were:

1. The feasibility of projecting 14 fragment layers was demonstrated in three design variations - spiral cylinders, concentric ring hyperboloids, and spiral hyperboloids.

2. The feasibility of controlling fragment beam spray angles was demonstrated with massive end confinement, hyperboloid shaping, explosive end plates, and combinations of these.

3. The capability of a 14 fragment layer warhead model to meet performance goals under dynamic rocket sled test conditions was demonstrated.

The warhead design that progressed to rocket sled tests is a hyperbolic configuration (for beam spray control), 10.75 inches in length and 9.75 inches in diameter, weighing 110 pounds. 30,000 one-quarter inch spherical fragments are projected radially by 3 pounds of sheet explosive.

DD FORM 1 JAN 64 1473

CONFIDENTIAL (Gp-4)

Security Classification

CONFIDENTIAL

CONFIDENTIAL

CONFIDENTIAL (Gp-4)

Security Classification

14. KEY WORDS	LINK A		LINK B		LINK C	
	ROLE	WT	ROLE	WT	ROLE	WT
Fragmentation Warheads Multilayered Fragments Projectors						

INSTRUCTIONS

1. ORIGINATING ACTIVITY: Enter the name and address of the contractor, subcontractor, grantee, Department of Defense activity or other organization *(corporate author)* issuing the report.

2a. REPORT SECURITY CLASSIFICATION: Enter the overall security classification of the report. Indicate whether "Restricted Data" is included. Marking is to be in accordance with appropriate security regulations.

2b. GROUP: Automatic downgrading is specified in DoD Directive 5200.10 and Armed Forces Industrial Manual. Enter the group number. Also, when applicable, show that optional markings have been used for Group 3 and Group 4 as authorized.

3. REPORT TITLE: Enter the complete report title in all capital letters. Titles in all cases should be unclassified. If a meaningful title cannot be selected without classification, show title classification in all capitals in parenthesis immediately following the title.

4. DESCRIPTIVE NOTES: If appropriate, enter the type of report, e.g., interim, progress, summary, annual, or final. Give the inclusive dates when a specific reporting period is covered.

5. AUTHOR(S): Enter the name(s) of author(s) as shown on or in the report. Enter last name, first name, middle initial. If military, show rank and branch of service. The name of the principal author is an absolute minimum requirement.

6. REPORT DATE: Enter the date of the report as day, month, year; or month, year. If more than one date appears on the report, use date of publication.

7a. TOTAL NUMBER OF PAGES: The total page count should follow normal pagination procedures, i.e., enter the number of pages containing information.

7b. NUMBER OF REFERENCES: Enter the total number of references cited in the report.

8a. CONTRACT OR GRANT NUMBER: If appropriate, enter the applicable number of the contract or grant under which the report was written.

8b, 8c, & 8d. PROJECT NUMBER: Enter the appropriate military department identification, such as project number, subproject number, system numbers, task number, etc.

9a. ORIGINATOR'S REPORT NUMBER(S): Enter the official report number by which the document will be identified and controlled by the originating activity. This number must be unique to this report.

9b. OTHER REPORT NUMBER(S): If the report has been assigned any other report numbers *(either by the originator or by the sponsor)*, also enter this number(s).

10. AVAILABILITY/LIMITATION NOTICES: Enter any limitations on further dissemination of the report, other than those imposed by security classification, using standard statements such as:

(1) "Qualified requesters may obtain copies of this report from DDC."

(2) "Foreign announcement and dissemination of this report by DDC is not authorized."

(3) "U. S. Government agencies may obtain copies of this report directly from DDC. Other qualified DDC users shall request through ________________."

(4) "U. S. military agencies may obtain copies of this report directly from DDC. Other qualified users shall request through ________________."

(5) "All distribution of this report is controlled. Qualified DDC users shall request through ________________."

If the report has been furnished to the Office of Technical Services, Department of Commerce, for sale to the public, indicate this fact and enter the price, if known.

11. SUPPLEMENTARY NOTES: Use for additional explanatory notes.

12. SPONSORING MILITARY ACTIVITY: Enter the name of the departmental project office or laboratory sponsoring *(paying for)* the research and development. Include address.

13. ABSTRACT: Enter an abstract giving a brief and factual summary of the document indicative of the report, even though it may also appear elsewhere in the body of the technical report. If additional space is required, a continuation sheet shall be attached.

It is highly desirable that the abstract of classified reports be unclassified. Each paragraph of the abstract shall end with an indication of the military security classification of the information in the paragraph, represented as *(TS), (S), (C), or (U)*.

There is no limitation on the length of the abstract. However, the suggested length is from 150 to 225 words.

14. KEY WORDS: Key words are technically meaningful terms or short phrases that characterize a report and may be used as index entries for cataloging the report. Key words must be selected so that no security classification is required. Identifiers, such as equipment model designation, trade name, military project code name, geographic location, may be used as key words but will be followed by an indication of technical context. The assignment of links, rules, and weights is optional.

CONFIDENTIAL (Gp-4)

Security Classification

CONFIDENTIAL